

**BIOLUBRICANT PRODUCTION OVER  
SULFATED TI-SBA-15 AND TIO<sub>2</sub>-SIO<sub>2</sub> BASED  
MESOPOROUS CATALYSTS**

**A Thesis Submitted to  
the Graduate School of Engineering and Sciences of  
İzmir Institute of Technology  
in Partial Fulfillment of the Requirements for the Degree of**

**MASTER OF SCIENCE**

**in Chemical Engineering**

**by  
Tuğçe ÖZPERÇİN**

**May 2022**

**İZMİR**

## ACKNOWLEDGMENTS

I would like to express my deepest appreciation to my supervisor Prof. Dr. Selahattin YILMAZ who made this work possible. He was very helpful and patient to me during my studies. I am grateful to him for helping me develop a better perspective on the subject and kept me motivated about my research. I feel pleased and privileged to have worked with him.

I would like to thank to Jury Members Assist. Prof. Dr. Bařar aęlar and Assoc. Prof. Emine Sert for suggestions and ideas they shared for my thesis.

I would like to thank to research specialists, Nesrin Ahıpařaoęlu, zlem Duvarcı, Deniz Őimřek, Mine Baheci, Burcu Akdaę aęlar, Hseyin zgener for their help and contributions in the characterization studies. Moreover, I am thankful to technical staff Nazil Karaca and Ahmet Kurul for their kind help and technical support.

I especially want to thank my dear lab friends Azime Arıkaya, Gnsev Dizoęlu, Begm Snmeztrk and Mustafa Kalkandelen for their valuable support, useful comments and friendships. I appreciate to meet each of them.

My special thanks go to my dear parents Orhan zperin and Nimet zperin. I am really thankful for their endless support and continuous encouragement throughout my studies. They never stopped to believing in me. This study could not be achieved without them.

This study was supported financially by Kansai Altan. I would like to thank to Selim Yetiř, Murat Gaffaroęulları and Pınar zkal.

## ABSTRACT

### BIOLUBRICANT PRODUCTION OVER SULFATED TI-SBA-15 AND TiO<sub>2</sub>-SiO<sub>2</sub> BASED MESOPOROUS CATALYSTS

Production of ecofriendly biodegradable lubricants from vegetable oils is an attractive alternative to petroleum derived lubricants for environmental protection. This study presents an investigation for the production of biolubricants via ring opening reaction of epoxidized soybean oil using the mesoporous solid acid catalysts. SO<sub>4</sub>/SBA-15, SO<sub>4</sub>/Ti-SBA-15, SO<sub>4</sub>/TiO<sub>2</sub>-SiO<sub>2</sub> and SO<sub>4</sub>/La-TiO<sub>2</sub>-SiO<sub>2</sub> catalysts were prepared and characterized. In addition, effect of increasing titanium content on SO<sub>4</sub>/Ti-SBA-15 (Si/Ti: 10, Si/Ti: 6) and effect of sulfation source (ammonium sulfate and chlorosulfonic acid) on Ti-SBA-15 and La-TiO<sub>2</sub>-SiO<sub>2</sub> properties, activities and stabilities were studied. Activity and stability of all the catalysts were tested in the ring opening reactions of epoxidized soybean oil with 2-propanol at 80 °C with 10/1 alcohol-epoxide mol ratio. After determination of the two most stable and active catalysts, reactions were also performed with 2-ethylhexanol at 100 °C with 6/1 alcohol-epoxide mol ratio. Products were analyzed by titration, FTIR and H-NMR. Also, thermal stability and low temperature behavior of products were determined by thermogravimetric analysis and differential scanning calorimetry.

Prepared catalysts had mesoporous structure and stronger acid sites by attachment of sulfate groups. The catalysts showed a serious leaching when they were sulfated with ammonium sulfate. On the other hand, chlorosulfonic acid treatment enhanced significantly stability of catalyst. Furthermore, increasing of titanium content and sulfation with chlorosulfonic acid increased the acidity of catalysts compared to ammonium sulfate. The SO<sub>4</sub>/Ti-SBA-15-6(CS) catalyst (Si/Ti:6 mole ratios and chlorosulfonic acid sulfated) was found as the most stable and active catalyst. It provided 62 % (12 h) and 90 % (18 h) conversion in the reactions with 2-propanol and 2-ethylhexanol, respectively. All products were found as thermally stable up to 300 °C showing that ring opening reaction did not affect thermal stability. Nevertheless, it affected positively low temperature properties and better low temperature properties were obtained from the products of reactions with 2-ethylhexanol. However, its influence on the products obtained from 2-propanol was not prominent.

## ÖZET

### SÜLFATLANMIŞ Ti-SBA-15 VE TiO<sub>2</sub>-SiO<sub>2</sub> BAZLI MEZOGÖZENEKLI KATALİZÖRLER ÜZERİNDEN BİYOYAĞLAYICI ÜRETİMİ

Bitkisel yağlardan çevre dostu biyolojik olarak parçalanabilen yağlayıcıların üretimi, çevresel koruma için petrol türevli yağlayıcılara karşı cazip bir alternatiftir. Bu çalışmada, mezogözenekli katı asit katalizörleri kullanılarak epoksitlenmiş soya fasulyesi yağının halka açma reaksiyonunda biyoyağlayıcı üretimi araştırılmıştır. SO<sub>4</sub>/SBA-15, SO<sub>4</sub>/Ti-SBA-15, SO<sub>4</sub>/TiO<sub>2</sub>-SiO<sub>2</sub> ve SO<sub>4</sub>/La-TiO<sub>2</sub>-SiO<sub>2</sub>, katalizörleri hazırlanmıştır ve karakterize edilmiştir. Ayrıca SO<sub>4</sub>/Ti-SBA-15'te artan titanyum içeriğinin (Si/Ti: 10, Si/Ti: 6), ve Ti-SBA-15 ve La- TiO<sub>2</sub>-SiO<sub>2</sub> katalizörlerinde sülfat kaynağının (amonyum sülfat ve klorosülfonik asit) katalizörlerin özellikleri, aktiviteleri ve stabiliteleri üzerine etkisi çalışılmıştır. Hazırlanan katalizörlerin aktivitesi ve stabilitesi, 2-propanol ile halka açma reaksiyonlarında test edilmiştir (80 °C.). En kararlı ve aktif iki katalizörün belirlenmesinden sonra, 2-etilheksanol ile de reaksiyonlar gerçekleştirilmiştir (100 °C.). Ürünler titrasyon, FTIR ve H-NMR ile analiz edilmiştir. Ayrıca termogravimetrik analiz ve diferansiyel taramalı kalorimetri ile ürünlerin termal stabilitesi ve düşük sıcaklık davranışı belirlenmiştir.

Hazırlanan katalizörler mezogözenekli bir yapıdadır ve sülfat gruplarının eklenmesiyle daha güçlü asit bölgelerine sahip olmuştur. Katalizörler, amonyum sülfat ile hazırlandıklarında ciddi bir liç göstermiştir. Öte yandan, klorosülfonik asit muamelesi katalizörün stabilitesini önemli ölçüde arttırmıştır. Ayrıca titanyum içeriğinin artırılması ve klorosülfonik asit ile sülfatlaması amonyum sülfata kıyasla katalizörlerin asitliğini arttırmıştır. SO<sub>4</sub>/Ti-SBA-15-6(CS) katalizörü (Si/Ti:6 mol oranı ve klorosülfonik asit sülfatlamış) en kararlı ve aktif katalizör olarak bulunmuştur. 2-propanol ve 2-ethylhexanol ile reaksiyonlarda sırasıyla 62 % (12h) ve 90 % (18 h) dönüşüm sağlamıştır. Tüm ürünler 300 °C'ye kadar termal olarak kararlı bulunmuştur ve halka açılma reaksiyonunun termal stabiliteyi etkilemediği görülmüştür. Bununla birlikte, düşük sıcaklık özelliklerini olumlu yönde etkilemiş ve 2-etilheksanol ile reaksiyon ürünlerinden daha iyi düşük sıcaklık özellikleri elde edilmiştir. Ancak 2-propanolden elde edilen ürünler üzerindeki etkisi belirgin değildi.

# TABLE OF CONTENTS

ABSTRACT .....	iii
ÖZET .....	iv
LIST OF FIGURES .....	vii
LIST OF TABLES.....	x
CHAPTER 1. INTRODUCTION .....	1
CHAPTER 2. OVERVIEW OF BIOLUBRICANTS .....	4
2.1. Role of Lubrication .....	4
2.2. Vegetable Oils and Biolubricants .....	5
2.3. Modification of Vegetable Oils .....	10
2.3.1. Esterification and Transesterification .....	10
2.3.2. Epoxidation and Ring Opening Reaction .....	12
CHAPTER 3. LITERATURE STUDIES ON BIOLUBRICANT PRODUCTION.....	14
3.1. Assessments of Literature Studies .....	24
3.2. Sulfated Ti-SBA-15 Catalysts .....	26
3.3. Sulfated TiO <sub>2</sub> -SiO <sub>2</sub> Catalysts .....	27
CHAPTER 4. EXPERIMENTAL STUDY .....	30
4.1. Materials .....	30
4.2. Catalyst Preparation .....	31
4.2.1. Preparation of SO <sub>4</sub> /Ti-SBA-15 and SO <sub>4</sub> /SBA-15.....	31
4.2.2. Preparation of SO <sub>4</sub> /La-TiO <sub>2</sub> -SiO <sub>2</sub> and SO <sub>4</sub> /TiO <sub>2</sub> -SiO <sub>2</sub> .....	32

4.3. Catalyst Characterization .....	33
4.3.1. N <sub>2</sub> Adsorption/Desorption Tests (BET).....	33
4.3.2. X-Ray Diffraction (XRD).....	33
4.3.3. Skeletal FTIR Spectroscopy .....	33
4.3.4. Temperature Programmed Desorption of Ammonia (NH <sub>3</sub> -TPD) .....	33
4.3.5. Thermal Gravimetric Analysis (TGA) .....	34
4.3.6. X-Ray Fluorescence Spectroscopy (XRF) .....	34
4.4. Catalyst Testing in Epoxide Soybean oil to Biolubricants .....	34
4.5. Reusability of the Catalysts .....	38
CHAPTER 5. RESULT AND DISCUSSION .....	39
5.1. Characterization of the Catalysts .....	39
5.1.1. SO <sub>4</sub> / Ti-SBA-15 and SO <sub>4</sub> /SBA-15 Catalysts .....	39
5.1.2. SO <sub>4</sub> / TiO <sub>2</sub> -SiO <sub>2</sub> and SO <sub>4</sub> /La-TiO <sub>2</sub> -SiO <sub>2</sub> Catalysts .....	45
5.2. Activity and Stability of the Catalysts .....	51
5.2.1. Biolubricant Production from Epoxidized Soybean Oil from reactions 2-propanol Reaction.....	51
5.2.2. Biolubricant Production from Epoxidized Soybean Oil with 2-ethyl hexanol.....	59
5.3. Physicochemical Properties of the Obtained Biolubricants.....	64
CHAPTER 6. CONCLUSIONS .....	67
REFERENCES .....	68

## LIST OF FIGURES

<u>Figure</u>	<u>Page</u>
Figure 2.1. Triglyceride structure .....	5
Figure 2.2. Life Cycles of Biolubricants.....	7
Figure 2.3. Scheme of biolubricant production via esterification or transesterification.	11
Figure 2.4. Schematic representation of epoxidation and ring opening reaction .....	13
Figure 3.1. Comparison of catalytic activities of Si-12Nb, SBA <sub>RT</sub> -12Nb, SBA <sub>H</sub> 12Nb and SBA <sub>TMB</sub> -12Nb .....	16
Figure 3.2. Oleic acid conversion with 2-ethylhexanol (A) and trimethylolpropane (B) in the presence of AC, ACS1, ACS2 and ACS3 catalysts.....	17
Figure 3.3. Thermal stability of epoxidized canola oil (ECO) and ring opening reaction products BCO: n-butanol, ACO: amyl alcohol and 2-EHCO: 2-ethylhexanol .....	18
Figure 3.4. SO <sub>4</sub> /Ti-SBA-15 and Ti-SBA-15 NH <sub>3</sub> -TPD profile .....	20
Figure 3.5. Reaction mechanism of epoxy ring opening of canola oil .....	21
Figure 3.6. Schematic representation of ring opening reaction of epoxidized canola oil and epoxidized canola biodiesel .....	22
Figure 3.7. DSC curves of (A) epoxy canola oil (B) epoxy canola biodiesel, (C) biolubricant based on epoxy canola oil, (D) biolubricant based on epoxy canola biodiesel.....	22
Figure 3.8. Configuration of SO <sub>4</sub> /TiO <sub>2</sub> -SiO <sub>2</sub> catalyst.....	28
Figure 4.1 Experimental Set-up and biolubricant obtained .....	35
Figure 4.2. Removal of excess alcohol with rotary evaporator .....	35
Figure 4.3. Removal of excess alcohol with Kugel vacuum distillation .....	36
Figure 4.4. Analysis of oxirane content by titration .....	37
Figure 5.1. N <sub>2</sub> Adsorption/Desorption isotherms of SO <sub>4</sub> /SBA-15-(CS), SO <sub>4</sub> /Ti-SBA-15-10(AS), SO <sub>4</sub> /Ti-SBA-15-10(CS) and SO <sub>4</sub> /Ti-SBA-15-6(CS) catalysts .....	40
Figure 5.2. XRD patterns of Ti-SBA-15-10, SO <sub>4</sub> / Ti-SBA-15-10(AS), SO <sub>4</sub> /Ti-SBA-15-10(CS) and SO <sub>4</sub> /Ti-SBA-15-6(CS) catalysts.....	40
Figure 5.3. XRD patterns of SBA-15 and SO <sub>4</sub> / SBA-15-(CS) catalysts.....	41

<b><u>Figure</u></b>	<b><u>Page</u></b>
Figure 5.4. FTIR spectra of SO <sub>4</sub> /SBA-15-(CS), SO <sub>4</sub> /Ti-SBA-15-10(AS), SO <sub>4</sub> /Ti-SBA-15-10(CS) and SO <sub>4</sub> /Ti-SBA-15-6(CS) catalysts .....	42
Figure 5.5. NH <sub>3</sub> -TPD analysis of Ti-SBA-15-10, SO <sub>4</sub> /Ti-SBA-15-10(AS), SO <sub>4</sub> /Ti-SBA-15-10(CS) and SO <sub>4</sub> /Ti-SBA-15-6(CS) catalysts .....	43
Figure 5.6. NH <sub>3</sub> -TPD analysis of SBA-15 and CS-SO <sub>4</sub> /SBA-15 catalysts .....	44
Figure 5.7. Thermal gravimetric analysis of SO <sub>4</sub> /SBA-15-(CS), Ti-SBA-15-10, SO <sub>4</sub> /Ti-SBA-15-10(AS), SO <sub>4</sub> /Ti-SBA-15-10(CS) and SO <sub>4</sub> /Ti-SBA-15-6(CS) catalysts .....	45
Figure 5.8. N <sub>2</sub> Adsorption/Desorption isotherms of SO <sub>4</sub> /TiO <sub>2</sub> -SiO <sub>2</sub> (AS), SO <sub>4</sub> /La-TiO <sub>2</sub> -SiO <sub>2</sub> (AS) and SO <sub>4</sub> /La-TiO <sub>2</sub> -SiO <sub>2</sub> (CS) catalysts .....	46
Figure 5.9. XRD patterns of TiO <sub>2</sub> -SiO <sub>2</sub> and SO <sub>4</sub> /TiO <sub>2</sub> -SiO <sub>2</sub> (AS) catalysts .....	47
Figure 5.10. XRD patterns of La-TiO <sub>2</sub> -SiO <sub>2</sub> , SO <sub>4</sub> /La-TiO <sub>2</sub> -SiO <sub>2</sub> (AS) and SO <sub>4</sub> /La-TiO <sub>2</sub> -SiO <sub>2</sub> (CS) catalysts .....	47
Figure 5.11. FTIR spectra of SO <sub>4</sub> /TiO <sub>2</sub> -SiO <sub>2</sub> (AS), SO <sub>4</sub> /La-TiO <sub>2</sub> -SiO <sub>2</sub> (AS) and SO <sub>4</sub> /La-TiO <sub>2</sub> -SiO <sub>2</sub> (CS) catalysts .....	48
Figure 5.12. NH <sub>3</sub> -TPD analysis of TiO <sub>2</sub> -SiO <sub>2</sub> and SO <sub>4</sub> /TiO <sub>2</sub> -SiO <sub>2</sub> (AS) catalysts .....	49
Figure 5.13. NH <sub>3</sub> -TPD analysis of La-TiO <sub>2</sub> -SiO <sub>2</sub> and SO <sub>4</sub> /La-TiO <sub>2</sub> -SiO <sub>2</sub> (AS) .....	49
Figure 5.14. Thermal gravimetric analysis of TiO <sub>2</sub> -SiO <sub>2</sub> , La-TiO <sub>2</sub> -SiO <sub>2</sub> , SO <sub>4</sub> /TiO <sub>2</sub> -SiO <sub>2</sub> (AS) and SO <sub>4</sub> /La-TiO <sub>2</sub> -SiO <sub>2</sub> (AS) catalysts .....	50
Figure 5.15. Washing of SO <sub>4</sub> /Ti-SBA-15-10(CS) catalyst .....	54
Figure 5.16. FTIR spectrum of epoxidized soybean oil and product of epoxidized soybean oil ring opening reaction (Alcohol: 2-propanol, Catalysts: SO <sub>4</sub> /Ti-SBA-15-10(CS) and SO <sub>4</sub> /Ti-SBA-15-6(CS) catalysts) .....	55
Figure 5.17. HNMR spectrum of epoxidized soybean oil .....	56
Figure 5.18. HNMR spectrum of ring opening product with 2-propanol by SO <sub>4</sub> /Ti-SBA-15-10(CS) catalyst .....	57
Figure 5.19. HNMR spectrum of ring opening product with 2-propanol by SO <sub>4</sub> /Ti-SBA-15-6(CS) catalyst .....	57
Figure 5.20. Reusability of SO <sub>4</sub> /Ti-SBA-15-10(CS) and SO <sub>4</sub> /Ti-SBA-15-6(CS) in the reactions of 2-propanol .....	58
Figure 5.21. Effect of the catalyst loading on the conversion .....	59
Figure 5.22. Effect of the reaction time on the conversion .....	59

<b><u>Figure</u></b>	<b><u>Page</u></b>
Figure 5.23. FTIR spectrum of epoxidized soybean oil and product of epoxidized soybean oil ring opening reaction (Alcohol: 2-ethyl hexanol, Catalysts: SO <sub>4</sub> /Ti-SBA-15-10(CS) and SO <sub>4</sub> /Ti-SBA-15-6(CS) catalysts).....	62
Figure 5.24. HNMR spectrum of ring opening product with 2-ethyl hexanol by SO <sub>4</sub> /Ti-SBA-15-10(CS) catalyst.....	62
Figure 5.25. HNMR spectrum of ring opening product with 2-ethyl hexanol by SO <sub>4</sub> /Ti-SBA-15-6(CS) catalyst.....	63
Figure 5.26. Reusability of SO <sub>4</sub> /Ti-SBA-15-6(CS) in the reactions of 2-ethyl hexanol.	63
Figure 5.27. Effect of the reaction time on the conversion.....	64
Figure 5.28. Thermal Stability of epoxidized soybean oil and obtained products .....	65
Figure 5.29. Low temperature properties of epoxidized soybean oil and biolubricant samples produced .....	66

## LIST OF TABLES

<u>Table</u>	<u>Page</u>
Table 2.1. The fatty acid composition of most popular vegetable oils .....	6
Table 2.2. Main application of vegetable oils .....	7
Table 2.3. Psychochemical properties of commonly used vegetable oils, some commercial lubricants and ISO standarts .....	9
Table 2.4. Relationship between structure and psychochemical properties of vegetable oils .....	9
Table 2.5. Reaction parameters and results of epoxidation of vegetable oil studies.....	12
Table 3.1. Textural and acidic properties of SBA and niobium incorporated SBA catalysts prepared by different methods.....	15
Table 3.2. Surface area and sulfur content of AC, ACS1, ACS2 and ACS3.....	17
Table 3.3. Viscosity and pour point of epoxidized canola oil (ECO) and ring opening reaction products. BCO: n-butanol, ACO: amyl alcohol and 2-EHCO: 2-ethylhexanol .....	18
Table 3.4. Activity results of prepared Ti-SBA-15 catalysts and Amberlyst-15.....	19
Table 3.5. Textural properties of Ti-SBA-15 (10) and sulfated Ti-SBA-15 (10).....	19
Table 3.6. Pour point values of epoxy canola oil, epoxy canola biodiesel, biolubricant based on epoxy canola oil and biolubricant based on epoxy canola biodiesel.....	22
Table 3.7. Physicochemical properties of epoxidized canola oil and epoxidized canola biodiesel derived biolubricants.....	24
Table 3.8. BET specific surface area and total acidity of HP-SZ/Mg-SBA-15, SR-SZ/MgSBA-15 and LR-SZ/Mg-SBA-15.....	27
Table 4.1. The reagents used for experimental study .....	30
Table 5.1. Textural properties and sulphur content of SBA-15 and Ti-SBA-15 based catalysts.....	40
Table 5.2. Total acidity of SBA-15, SO <sub>4</sub> / SBA-15-(CS), Ti-SBA-15-10, SO <sub>4</sub> / Ti-SBA-15-10(AS), SO <sub>4</sub> /Ti-SBA-15-10(CS) and SO <sub>4</sub> /Ti-SBA-15-6(CS) .....	44

<b><u>Table</u></b>	<b><u>Page</u></b>
Table 5.3. Textural properties and sulphur content of La-TiO <sub>2</sub> -SiO <sub>2</sub> , TiO <sub>2</sub> -SiO <sub>2</sub> , SO <sub>4</sub> /TiO <sub>2</sub> -SiO <sub>2</sub> (AS), SO <sub>4</sub> /La-TiO <sub>2</sub> -SiO <sub>2</sub> (AS) and SO <sub>4</sub> /La-TiO <sub>2</sub> -SiO <sub>2</sub> (CS) catalysts .....	46
Table 5.4. Total acidity of La-TiO <sub>2</sub> -SiO <sub>2</sub> , TiO <sub>2</sub> -SiO <sub>2</sub> , SO <sub>4</sub> /TiO <sub>2</sub> -SiO <sub>2</sub> (AS), SO <sub>4</sub> /La-TiO <sub>2</sub> -SiO <sub>2</sub> (AS) and SO <sub>4</sub> /La-TiO <sub>2</sub> -SiO <sub>2</sub> (CS) catalysts .....	50
Table 5.5. Ring opening reaction epoxidized soybean oil with 2-propanol in the presence of Amberlyst-15 .....	51
Table 5.6. Activity and Stability of SO <sub>4</sub> /Ti-SBA-15-10(AS), SO <sub>4</sub> /La-TiO <sub>2</sub> -SiO <sub>2</sub> and SO <sub>4</sub> /TiO <sub>2</sub> -SiO <sub>2</sub> catalysts .....	52
Table 5.7. Activity and Stability of SO <sub>4</sub> /Ti-SBA-15-10(AS), SO <sub>4</sub> /Ti-SBA-15-10(CS), SO <sub>4</sub> /Ti-SBA-15-6(CS), SO <sub>4</sub> /SBA-15-(CS) with reactions of 2-propanol .....	52
Table 5.8. Activity and stability of hot filtrated SO <sub>4</sub> /Ti-SBA-15-10(CS) catalyst.....	54
Table 5.9. H-NMR spectrum peak assignment.....	56
Table 5.10. Ring opening reaction epoxidized soybean oil with 2-ethyl hexanol in the presence of Amberlyst-15 .....	60
Table 5.11. Activity and Stability of SO <sub>4</sub> /Ti-SBA-15-10(AS), SO <sub>4</sub> /Ti-SBA-15-10(CS), SO <sub>4</sub> /Ti-SBA-15-6(CS) reactions of 2-ethylhexanol .....	61
Table 5.12. Names of products obtained with more active and stable catalysts.....	64

# CHAPTER 1

## INTRODUCTION

Lubricants are essential products in the industry for protection of mechanical systems from corrosion and reduction of friction between surfaces. Global lubricant demand is increasing significantly in recent times due to fast growth of industrialization. Thereby, lubricants have an important place in the world market and Royal Dutch Shell, ExxonMobil, BP, Chevron, Sinopec, Lukoil, Total, FUCHS, Nippon Oil are the major players of lubricant market [1]. On the other hand, they are petroleum derived products and development of green and sustainable processes has gained much interest day by day because of harmful effect of petroleum products on environment. In addition, growth of world population increased global energy demand and depletion of fossil fuel reserves have started. In this context, researchers have focused on finding alternative raw materials based on renewable sources and reducing dependency on petroleum products to protect environment and overcome the energy crisis. Utilization of biomass as feedstock is a reasonable approach to solve environmental concerns and achieve sustainability objectives due to its unique features such as cost effectiveness and abundancy [2,3]. Vegetable oils are promising biomass sources and green lubricants can be obtained from them. Canola oil, soybean oil and castor oil are the most common vegetable oils that are used in the biolubricant production. They are non-toxic and they have excellent lubrication properties. However, it is not suitable to use vegetable oils directly as biolubricant since they have unsaturated bonds in their structure. Unsaturation limits good cold flow properties and high thermal stability that lubricants should have to utilize them effectively in the industry. Hence, modification of vegetable oils should be carried out to enhance their stability and low temperature properties [4].

There are various methods for the modification of vegetable oils such as esterification, transesterification and epoxidation. Epoxidation is attractive method for the elimination of unsaturation [5]. Otherwise, the reactivity of oxirane rings formed by epoxidation is quite high and they have a negative influence on low temperature

properties. Therefore, epoxidized oils should be further modified via ring opening reactions. Ring opening reactions can be performed using homogenous or heterogenous catalysts [6]. Nevertheless, homogenous catalysts cannot meet the target of green chemistry as they are corrosive, harmful on environment and non-reusable. Also, their separation is difficult and product purification requires high volumes of water. On the other hand, solid acid catalysts are advantageous due their reusability, non-corrosive nature and ease of separation and heterogeneous catalysis is a cornerstone for an ecofriendly process. Thus, there is an enormous effort to replace homogenous catalysts by heterogenous catalysts [7]. In the literature, various solid acid catalysts were used in the ring opening reaction to produce biolubricant but most study was carried out with commercial solid catalysts that have also low thermal stability [8]. Although some study tested the activity of novel heterogenous catalysts, there is limited information about their stability which has great importance for the reusability of catalyst. In this context, additional investigations should be pursued to find active and stable catalysts for the development of ecofriendly biolubricants.

The catalysts can have Brønsted acid sites or Lewis acid sites. Brønsted acid sites have proton donor properties and reaction on the Brønsted sites generally takes place via proton transfer. On the other hand, Lewis acid sites behave as an electron acceptor and reactions occur by electron transfer [9]. Studies with commercial solid acid catalysts show that Brønsted acid sites are essential in the ring opening reactions of epoxidized oil. These acid sites can be formed by the attachment of sulfate groups to the surface of the catalysts. In addition, strength and concentration of the acid sites of the catalysts are closely related with their activity. As a result, sulfation of catalysts is a crucial criterion in the reactions. Beside acidity, surface area and porosity have a significant importance and high surface area and mesopore catalysts was found as suitable for the ring opening reactions [10]. Today, many studies were performed with sulfated catalysts. Sulfated SBA-15 supported metal incorporated catalysts play an important role in the heterogenous catalysis due to their stability, high surface area and acidity. Also, in recent years mixed oxides are popular regarding their remarkable catalytic performance [11].

There are various parameters affecting during biolubricant production. Feedstock determination has great importance. Among vegetable oils, soybean oil is one of the promising options. It might be obtained cost effective way with soybean oil-based

lubricants since production capacity of soybean oil is quite high around the world. In 2021, world production capacity of soybean oil was nearly 60.4 million ton [12]. Furthermore, soybean oil has significant amount unsaturated fatty acids and this makes it a favorable feedstock for the epoxidation reaction [13]. Production of epoxidized soybean oil has increased gradually and it has become an easily accessible commercial product. In this context, it might be an attractive route to prefer epoxidized soybean oil as feedstock in the ring opening reaction for biolubricant production. Beside feedstock consideration, alcohol is also an important parameter for the ring opening reaction of epoxidized soybean oil. It has an influence on the conversion and physicochemical properties of product [14].

In this thesis study, the production of biolubricants via ring opening reaction of epoxidized soybean oil with the mesoporous solid acid catalysts is investigated. In accordance with this purpose,  $\text{SO}_4/\text{SBA-15}$ ,  $\text{SO}_4/\text{Ti-SBA-15}$ ,  $\text{SO}_4/\text{TiO}_2\text{-SiO}_2$  and  $\text{SO}_4/\text{La-TiO}_2\text{-SiO}_2$  catalysts were prepared. Effect of titanium and lanthanum incorporation on catalyst activity and properties were analyzed. In addition, the catalysts were sulphated with two different sulphate sources which are ammonium sulfate and chlorosulfonic acid in order to determine influence of sulphate source on acidity and stability of catalysts. The prepared catalysts were characterized by  $\text{N}_2$  adsorption, XRD, FTIR,  $\text{NH}_3$ -TPD and TGA. Also, stability of catalysts was studied with XRF. Reusability tests were performed for the most stable catalyst. Furthermore, ring opening reactions were performed using 2-propanol and 2-ethylhexanol to evaluate length and branching effect of alcohol.

## CHAPTER 2

### OVERVIEW OF BIOLUBRICANTS

#### 2.1 Role of Lubrication

Lubricants are crucial in all mechanical systems. Primary objective of lubrication is to reduce the friction and wear between surfaces so prevention of energy and heat losses. In addition, lubricants protect machines against to corrosion. Thus, service life of machinery and its components can be extended. In many areas of industry, lubricants are used for a variety of functions such as engine oils, chainsaw oils, transmission oils, metal and hydraulic oils [14,15]. In each application, oils have specific purposes. For instance;

- Engine oils cool the engine and clean the engine system by carrying impurities and wear particles away from the moving parts.
- Hydraulic oils are essential in the tractors, excavators, harvesters, and trucks systems. These systems need high power for movement. Hydraulic fluid serves as an interface between power and energy where the force is transmitted by the movement of the hydraulic fluid. They have low compressibility so faster rate of the pressure transfer, the better power transfer, and the higher efficiency is obtained in the systems.
- Application areas of transmission fluids are gears and transmissions in machineries or vehicles. Their thermal property is quite important due to the heat generation during the operation. They should resist to thermal stress and dissipate the heat efficiently.
- Metalworking fluids are widely used in automobiles, aerospace, and marine industries. Machining process quality is enhanced with lubrication of cutting edge via metalworking fluids. They provide the removal of chips on cutting parts and tools which can affect the process negatively [17].

The major part of the lubricant formulation is the base oils. They compose 70-99 % of lubricants. Also, additives can be added to formulation for improvement of the physical and chemical properties of the base oil. Antioxidants, anti-wear, viscosity

modifiers and pour point depressants are the most common additives. Lubricants should have high flash point, high oxidative stability and low pour point for an efficient process [15]. Beside these properties, they should show excellent tribological performances which are related about lubricity, friction and wear [18].

## 2.2 Vegetable Oils and Biolubricants

Vegetable oils are obtained from oil bearing crops via extraction and they can be classified as edible and non-edible. Soybean, canola, rapeseed, palm, olive, sunflower, and coconut oil are the most popular edible feedstocks whereas castor, jatropha, karanja oils are non-edible [14, 15]. All vegetable oils consist of triglyceride molecules. In triglyceride structure, three fatty acids are connected to a glycerol backbone by ester linkage as shown Figure 2.1. Fatty acids have larger percentage in triglycerides so fatty acids play more important role for specifying the physical and chemical properties of vegetable oils [18]. Fatty acids are straight chain aliphatic carboxylic acids and their chain length is between 12-24 carbon atoms with varying degrees of unsaturation. Vegetable oils contain saturated, monounsaturated and polyunsaturated fatty acids. There is only carbon-carbon single bond in composition of saturated fatty acids whereas monounsaturated fatty acids have one carbon-carbon double bond and polyunsaturated fatty acids include two or more carbon-carbon double bond in their back-bone structure [19]. The fatty acid composition of most popular vegetable oils and their saturation degree are given in Table 2.1. As shown in Table 2.1, castor oil has a special type of fatty acid which is ricinoleic acid and its structure contains a hydroxyl group.

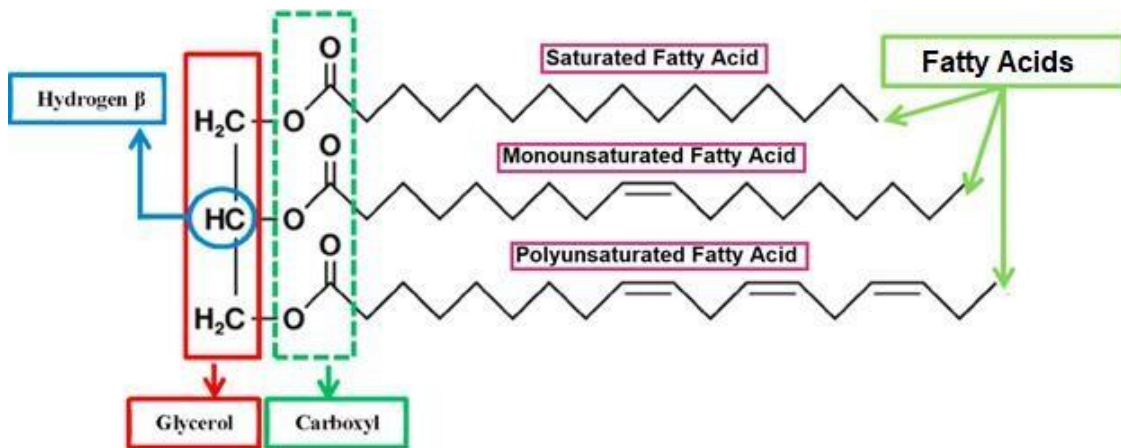


Figure 2.1. Triglyceride structure [15]

Table 2.1. The fatty acid composition of most popular vegetable oils [20]

<b>Saturation degree</b>	<b>Fatty acid composition (%)</b>	<b>Karanja oil</b>	<b>Jatropha Oil</b>	<b>Sunflower oil</b>	<b>Soybean oil</b>	<b>Rapeseed oil</b>	<b>Canola oil</b>	<b>Castor oil</b>	<b>Palm oil</b>	<b>Olive oil</b>
<b>Saturated</b>	Lauric C12:0	-	-	-	-	-	-	-	0.46	-
	Myristic C14:0		1.4						1.22	
	Palmitic C16:0	11.65	15.6	6.18	11.28	4.8	3	2.63	47.9	11.7
	Stearic C18:0	7.5	9.7	2.16	2.70	1.8	3	1.51	4.23	3.0
<b>Mono unsaturated</b>	Palmitoleic 16:1	-	-	-	-	-	-	-	-	0.8
	Oleic C18:1	51.59	40.8	26.13	24.39	62.7	60	4.74	37.0	77.9
	Ricinoleic C18:1:OH	-	-	-	-	-	-	82.80	-	-
<b>Poly unsaturated</b>	Linoleic C18:2	16.64	32.1	65.52	56.28	19.5	30	8.36	9.07	7.2
	Linolenic C18:3	-	-	-	5.34	8.6	7	-	0.26	-

Vegetable oils are ecofriendly, inexpensive and non-toxic biomass feedstocks. They are attractive sources due to their worldwide availability, competitive cost, renewability and inherent structure. In this context, today there has been an increasing interest in the usage of vegetable oils for the production of various chemicals. Table 2.2 shows main application of vegetable oils. For instance, lubricants can be derived from vegetable oils which are called as biolubricant. Biolubricants are promising alternatives to petroleum-based lubricants since they can provide green and sustainable process as shown Figure 2.2 and biolubricant market is expected to rise about 15-30% in the near future of 15-20 years [14, 18].

Table 2.2. Main application of vegetable oils [8]

Vegetable Oil	Main Applications
Soybean oil	Engine oils, hydraulic oils, transmission fluids, chainsaw oils, biodiesel fuel, paints, printing inks, coatings, detergents, shampoos, pesticides
Canola oil	Transmission fluids, hydraulic fluids, penetrating oils, metal-working fluids, food-grade lubes
Rapeseed oil	Greases, hydraulic fluids, chainsaw oils
Castor oil	Greases, gear lubricants
Palm oil	Greases, metal-working fluids
Olive oil	Engine oils
Sunflower oil	Greases, diesel fuels

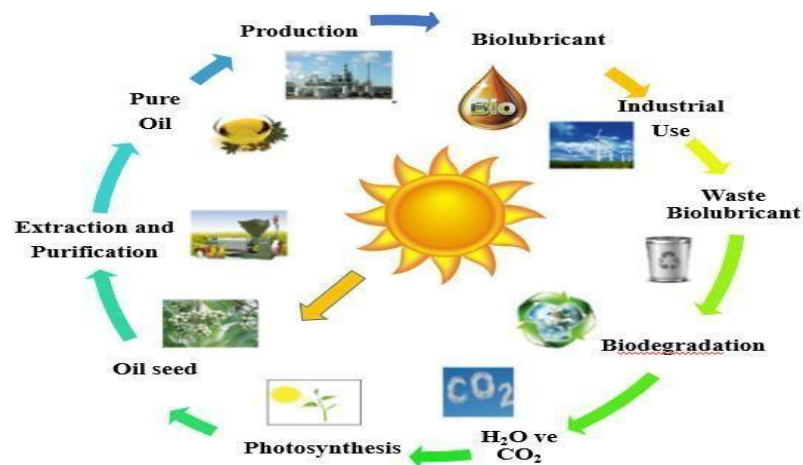


Figure 2.2. Life Cycles of Biolubricants [21]

The utilization of vegetable oils as a lubricant has many advantages. Biolubricants have higher flash point and viscosity index than petroleum-based lubricants. Flash point is the minimum temperature at which the vapor over oil sample will instantaneously ignite when exposed to an ignition source and viscosity index is the viscosity change of sample with temperature. High viscosity index implies the slight variance in the viscosity regarding in temperature change. Thus, biolubricants can provide safer operation and are more useful in wide temperature range due to their high viscosity index and flash point. In addition, vegetable oils show excellent boundary lubrication properties due to the polar group with a long hydrocarbon chain in their triglyceride structure. Strong lubricating film on the metallic surfaces forms so wear and friction reduces significantly [22]. Psychochemical properties of commonly used vegetable oils, some commercial lubricants and ISO standards is given Table 2.3. As it was stated flash point and viscosity index of vegetable oils are more favorable than petroleum based commercial lubricants. In addition, they satisfy ISO standards requirement for viscosity index and flash point.

On the other hand, direct usage of vegetable oil as biolubricant is limited in industrial application because of some disadvantages [16]. Oxidative and thermal stability of vegetable oils are quite low due to reactivity of unsaturated fatty acids. Low oxidation stability demonstrates that lubricant can oxidize rapidly. Oxidation is undesired situation because it causes degradation and polymerization of lubricant. Consequently, functionality of lubricant decreases. Lubricants should have high oxidation stability for longer service life. Otherwise, presence of saturated fatty acids causes high pour point. Pour point is the lowest temperature at which the lubricant becomes semi-solid and loses its flow characteristics. As shown Table 2.3, vegetable oils provide ISO standards of pour point however commercial lubricants are more favorable regarding their lower pour point. When the pour point is not low enough, lubricant cannot flow properly and so equipment can be damaged owing to excessive friction, wear and heat in the system. Furthermore, hydrogen  $\beta$  in the glycerol part is not stable. It can be easily removed from the molecular structure and undesired products can be formed. As result there is strong relationship between structure and psychochemical properties of triglyceride as shown Table 2.4. The shortcomings of vegetable oils can be eliminated via chemical modification.

There are various methods for enhancement of psychochemical properties. Esterification, transesterification, epoxidation are the most common techniques for chemical modification [20]. They are explained with details in the next section.

Table 2.3. Psychochemical properties of commonly used vegetable oils, some commercial lubricants and ISO standarts [8]

	Kinematic Viscosity at 40 °C (cst)	Kinematic Viscosity at 100 °C (cst)	Viscosity index	Pour Point (°C)	Flash Point (°C)
<b>Vegetable Oils</b>					
Soybean oil	28.86	7.55	246	-9	325
Rapeseed oil	45.60	10.07	180	-12	252
Castor oil	220.6	19.72	220	-27	250
Palm oil	52.4	10.2	186	-5	267
<b>ISO Standards</b>					
ISO VG32	>28.8	>4.1	>90	-6	204
ISO VG46	>41.4	>4.1	>90	-6	220
ISO VG68	>61.4	>4.1	>198	-6	226
<b>Commercial Lubricants (petroleum based)</b>					
SAE 20W-40	105	13.9	132	-21	200
AG100	216	19.6	103	-18	244

Table 2.4. Relationship between structure and psychochemical properties of vegetable Oils [17, 19]

	Viscosity index	Kinematic viscosity	Pour Point	Oxidative stability	Tribofilm Adhesion
Chain length ↑	+	+	- *	-	No effect
Chain branching ↑	-	+	+	+	-
Degree of unsaturation ↑	+	-	+	-	-

(+: positive effect, -: negative effect, \*: except molecules with steric hindrance)

## 2.3 Modification of Vegetable Oils

### 2.3.1 Esterification and Transesterification

Acyl moieties in vegetable oils can be modified via esterification or transesterification. Both reactions consist of two steps to obtain biolubricant with enhanced physical properties [16]. A schematic representation of biolubricant production via esterification or transesterification is given in Figure 2.3. In esterification reaction, firstly vegetable oils are hydrolyzed to obtain free fatty acids. Then, free fatty acids are reacted with an alcohol to form their respective esters [8]. On the other hand, in the first step of transesterification, fatty acid methyl esters (FAMES) are synthesized as a result of reaction between triglyceride and a short chain alcohol (in general methanol) in the presence of base catalyst (in general KOH). After that, FAMES are reacted with various types of alcohol such as Trimethylolpropane (TMP), Neopentyl glycol (NPG), and Pentaerythritol (PET). TMP is cheaper and it can react at lower temperature. In this context, TMP is generally preferred over other alcohols since it can decrease the cost of process. During the transesterification, glycerol is the side product of first step and methanol is the side product of second step. Transesterification is an effective approach for the elimination of unstable hydrogen atom in the  $\beta$  position in the glycerol molecule [15].

In general, homogenous acid catalysts such as HCl, H<sub>2</sub>SO<sub>4</sub> and p-toluensulfonic acid, are used in esterification reactions. However, they are corrosive, harmful on environment and separated hardly. Therefore, development solid acid catalysts showed much interest in recent times [8]. Transesterification can be performed with acidic or basic catalyst. However, acid-catalyzed reaction is roughly 4000 times slower so base catalysts are more effective. Calcium oxide, sodium and calcium methoxide, sodium and potassium hydroxide and potassium carbonate are the most popular base catalysts for the transesterification [22].

Physical properties of products are closely related with alcohols used in the reaction. In addition, temperature of the reaction, catalyst, alcohol to oil molar ratio and amount of catalyst have significant effect for the esterification and transesterification [22]. Various studies carried out in recent times which will be given in the Chapter 3.

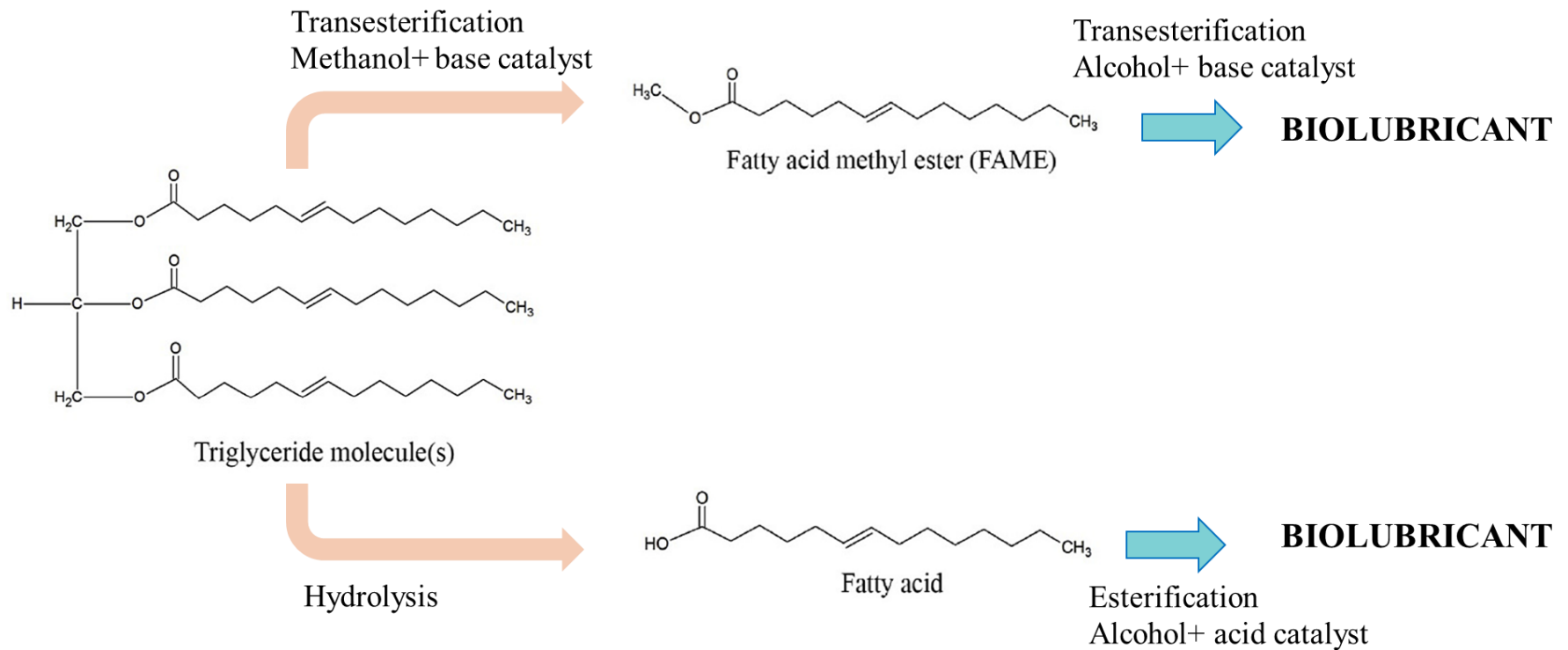


Figure 2.3. Scheme of biolubricant production via esterification or transesterification [17]

## 2.3.2 Epoxidation and Ring Opening Reactions

Unsaturated fatty acids in structure of vegetable oils have a negative effect for the oxidative stability. Double bonds between two carbons can be converted into epoxide groups via epoxidation reaction. Epoxides are cyclic ethers which consist of two carbon atoms and an oxygen atom and they can be also called as oxirane rings. In the reaction, peracids are used as oxidizing agent. In general, they are produced in situ via reaction of acetic or formic acid with hydrogen peroxide in the presence of homogenous or heterogenous catalysts [23]. Amberlite IR-120H is one of the widely used heterogenous catalyst for the epoxidation reaction and it is preferred over homogenous catalysts to achieve an ecofriendly process. Ratio of ethylenic unsaturation to per carboxylic acids, temperature and catalyst concentration are important parameters. Also, addition period of H<sub>2</sub>O<sub>2</sub> has significant impact for the reaction. It should be added slowly for prevention of side reaction and overheating of reactor [22]. Furthermore, reaction is generally carried out at moderate temperatures which is more favorable for the systems. Table 2.5 shows that various epoxidation studies.

Table 2.5. Reaction parameters and results of epoxidation of vegetable oil studies

Oil	Acid	H <sub>2</sub> O <sub>2</sub> concentration	Ethylene unsaturation: Acid:H <sub>2</sub> O <sub>2</sub>	Catalyst	Reaction Condition	Yield	Reference
Castor Biodiesel	Acetic acid	50%	1:0.5:1.5	Amberlite IR-120	60°C, 10 h 1000-1100 rpm	96%	[24]
Canola	Acetic acid	30%	1:0.5:1.5	Amberlite IR-120	65°C,	90%	[25]
Canola	Acetic acid	50%	1:0.5:2	Amberlite IR-120	75° C, 5.5 h	93%	[26]
Rice bran	Formic acid	30%	1:0.5:1.5	H <sub>2</sub> SO <sub>4</sub> , 3%	60° C, 6 h, 1600 rpm	92%	[27]
Canola	Acetic acid	30%	1:0.5:1.5	Amberlite IR-120	65° C, 8 h	-	[19]
Canola Biodiesel	Acetic acid	30%	1:0.5:1.5	Amberlite IR-120	65° C, 8 h	-	[28]
Canola	Acetic acid	30%	1:0.5:1.5	Amberlite IR-120	65° C, 8 h	-	[29]

Epoxidation is an effective approach for the improvement of lubricity, thermal and oxidative stability. Beside these advantages, pour point and viscosity index are affected adversely because of high reactivity of oxirane rings. Therefore, the

epoxidation reaction is followed by combination of oxirane ring opening, esterification, and/or acetylation. Ring opening reactions are performed with various linear or branched alcohols and one of the C–O bonds is cleaved. As a result, different functional groups are introduced to the structure which has great influence for properties of lubricant [23]. A schematic representation of epoxidation and ring opening reaction is given in Figure 2.4. There are many studies for improvement of epoxidized product properties with various feedstocks, catalysts and reaction parameters. They are analyzed in details in literature survey part (Chapter 3).

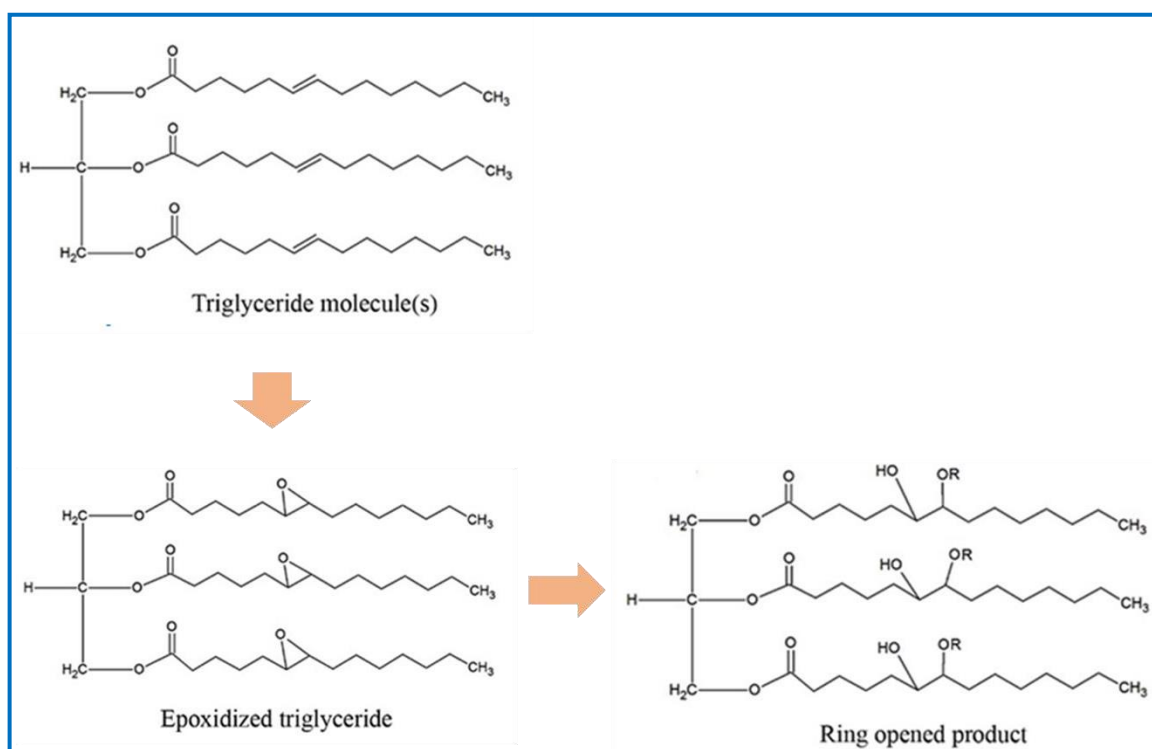


Figure 2.4. Schematic representation of epoxidation and ring opening reaction [17]

## CHAPTER 3

### LITERATURE STUDIES ON BIOLUBRICANT PRODUCTION

Esterification, transesterification and epoxidation are commonly carried out for biolubricant production. In the literature, many studies were performed with homogenous or heterogenous catalyst. Conventional mineral acids such as  $H_2SO_4$ , p-toluenesulfonic acid, HCl,  $HNO_3$  provides high catalytic activity in short reaction times and they are mostly used in industrial application. However, homogenous acid catalysts have several disadvantages. They are corrosive and harmful on environment. Also, high volume of water is required for product purification. In this context, heterogeneous catalyst can be promising alternative due to their ease of separation, reusability and ecofriendly feature. Thus, there are many investigations on using heterogeneous catalysts.

Saboya et al. (2017) used cationic exchange resins in esterification reaction between free fatty acids of castor oil and 2-ethylhexanol. The reaction was carried out at 120 °C with 5 % catalyst loading. Three cationic exchange resins (PD206, CT269DR and CT275DR) which have different psychochemical properties, were compared in the reactions. The results showed that macroreticular-type resins (CT269DR and CT275DR) have better catalytic activity than gel-type resin (PD206). Macroreticular-type resins provided 95 % conversion after 4 h whereas gel type resin provided 72 %. Better catalytic activity of the macroreticular resins was attributed to their higher surface area and existence of larger amount of Brönsted sites on their surface. The obtained biolubricant exhibited good psychochemical properties. Pour point and viscosity index was found as -39 °C and 132, respectively. Also, oxidative stability is improved from 3600 h to 5000 h [30]. In another study, Saboya et al. (2017) compared Amberlyst-15, Dowex 50W-X8 and Purolite-CT275DR catalysts and they found that Amberlyst-15 had the highest sulfur content and surface area so it was found as the most active catalyst which showed 90 % conversion after 1 h and 100 % after 4 h of reaction [31].

Sancho et al. (2017) analyzed the activity of niobium oxide supported on SBA-15 acid catalysts in the esterification of free fatty acid of castor oil with 2-ethyl hexanol for biolubricant production. Reaction was carried out at 120 °C with 10 % catalyst loading.

Effect of synthesis method of mesoporous SBA-15 silica and niobium oxide loading was evaluated. Mesoporous SBA-15 silica was synthesized with three different procedures. In one of them, it was prepared at room temperature. In another procedure, hydrothermal synthesis was applied. In latter case, 1,3,5-trimethylbenzene (TMB) was used as swelling agent. They were denoted as  $SBA_{RT}$ ,  $SBA_{HT}$  and  $SBA_{TMB}$ , respectively. These different preparation methods affected the pore size of catalyst as shown Table 3.1. Addition of swelling agent 1,3,5-trimethylbenzene (TMB) increased significantly pore volume and pore size of catalyst since it decreased the microporosity. Also, incorporation of niobium oxide to the prepared SBA-15 were carried out via incipient wetness impregnation of niobium oxalate. Niobium oxide loading caused a reduction in the surface area, pore volume and pore size. It was attributed to blocking of the micropores by the niobium oxide particles. Furthermore, it was noticed that  $SBA_{RT}$ ,  $SBA_{HT}$ ,  $SBA_{TMB}$  catalysts had no acidity whereas niobium oxide incorporation improved their acidity and the highest amount of acid sites existed in the  $SBA_{RT-12Nb}$  [32].

Table 3.1. Textural and acidic properties of SBA and niobium incorporated SBA catalysts prepared by different methods [32].

Catalyst	$S_{BET}$ ( $m^2 g^{-1}$ )	$V_P$ ( $cm^3 g^{-1}$ )	Pore size(nm)	Acidity ( $\mu moles NH_3/ g cat$ )
$SBA_{RT}$	636	0.4	3.6	-
$SBA_{HT}$	430	1.0	8.8	-
$SBA_{TMB}$	460	2.7	19.4	-
$SBA_{RT-12Nb}$	439	0.3	3.5	309
$SBA_{HT-12Nb}$	333	0.8	8.5	165
$SBA_{TMB-12Nb}$	343	1.2	16.3	138

Activity of different supports and commercial silica with 12% niobium oxide loading was compared. Commercial silica (Si-12Nb) showed considerably low activity because it had no intrinsic porosity. Although the most acidic catalyst was  $SBA_{RT-12Nb}$ , the highest conversion was obtained when SBA-15 synthesized via hydrothermal treatment ( $SBA_{HT-12Nb}$ ) as shown Figure 3.1. This catalytic result was attributed to difference in pore size of supports. Pore size of  $SBA_{RT-12Nb}$  was found as narrow to access of free fatty acid molecules to the active sites located inside the pores. On the other

hand, pore size of SBATMB-12Nb was observed as quite large for the interaction of free fatty acid molecules and alcohol molecules with active sites. As a result, it was concluded that pore size affected the catalytic activity. In addition, niobium oxide loading was varied between 2 and 16wt%. 12 wt% Nb<sub>2</sub>O<sub>5</sub> loading provided the highest conversion [32].

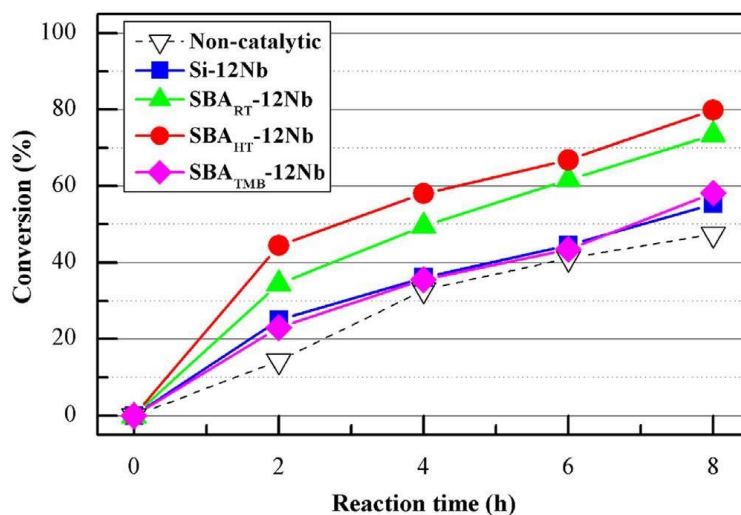


Figure 3.1. Comparison of catalytic activities of Si-12Nb, SBA<sub>RT</sub>-12Nb, SBA<sub>HT</sub>-12Nb and SBA<sub>TMB</sub>-12Nb [32]

Ferria et al. (2020) investigated sulfonation method of catalyst for the biolubricant production. For this purpose, they sulfated commercial activated carbon under different condition and tested their activity in the esterification of oleic acid with 2-ethylhexanol and trimethylolpropane at 90 °C. 5 g activated carbon samples were sulfated with 50 mL concentrated sulfuric acid under reflux at 100 °C, 150 °C and 200 °C for 5 h. Then, they were washed with deionized water several times up to reach neutral pH and they were dried at 110 °C for 24 h. Finally, they were labeled as ACS1, ACS2 and ACS3, respectively. Sulfation at different temperatures affected the sulfur content of catalysts. As shown Table 3.2, the highest sulfur content was obtained with ACS1. Moreover, surface area of commercial activated carbon (AC) and prepared catalysts were investigated. Sulfuric acid treatment resulted a decrease in the surface area of ACS1 and ACS3 and it was observed that this decrease was more pronounced for the ACS1 as more sulfate groups were attached to ACS1. All catalyst showed better catalytic activity than commercial activated carbon however catalytic performance of ACS1 was higher than ACS2 and ACS3 due to its more enhanced sulfur content (see Figure 3.2). In addition, almost 100 % conversion was achieved in the presence of 2-ethylhexanol whereas

the conversion was just 70 % was with trimethylolpropane. This was attributed to steric effect and lower nucleophilicity of the alcohol [33].

Table 3.2. Surface area and sulfur content of AC, ACS1, ACS2 and ACS3 catalysts [33]

	AC	ACS1	ACS2	ACS3
$S_{BET}$ ( $m^2 g^{-1}$ )	931	714	954	869
Atomic percentage of S (%)	-	0.36	0.17	0.20

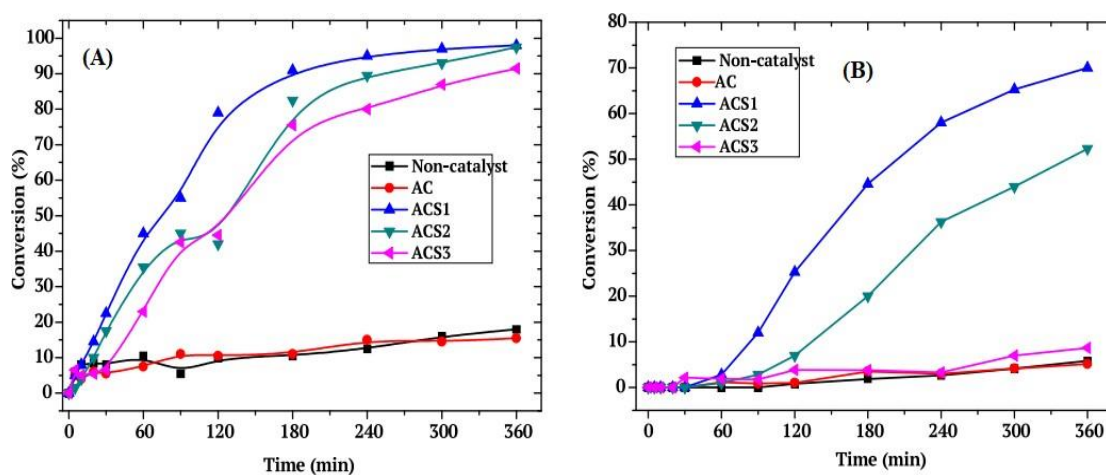


Figure 3.2. Oleic acid conversion with 2-ethylhexanol (A) and trimethylolpropane (B) in the presence of AC, ACS1, ACS2 and ACS3 catalysts [33]

In the study performed by Borugadda et al. (2014) castor oil fatty acid methyl esters were epoxidized using Amberlite IR 120 catalyst at 60 °C for 10 h. Thereby, unsaturated double bonds were completely converted into oxirane rings and it was confirmed with FTIR and NMR analysis. Removal of unsaturated part enhanced the thermal and oxidative stability of the oil. Castor oil fatty acid methyl ester was thermally stable up to 203 °C whereas epoxidized castor oil fatty acid methyl ester was found as thermally stable up to 340 °C. However, pour point (8 °C) was found as quite high and it was concluded that epoxidized oil should be further modified [24].

Madankar et al. (2013) studied the ring opening reaction of epoxidized canola oil with different alcohols over Amberlyst-15 catalyst to develop an ecofriendly alternative for lubricant formulation. Ring opening reactions were performed at 100 °C for 15 h using amyl alcohol, n-butanol and 2-ethylhexanol. Complete epoxide conversion was obtained with all alcohols however product of ring opening reaction of epoxidized canola oil (ECO) with n-butanol (BCO), amyl alcohol (ACO) and 2-ethyl hexanol (2-

EHCO) showed different psychochemical properties. Higher viscosity was observed with shorter alcohols. Product of ring opening reaction with n-butanol demonstrated the highest kinematic viscosity (251.7 mm<sup>2</sup>/s). It was attributed to polar structure of n-butanol which provides stronger intermolecular bonds. Furthermore, the lowest pour point (-15) and the highest thermal stability were obtained with 2-EHCO as shown Table 3.3 and Figure 3.3. It was found that large branching is favored for lower pour point. Because, it results a steric barrier and prevents the crystallization so pour point is improved significantly [29].

Table 3.3. Viscosity and pour point of epoxidized canola oil (ECO) and ring opening reaction products. BCO: n-butanol, ACO: amyl alcohol and 2-EHCO: 2-ethylhexanol [29]

Product	Kinematic viscosity at 40 °C (mm <sup>2</sup> s <sup>-1</sup> )	Pour point (°C)
ECO	151	10
BCO	251.7	-5
ACO	190.5	-8
EHCO	85.5	-15

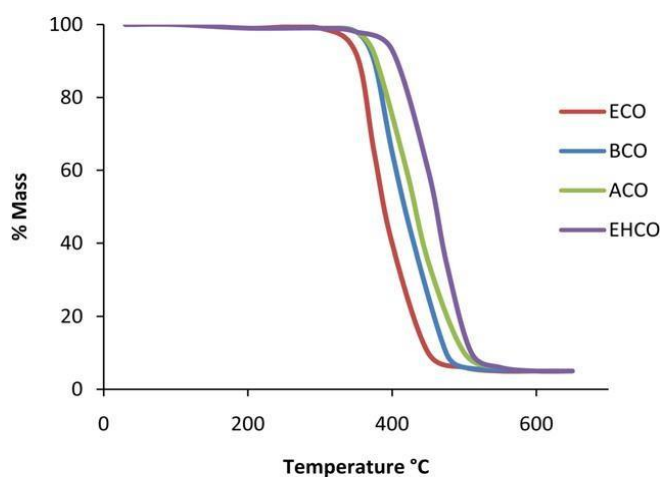


Figure 3.3. Thermal stability of epoxidized canola oil (ECO) and ring opening reaction products BCO: n-butanol, ACO: amyl alcohol and 2-EHCO: 2-ethylhexanol [29]

Sharma et al. (2013) tested activity of sulfated Ti-SBA-15 solid acid catalyst for the ring opening reaction of epoxidized canola oil with acetic anhydride and chlorosulfonic acid was used for the sulfation of Ti-SBA-15. The catalyst was prepared by sol-gel method and then it was calcined at 550 °C for 6 h. For the sulfation, it was

mixed with chlorosulfonic acid in methylene dichloride (1 g catalyst/ 15 mL, 0.5 M chlorosulfonic acid solution). After, it was calcined at 550 °C for 3 h. First of all, they compared catalytic activity of Ti-SBA-15 with various Si/Ti ratios (10, 20, 40 and 80). Catalysts showed better activity with increasing of titanium content since higher titanium content provided enhanced acidity to the catalyst. Furthermore, it was observed that sulfation of the catalysts had significant effect on improvement of conversion. Also, authors found that sulfated Ti-SBA-15 (10) was more active than commercial catalyst Amberlyst-15 [10]. Catalytic results are given in Table 3.4. Sulfated Ti-SBA-15 (10) catalyst was characterized in details and its textural properties are given in Table 3.5. The catalyst had mesopore structure and large surface area. Sulfation of Ti-SBA-15 (10) decreased its surface area since sulfate linkage was formed.

Table 3.4. Activity results of prepared Ti-SBA-15 catalysts and Amberlyst-15 [10]

Catalysts	Conversion (%)
Ti-SBA-15 (80)	11
Ti-SBA-15 (40)	19
Ti-SBA-15 (20)	26
Ti-SBA-15 (10)	32
Sulfated Ti-SBA-15 (10)	100
Amberlyst-15	55

Table 3.5. Textural properties of Ti-SBA-15 (10) and sulfated Ti-SBA-15 (10) [10]

Catalyst	$S_{BET}$ (m <sup>2</sup> /g)	$d_p$ (nm)	$V_p$ (cm <sup>3</sup> /g)
Ti-SBA-15 (10)	993	5.5	1.36
Sulfated Ti-SBA-15 (10)	594	6.6	0.99

$V_p$ , pore volume determined by nitrogen adsorption at a relative pressure of 0.98;  $d_p$ , mesopore diameter corresponding to the maximum of the pore size distribution obtained from the adsorption isotherm by the BJH method

Acidities of  $SO_4/Ti-SBA-15$  (10) and Ti-SBA-15 (10) were determined by  $NH_3$ -TPD analysis and the results are given in Figure 3.4. After chlorosulfonic acid treatment,  $SO_4/Ti-SBA-15$  showed a broad peak that indicated improvement of the catalyst acidity.

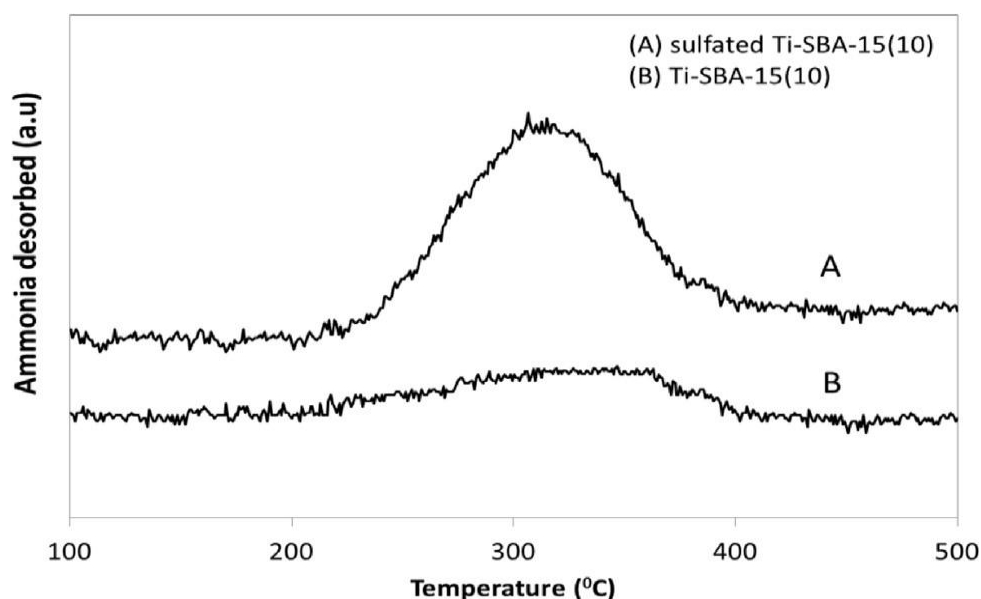


Figure 3.4. SO<sub>4</sub>/Ti-SBA-15 and Ti-SBA-15 NH<sub>3</sub>-TPD profile [10].

Besides catalysts comparison, parametric study was performed to investigate the effect of reaction conditions. For this purpose, the reactions were carried out between 100-130 °C with 0-20 % catalyst loading. In addition, stirring rate was varied from 600 rpm to 1200rpm. Optimum reaction conditions were found as 130 °C with 1000 rpm agitation speed and 10 wt.% catalyst loading. No effect was observed with further increase amount of catalyst and stirring rate whereas 140 °C and higher temperatures caused the polymerization in the reaction. Also, acetic anhydride amount (1.5, 2.25, 3 and 4 wt% of epoxy canola oil) was analyzed. The suitable amount of acetic anhydride was found as 1.5 wt% of epoxy canola oil and increasing amount of acetic anhydride had a negative effect on conversion which may be due to adsorption of acetic anhydride on the catalyst's active sites. Improved tribological properties were obtained with these reaction conditions. Oxidative stability increased from 0.6 h to 56.1 h and pour point of biolubricant was found as -9 °C. Furthermore, reaction mechanism was analyzed and it was found that ring opening reaction of epoxidized canola oil followed Langmuir–Hinshelwood–Hougen–Watson (LHHW) type mechanism [10]. Its schematic representation is given in Figure 3.5. Firstly, the active sites of the catalyst adsorbed the epoxy canola oil and acetic anhydride and then mono acylated intermediate product formed by nucleophilic attack of epoxy groups to acetic anhydride. Finally, diacylated product produced and it desorbed from the catalyst.

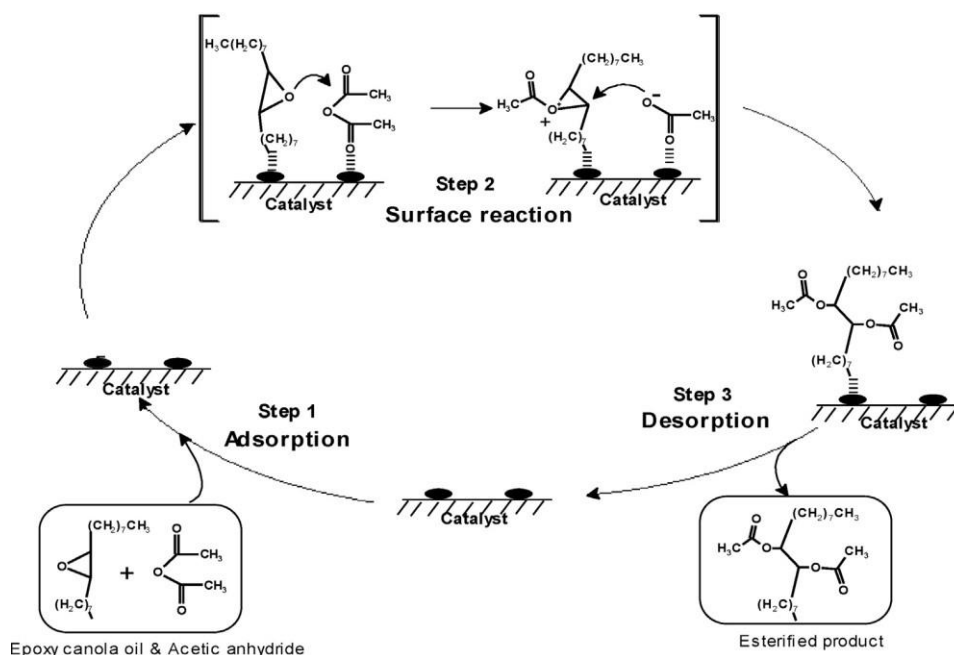


Figure 3.5. Reaction mechanism of epoxy ring opening of canola oil [10]

A ring opening reaction of epoxidized canola oil and epoxidized canola biodiesel with Acetic Anhydride using Amberlyst-15 was performed by Sharma et al. (2015). Reaction scheme and reaction condition are given in the Figure 3.6. Complete epoxide conversion was obtained and biolubricants showed good psychochemical properties. Pour point values are given in the Table 3.6 and lower pour point were obtained for biolubricant based on epoxy canola biodiesel due to fewer aliphatic carbon in their structure. Low temperature properties were further confirmed with differential scanning calorimetry (DSC) analysis. As shown Figure 3.7, exothermic crystallization peaks were observed at  $-7$ ,  $-12$  and  $-118$  °C for the epoxy canola oil, epoxy canola biodiesel and biolubricant based on epoxy canola oil, respectively. There was no peak for the biolubricant based on epoxy canola biodiesel between the  $0$ - $140$  °C that indicates the its more advanced low temperature properties. Otherwise, biolubricant based on epoxy canola oil and epoxy canola biodiesel were found as thermally stable up to  $309$  °C and  $194$  °C, respectively. Epoxy canola oil biolubricant showed higher thermal stability which might be due to the existence of intra molecular hydrogen bonding. As a result, it was concluded that canola oil based biolubricants are more effective for high temperature application whereas canola biodiesel-based lubricants are more useful for low temperature application [28].

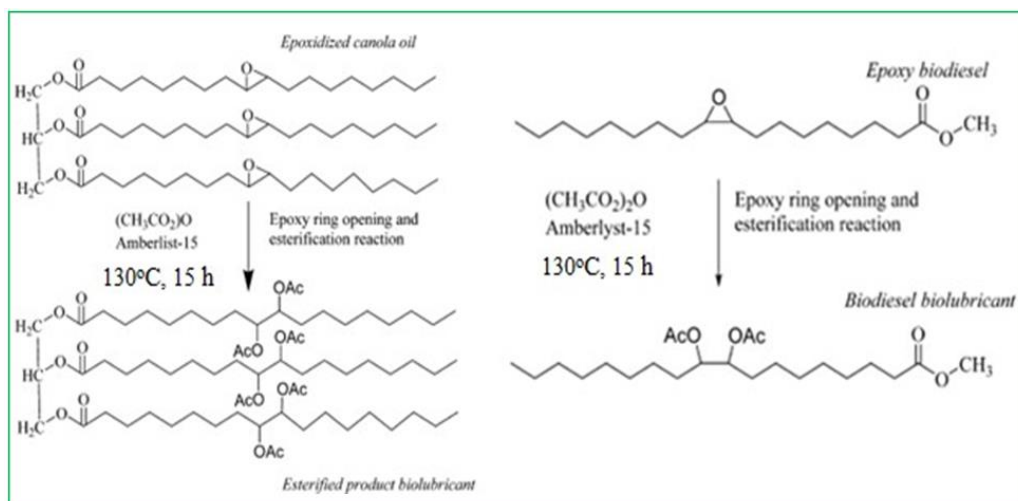


Figure 3.6. Schematic representation of ring opening reaction of epoxidized canola oil and epoxidized canola biodiesel [28]

Table 3.6. Pour point values of epoxy canola oil, epoxy canola biodiesel, biolubricant based on epoxy canola oil and biolubricant based on epoxy canola biodiesel [28]

	Epoxy canola oil	Epoxy canola Biodiesel	Biolubricant from epoxy canola oil	Biolubricant from epoxy canola biodiesel
pour point ( $^\circ\text{C}$ )	9	0	-9	-18

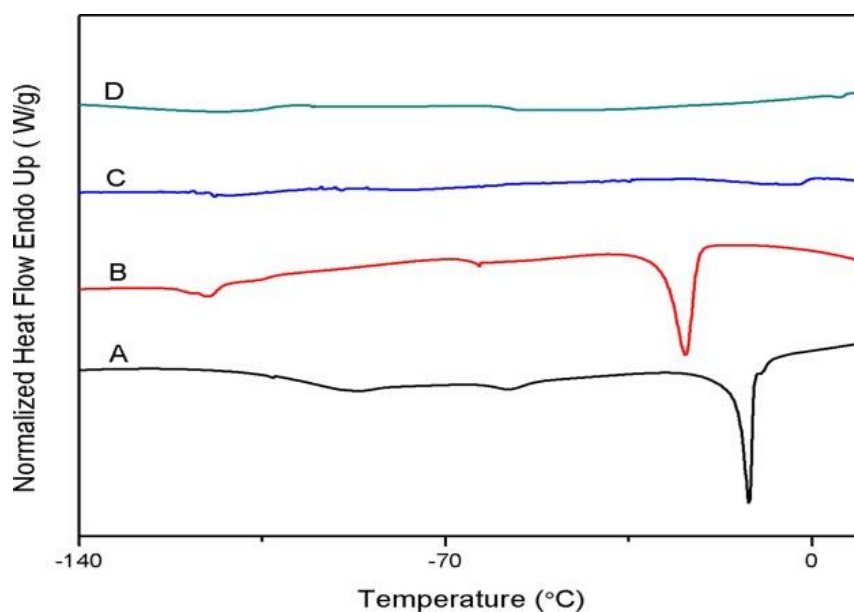


Figure 3.7. DSC curves of (A) epoxy canola oil (B) epoxy canola biodiesel, (C) biolubricant based on epoxy canola oil, (D) biolubricant based on epoxy canola biodiesel [28]

A illustrative study on the optimization of reaction condition for ring opening reaction of epoxidized canola oil methyl ester with 2-ethyl hexanol was pursued by Ren et al. (2015). Reactions were carried out using Amberlyst D001 (dry) catalyst. Amberlyst D001 is strong-acid cation-exchange resin that has macroporous structure. First of all, reactions were carried out between 60 °C and 100 °C for 18 h. It was found that 90 °C was optimum condition for complete epoxide conversion and it was determined that there was negligible effect of higher temperatures. Also, the catalyst amount was varied from 2 wt.% to 10 wt.% and 7 wt.% catalyst amount was observed as optimum for the reaction. Furthermore, 4/1, 5/1 and 6/1 2-Ethyl hexanol/oil molar ratio were investigated. It was noted that 4/1 2-Ethyl hexanol/oil molar ratio was suitable for the reaction since higher amounts showed no influence on the conversion. In this reaction condition, pour point was improved from 0 to -10 °C [34].

Borugadda et al. (2017) investigated ring opening reaction of epoxidized canola oil and epoxidized canola biodiesel in the presence of montmorillonite catalyst using 2- propanol and tert-butanol. Montmorillonite (K<sub>10</sub>) is a type of commercial silicates based heterogenous catalyst and it has strong Brønsted acid sites. Reaction was carried out with 6/1 epoxide to alcohol mol ratio and 10 wt.% catalyst loading at 90 °C for 6 h with 2- propanol and 8 h with tert-butanol to achieve of complete epoxide conversion. Table 3.7 shows that viscosity of ring opening product of epoxidized canola oil was higher than ring opening product of epoxidized canola biodiesel due to the existence of glycerol molecule in epoxidized canola oil. All products demonstrated higher viscosity index than 90 so they met the requirement of ISO standards. In addition, lubricity characteristics of products analyzed according to wear scar diameter. The obtained products were mixed with standard diesel fuel which has 600 µm wear scar diameter. As shown below, obtained lubricant provided great lubricity to standard diesel fuel and wear scar diameter decreased significantly since chain length increased via alkoxylation and strong chemical and physical adsorption on the contact surface were formed that reduced friction. Alkoxy derivatives of epoxidized canola biodiesel had lower wear scar diameter owing to their ester functionalities that stick to metal surface and provide an anti-frictional film. Also, they were less viscous and less non-polar due to their lower number of aliphatic carbons. Thus, their solubility was higher in the standard diesel fuel and they showed better lubricity properties. Furthermore, better pour point values were obtained from the ring opening reaction of epoxidized canola biodiesel. However, there was no comment about this result [35].

Table 3.7. Physicochemical properties of epoxidized canola oil and epoxidized canola biodiesel derived biolubricants [35]

Property	PCOB	BCOB	PCBB	BCBB
Viscosity (40°C, cst)	1822.22	661.23	21.49	18
Viscosity (100°C, cst)	102	45	4.79	4.2
Viscosity Index	135	115	150	142
Wear Scar diameter (µm)	142	154	112	127
Pour Point (°C)	8	2	-21	-7

**PCOB**: propylated canola oil biolubricant, **BCOB**:butylated canola oil biolubricant, **PCBB**:propylated canola biodiesel biolubricant, **BCBB**:butylated canola biodiesel biolubricant

Turco et al. (2017) compared various alcohols which were methanol, ethanol, 2-propanol and 2-butanol using SAC-13 catalyst in the ring opening reaction of epoxidized soybean oil. SAC-13 is strongly acidic resin catalyst and its pore size is above 10 nm. The reactions were performed at 80 °C with 10 wt% catalyst loading for 6 h. It was reported that ring opening product with 2-butanol provided the highest kinematic viscosity (about 600 mm<sup>2</sup>s<sup>-1</sup>) due its branched structure which can be an attractive alternative for renewable lubricant formulation. Also, powder and pellet form of catalyst were compared in the reactions. 100 % and 27.1 % conversions were obtained with the powder and pellet forms of catalyst, respectively. Lower activity of pellet form was attributed to difference of mass transfer phenomenon takes place in the liquid-solid film or for intraparticle diffusion. It had an influence on internal diffusion and caused a lower kinetic behavior of pellet form [36].

### 3.1. Assessments of Literature Studies

Literature studies show that biolubricant can be produced in the presence of different alcohols and solid acid catalysts. It was observed that promising physicochemical biolubricant properties could be obtained via esterification. On the other hand, elimination of double bonds via epoxidation, which are one of the major drawbacks of vegetable oils and cause poor stability, was found as an effective approach for improvement of the thermal stability. However, it was observed that it is required to further optimize epoxidized oil to improve low temperature properties of lubricant and

studies was concentrated on ring opening reaction of epoxidized oil.

Although many studies were performed, it was found that heterogenous catalyst studies were limited with commercial solid acid catalysts such as Amberlyst-15, SAC-13. It is noticed that there is lack of studies about development of heterogenous catalysts for ring opening reactions in the literature. In addition, catalytic activity is closely related with textural and acidic properties of catalysts as shown in studies of Sancho et al. (2017) and Sharma et al. (2013). However, it was not given any information relating results to catalyst properties in the other studies that was investigated above.

Furthermore, reusability and stability are crucial parameters for an heterogenous catalyst but roughly investigations were carried out regarding catalyst reusability. In this context, development of solid acid catalysts for ring opening reactions and their characterization results will provide valuable research to the literature and an important insight for achievement of green chemistry objective. Therefore, in this study it is proposed to develop active, selective and reusable heterogeneous catalysts for the biolubricant production and it is aimed to characterize catalysts properties.

Studies also showed that catalysts should have Brønsted acid sites, mesopore structure and high surface area for an effective catalytic activity in the ring opening reactions. In this context, various catalyst research studies were analyzed. Recent studies showed that mesoporous silica such as SBA-15 could be an attractive alternative due to its inherent features. Its hydrothermal stability is high and surface area is large. Also, it possesses well-ordered hexagonal mesoporous structure. On the other hand, their surface acidity is quite weak. However, researchers reported that it can be modified via incorporation of transition metals [37]. Chen et al. (2013) obtained high quality biodiesel with Ti-SBA-15 catalyst [38] and Chirra et al. (2021) reported that incorporation Ti as a transition metal into SBA-15 framework is an effective method since titanium is readily available, non-toxic and low-priced [39]. Furthermore, titania-silicates via prepared sol-gel method have mesopore structure, high stability and super acid centers as reported by Kılıç et al. (2015). It was obtained as 100 % conversion in fructose dehydration to 5-Hydroxymethylfurfural and was found as highly stable [40].

In the light of the literature review, this study aims that preparation of sulfated Ti-SBA-15 and sulfated titania-silica catalysts for the ring opening reaction of epoxidized soybean oil.

### 3.2. Sulfated Ti-SBA-15 Catalysts

Sharma et al. (2014) carried out sulfation of Ti-SBA-15 using 0.5 M chlorosulfonic acid. Yadav et al. (2004) stated that 0.5 M chlorosulfonic acid treatment provided more sulfate species in other words higher amount of acid sites than 0.5 M sulfuric acid. For the sulfation, the catalyst was mixed with 0.5 M chlorosulfonic acid solution in methylene dichloride at room temperature using 15 ml per gram of catalyst. Strong acid sites of SO<sub>4</sub>/Ti-SBA-15 was confirmed with NH<sub>3</sub>-TPD analysis. Moreover, density of Brønsted acid sites increased by attachment sulfate species to the catalyst surface [40, 41]. In addition, stabilization of the anatase titanium by sulfation and so prevention of the sintering of titanium crystallite to lower crystallites was stated by Sunajadevi et al. (2005) [43]. This outcome was confirmed in another study of Sharma et al. (2012) from their XRD results. Intensity of diffraction peaks of anatase titanium (25.5, 37.4, 48 and 53) decreased after sulfation of the Ti-SBA-15 [44].

Mungia et al. (2017) incorporated aluminum, titanium and –PrSO<sub>3</sub>H groups into SBA-15 and investigated their effect in the oleic acid esterification reaction with methanol. Catalysts were prepared via sol-gel method with a molar ratio of Si/M=10, (M=Al or Ti). It was observed as SBA-15 had mainly Lewis acid sites (86%). On the other hand, Brønsted acid sites was more significant for Ti-SBA-15-SO<sub>3</sub>H (69%) and Al- SBA-15-SO<sub>3</sub>H (51%). Ti-SBA-15-SO<sub>3</sub>H and Al- SBA-15-SO<sub>3</sub>H showed 97% and 79.93 oleic acid conversion, respectively whereas SBA-15 provided just 10% conversion. Thus, it was confirmed that Brønsted acid sites were effective in the esterification reaction. Also, lower activity of Al- SBA-15-SO<sub>3</sub>H was attributed to weak interaction of oleic acid molecule to the acid sites since hydrophilic sites formation when Al replace Si atoms. Moreover, reusability study of the catalysts was performed. Catalytic activity of Ti-SBA-15-SO<sub>3</sub>H decreased to 29% after 3 cycles [45].

Synthesis condition of SBA-15 silica support is also an important parameter for the catalytic activity and resulting properties of metal incorporated SBA-15 catalysts. Rashid et al. (2019) calcined the SBA-15 at different temperatures (200-700 °C) to investigate the effect of calcination temperature over the SBA-15 synthesis. The highest surface area and porosity was obtained at 500 °C and it was determined as optimum

calcination temperature. It was reported that surfactant removal could not be achieved for the calcination temperatures 110 °C and 200 °C. Furthermore, calcination at 700 °C caused damage for the hexagonal ordered porous structure [46]. Yan et al. (2021), reported that morphology of SBA-15 can be changed according to synthesis temperature. SBA-15 synthesized at 35 °C, 45 °C and 55 °C had hexagonal prisms (HP), short rods (SR) and long rods (LR) morphologies, respectively. After that magnesium was incorporated by wet impregnation and sulfated zirconia was grafted into SBA-15 catalysts that have different morphologies and they were denoted as HP-SZ/Mg-SBA-15, SR-SZ/Mg-SBA-15 and LR-SZ/Mg-SBA-15. As shown Table 3.8, SR-SZ/Mg-SBA-15 had the highest surface area and total acidity. Catalytic activities were compared and the highest yield (98.6%) for the fructose dehydration into 5-HMF was achieved with the SBA-15 prepared at 45 °C as a result of its textural and acidic properties [47].

Table 3.8. BET specific surface area and total acidity of HP-SZ/Mg-SBA-15, SR-SZ/Mg-SBA-15 and LR-SZ/Mg-SBA-15 [47].

	HP-SZ/Mg-SBA-15	SR-SZ/Mg-SBA-15	LR-SZ/Mg-SBA-15
$S_{BET}$ (m <sup>2</sup> /g)	423	586	284
Total acidity (mmol/g)	0.76	1.74	0.68

As a result of literature studies, the method of Sharma et al. (2014) is determined for catalyst preparation in this thesis study. On the other hand, calcination temperature after sulfation can be revised regarding the study of Guo et al. (2008). They indicated that calcination temperature should be below the 460 °C since acidic protons can be lost above this temperature.

### 3.3. Sulfated TiO<sub>2</sub>-SiO<sub>2</sub> Catalysts

Sulfated metal oxides firstly used by Tanabe et al. in 1976 [48] and they have had an important place in the heterogenous catalysis since that time. Literature studies suggest that mixed metal oxides provide better catalytic activity than their single oxide form due to their improved acidity and thermal stability. Moreover, mixed metal oxides can offer

a solution to the sulfur leaching problem of single metal oxide [49].

Titania silicates are one of the most used catalysts among mixed oxides. Yang et al. (2003) showed the possible configuration of  $\text{SO}_4/\text{TiO}_2\text{-SiO}_2$  catalyst which is given in Figure 3.8.  $\text{TiO}_2\text{-SiO}_2$  catalyst was prepared with 13.8 wt.%  $\text{TiO}_2$  content and it was sulfated with 1.0 M sulfuric acid solution by mixing at room temperature for 1 h. Its catalytic activity was tested in the esterification of acetic acid reaction with glycerin and 91% acetic acid conversion was obtained. Thus, it was determined as an effective catalyst for the reaction. Also, its activity was found better than  $\text{SO}_4/\text{SiO}_2$ .  $\text{SO}_4/\text{SiO}_2$  provided just 56% conversion. Furthermore, effect of calcination temperature was analyzed. For this purpose,  $\text{SO}_4/\text{TiO}_2\text{-SiO}_2$  catalyst was calcined at 400, 450, 500, 550 and 600 °C and it was reported that 450 °C is the optimum calcination temperature and the highest surface and the highest surface area (550  $\text{m}^2/\text{g}$ ) was obtained at this temperature [50]. This result was further confirmed by Shao et al. (2013). In their work, sol-gel method was used for the preparation of  $\text{TiO}_2\text{-SiO}_2$  oxides and they calcined at different temperatures (450, 550, 650 and 800 °C). The highest surface area (457  $\text{m}^2/\text{g}$ ) was observed for the catalyst calcined at 450 °C and it provided best conversion (77 %) for the transesterification of waste oil [51].

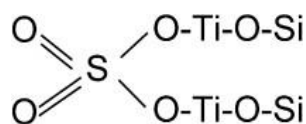


Figure 3.8. Configuration of  $\text{SO}_4/\text{TiO}_2\text{-SiO}_2$  catalyst [50].

Synthesis strategies is also an important criterion for the  $\text{TiO}_2\text{-SiO}_2$  catalysts. There are many other methods for the preparation of them such as impregnation, coprecipitation, flame hydrolysis, chemical vapor deposition. The sol-gel method is an effective preparation route for the tuning of catalyst surface properties [51]. Aguado et al. (2006) pointed out that  $\text{TiO}_2\text{-SiO}_2$  are obtained via sol-gel synthesis are mostly amorphous and titanium atoms are present in tetrahedral position of the silica network [52]. Furthermore, research of Li et al. (2013) proposed that activity and stability of sulfated mixed oxide could be improved with addition of rare earth elements. In this study, sulfated titania silicates were prepared with addition of lanthanide ion ( $\text{Ln} = \text{La}^{3+}$ ,  $\text{Ce}^{4+}$ ,  $\text{Sm}^{3+}$ ) and analyzed their activity in the esterification of itaconic acid. The highest activity (94.3%) was attained with the  $\text{La}^{3+}\text{-SO}_4^{2-}/\text{TiO}_2\text{-SiO}_2$  and it was further compared

with  $\text{La}^{3+}\text{-SO}_4^{2-}/\text{TiO}_2$  and  $\text{SO}_4^{2-}/\text{TiO}_2$  catalysts. Although catalytic activity was similar for all of them, they showed quite different reusability behavior. A dramatic decrease was observed for the activity of  $\text{SO}_4^{2-}/\text{TiO}_2$  whereas  $\text{La}^{3+}\text{-SO}_4^{2-}/\text{TiO}_2$  was found as highly stable. It provided still 84% itaconic acid conversion after eight cycles. Furthermore, it was confirmed by FTIR analysis that  $\text{La}^{3+}\text{-SO}_4^{2-}/\text{TiO}_2\text{-SiO}_2$  had stronger Brønsted acid sites and high dispersion of Si and La on the catalyst was observed from XRD analysis. Hereby, it was concluded that sulfur leaching can be prevented with combination of Si and  $\text{La}^{3+}$  ion and so stability of catalyst can be enhanced [53].

The presented studies showed that sulfated  $\text{TiO}_2\text{-SiO}_2$  are favorable catalysts for reactions that involves long chain reactants by considering the literature studies. Although no one employed this catalyst in the biolubricant production, it can be suitable for this study with its acidic and surface properties. In this context, sulfated titania silica and sulfated La incorporated titania-silica catalysts will be prepared and their activity will be tested for the ring opening reaction of epoxidized soybean oil.

Objective of present study is the production of biolubricant using epoxidized soybean oil via ring opening reaction. In the literature, most of study was performed with epoxy canola oil. On the other hand, usage of epoxy soybean oil can be favorable alternative since it is cheap and highly available feedstocks. Also, it can provide a different study to literature. Furthermore, literature studies demonstrated that length and branching of alcohol has a significant effect in the ring opening reactions. In this regard, it is suggested that comparison of 2-propanol and 2-ethylhexanol can be effective.  $\text{SO}_4/\text{Ti-SBA-15}$ ,  $\text{SO}_4/\text{SBA-15}$ ,  $\text{SO}_4/\text{La-TiO}_2\text{-SiO}_2$  and  $\text{SO}_4/\text{TiO}_2\text{-SiO}_2$  catalysts will be prepared for the ring opening reactions. Catalyst characterizations will be carried out with details since acidic, textural and structural properties of catalysts have great importance for their activity. Last but not the least, stability of catalysts will be analyzed.

## CHAPTER 4

### EXPERIMENTAL STUDY

#### 4.1 Materials

This study was performed using the chemicals given in Table 4.1.

Table 4.1. The reagents used for experimental study

Chemicals	Brand and Purity
2-Ethyl hexanol	Sigma-Aldrich, $\geq 99$ %
2-Propanol	Isolab Chemicals, $\geq 99.5$ %
Acetic acid	Isolab Chemicals, glacial (100 %)
Amberlyst-15	Sigma Aldrich, 216380
Ammonium hydroxide solution	Sigma Aldrich, 28-30 %
Ammonium sulfate	Isolab Chemicals, $\geq 99.5$ %
Chlorosulfonic Acid	Sigma-Aldrich, $\geq 99$ %
Deuterated chloroform	Eurisotop, 99.8%
Dichloromethane	Sigma-Aldrich, $\geq 99.5$ %
Epoxidized Soybean Oil	Olexol, 97%
Ethanol	Isolab Chemicals, $\geq 99.9$ %
Hydrochloric acid	Isolab Chemicals, 37%
Hyrogen Bromide Solution in Acetic Acid	Sigma-Aldrich, 33 wt %
Lanthanum (III) nitrate hexahydrate	Sigma-Aldrich, 99.9 %
Pluronic P123	Sigma-Aldrich, 435465
Potassium bromide	Merck, $\geq 99$ %
Potassium hydrogen pthalate	Merck, $\geq 99.5$ %
Sulfuric acid	Isolab Chemicals, 95-98%
Tetraethyl orthosilicate	Sigma-Aldrich, 98%
Titanium(IV) isopropoxide	Sigma Aldrich, 97 %

## 4.2. Catalyst Preparation

### 4.2.1 Preparation of SO<sub>4</sub>/Ti-SBA-15 and SO<sub>4</sub>/SBA-15

Ti-SBA-15 was prepared with sol-gel method using method given by Sharma et al. (2013) [10]. First of all, 9.28 g pluronic P123 and 228.6 g water were mixed at 40°C for 2h. At the end of 2 h, P123 was completely dissolved and a clear solution was obtained. After that 4.54 g of HCl (37 wt%) was added to the solution and left to stir for another 2 h and then 20.83 g tetraethylorthosilicate (TEOS) and 2.84 g titanium isopropoxide (TISOP) was added drop wise. After the addition was completed, the solution was left stirring for 24 h at 40°C. Subsequently, the solution was placed in a teflon bottle and hydrothermal treatment was applied at 100 °C for 24 h. The solid material was recovered by centrifugation, washed with water three times and dried at 100 °C for 12 h. Finally, the catalyst was calcined at 550 °C for 6 h and it was named as Ti-SBA-15-10 since molar ratio of Si/Ti was 10. Also, Ti-SBA-15 catalyst was prepared with molar ratio of Si/Ti:6 using same procedure with 4.74 g of TISOP instead of 2.84 g and it was named as Ti-SBA-15-6. Furthermore, SBA-15 was prepared for the comparison with Ti-SBA-15. SBA-15 was synthesized using the same procedure without titanium isopropoxide addition.

Ti-SBA-15 catalysts were sulfated with using two different sulfate sources. First of all, sulfation was carried out with 1 M ammonium sulfate solution. 5 mL of (NH<sub>4</sub>)<sub>2</sub>SO<sub>4</sub> aqueous solution was used per gram of catalyst and they were stirred at room temperature for 1 h. Also, sulfation was performed with 0.5 M chlorosulfonic acid in dichloromethane. For this purpose, 1 g Ti-SBA-15 was mixed with 15 mL chlorosulfonic acid solution for 5 minutes at room temperature. The catalysts prepared by ammonium sulfate and chlorosulfonic acid were denoted as SO<sub>4</sub>/Ti-SBA-15-10(AS), SO<sub>4</sub>/Ti-SBA-15-10(CS) and SO<sub>4</sub>/Ti-SBA-15-6(CS), respectively. In addition, SBA-15 was sulfated with chlorosulfonic acid using same procedure and denoted as SO<sub>4</sub>/SBA-15-(CS). Finally, obtained products were calcined at 450 °C for 6 h.

#### 4.2.2 Preparation of SO<sub>4</sub>/La-TiO<sub>2</sub>-SiO<sub>2</sub> and SO<sub>4</sub>/TiO<sub>2</sub>-SiO<sub>2</sub>

Sol-gel method was used for preparation of SO<sub>4</sub>/La-TiO<sub>2</sub>-SiO<sub>2</sub> and SO<sub>4</sub>/TiO<sub>2</sub>-SiO<sub>2</sub> catalysts. They were synthesized according to method given by Aguado et al. (2006) [52]. TiO<sub>2</sub>-SiO<sub>2</sub> (10 wt.%) with and without La incorporation was prepared according to the following mole ratios:

Ethanol:TEOS mol ratio: 2:1, H<sub>2</sub>O:TEOS mol ratio: 1.2:1, TISOP-Isopropanol mass ratio: 1:1

Firstly, 6.6 mL TEOS, 3.51 mL ethanol and 0.648 mL 0.05 M HCl were mixed (about 500 rpm) at room temperature for 90 min. Then TISOP-Isopropanol solution and 0.1 g lanthanum nitrate hexahydrate (for La incorporated catalyst) were added and were stirred for 45 min. After that, 2.35 mL deionized water was added and was stirred another 1 h. Finally, 1 M ammonia solution was added dropwise until the gelation was occurred. In this point, it is quite important to add ammonia solution drop by drop to obtain a homogeneous gel. Addition of ammonia solution increased pH and solution became transparent gel. After obtaining the transparent gel, it was aged at room temperature for 24 h and then dried at 80 °C for 24 h. Finally, the obtained product was milled and calcined at 500 °C for 4 h.

Sulfation of TiO<sub>2</sub>-SiO<sub>2</sub> and La-TiO<sub>2</sub>-SiO<sub>2</sub> was carried out with 1 M ammonium sulfate solution. 5 mL of (NH<sub>4</sub>)<sub>2</sub>SO<sub>4</sub> aqueous solution was used per gram of catalyst with stirring at room temperature for 1 h. It was named as SO<sub>4</sub>/TiO<sub>2</sub>-SiO<sub>2</sub>(AS) and SO<sub>4</sub>/La-TiO<sub>2</sub>-SiO<sub>2</sub>(AS), respectively. Also, La-TiO<sub>2</sub>-SiO<sub>2</sub> was sulfated with 0.5 M chlorosulfonic solution by mixing 15 mL solution per gram catalyst at room temperature for 5 min. It was named as SO<sub>4</sub>/La-TiO<sub>2</sub>-SiO<sub>2</sub>(CS). Finally, they were calcined at 450 °C for 6 h.

### **4.3. Catalyst Characterization**

#### **4.3.1. N<sub>2</sub> Adsorption/Desorption Tests (BET)**

The analysis was performed with Micromeritics ASAP 2010 model static volumetric adsorption instrument. The catalysts were degassed at 200 °C for 6 h and N<sub>2</sub> adsorption was carried out at – 196 °C.

#### **4.3.2. X-Ray Diffraction (XRD)**

XRD analysis was performed using Philips X'Pert diffractometer with CuK $\alpha$  radiation for the determination of the crystalline structures of catalysts. The scattering angle  $2\theta$  was varied from 5 °C to 80 °C, with a step length of 0.02.

#### **4.3.3. Skeletal FTIR Spectroscopy**

The characterization was performed by Shimadzu FTIR 8400S model Fourier Transformed Infrared Spectrometer using KBr pellet technique between 400 - 2000 cm<sup>-1</sup> wavenumbers with a resolution of 4 cm<sup>-1</sup> and the framework vibration of the catalysts was analyzed. Mixture of 3 mg catalyst sample and 150 mg KBr was pressed for the preparation of KBr pellets.

#### **4.3.4. Temperature Programmed Desorption of Ammonia (NH<sub>3</sub>-TPD)**

NH<sub>3</sub>-TPD analysis was carried out with Micromeritics AutoChem II Chemisorption Analyzer instrument for the determination of the catalysts acidic strength. Firstly, the catalysts were heated up to 500 °C with a 5 °C/min heating rate and then they were kept at this temperature for 1 h under 70 ml/min He flow. After that, the temperature of samples was decreased to 90°C (5 °C/min) under He flow of 30 ml/min and the gas flow was switched to NH<sub>3</sub>-He of 30 ml/min for 30 min. It is followed by 70 ml/min He

flow during 2 h for the removal of the physisorbed NH<sub>3</sub>. Finally, ammonia desorption from the catalysts was examined by heating the sample from 90 °C to 600 °C (10 °C/min).

#### **4.2.1. Thermal Gravimetric Analysis (TGA)**

Thermogravimetric analysis was performed with Shimadzu TGA-51 instrument for the investigation of the thermal stability of catalysts. The samples were heated from 25°C to 800°C with a 5 °C/min heating rate under air flow.

#### **4.3.6 X-Ray Fluorescence Spectroscopy (XRF)**

Elemental compositions of the catalysts were determined by XRF analysis using Spectro IQ II instrument with CuK $\alpha$  radiation. The analysis was carried out by powder method.

#### **4.4. Catalyst Testing in Epoxide Soybean oil to Biolubricants**

Activities of prepared catalysts were tested in the ring opening reaction of epoxidized soybean oil. Experiments were performed in a 100 mL three necked round bottom flask that was placed in a heating mantle with magnetic stirrer and equipped with a reflux condenser at the center neck of the flask. Reactions were carried out with alcohols which were 2-propanol and 2-ethyl hexanol. Experimental set-up and obtained biolubricant are given in Figure 4.1.

##### Experiments with 2-propanol

For this reaction, 10 g epoxidized soybean oil, 2-propanol (alcohol-epoxide mol ratio: 10/1) and 10 wt% catalyst (according to amount of epoxidized soybean oil) were added to the flasks and the mixture was continuously stirred with 1000 rpm for 6 h at 80°C. At the end of reaction, the catalyst was separated by centrifugation and excess

alcohol was removed by rotary evaporator as shown Figure 4.2. Evaporation was carried out at 80 °C under 55 mbar for 1 h.



Figure 4.1 Experimental Set-up and biolubricant obtained



Figure 4.2. Removal of excess alcohol with rotary evaporator

#### Experiments with 2-ethyl hexanol

In this reaction, 10 g epoxidized soybean oil, 2-ethylhexanol (alcohol-epoxide molratio: 6/1) and 7 wt% catalyst (according to amount of epoxidized soybean oil) were added to the flasks and the mixture was continuously stirred with 1000 rpm for 18 h at 100 °C. At the end of reaction, the catalyst was separated with centrifugation and excess alcohol was removed using Kugel vacuum distillation

at 100 °C under 1 mbar for 40 min as shown Figure 4.3.



Figure 4.3. Removal of excess alcohol with Kugel vacuum distillation

Product analysis was performed with analytical and instrumental methods. First of all, conversion was determined by analyzing the oxirane oxygen content of samples using the standard AOCS Cd 9–57 method [10]. Following procedure was applied for this method.

- 0.1 M HBr solution in acetic acid was prepared and standardized. For standardization, 0.4 g potassium hydrogen phthalate was dissolved with 10 mL acetic acid in 50 mL Erlenmeyer flask and 3 drops methyl violet indicator was added. Then, it was titrated with prepared HBr in acetic acid solution. Molarity of HBr solution was calculated from the following formula;

$$\text{Molarity of HBr} = \frac{\text{mass of potassium hydrogen phthalate, g}}{0.2042 * \text{mL of HBr solution}}$$

- After standardization of HBr solution, 0.4 g product was dissolved with 10 mL acetic acid in 50 mL Erlenmeyer flask and 3 drops methyl violet indicator was added.
- It was titrated with the HBr solution and observation of the color change from purple to blue-green was considered the end point of the titration. The color change is shown in Figure 4.4. Finally, oxirane content of products and conversion was determined from the following formula;

Oxirane oxygen content

$$= \frac{\text{mL of HBr solution required to titrate sample} \times N \times 1.60}{\text{mass of sample (g)}}$$

N: Normality of HBr solution

Conversion

$$= \frac{\text{Oxirane oxygen content at time t0} - \text{Oxirane oxygen content at time t1}}{\text{Oxirane oxygen content at time t0}} * 100$$

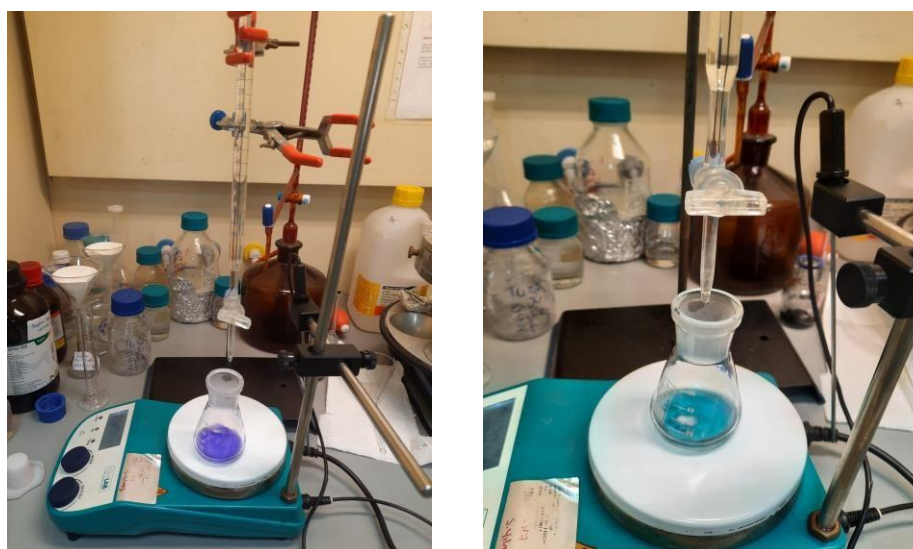


Figure 4.4. Analysis of oxirane content by titration

The products were further confirmed with FTIR and H-NMR analysis. For the FTIR analysis, 150 mg KBr pellets were pressed and 2-3 drops oil products were dispersed on the pellets. The analysis was performed by Shimadzu FTIR 8400S model Fourier Transformed Infrared Spectrometer between 400 - 2000  $\text{cm}^{-1}$  wavenumbers with a resolution of 4  $\text{cm}^{-1}$ . For the H-NMR analysis, 10 mg oil products and 0.6 ml deuteratedchloroform were mixed in an eppendorf and then the mixture was transferred to the NMRtube. The analysis was carried out with Varian Inova 300 MHz spectrometer instrument using 32 scan number.

## 4.5 Reusability of the Catalysts

Reusability is an important criterion in the heterogenous catalysis. In this context, stability of catalyst against leaching and their reusability was tested. For this purpose, after each reaction, separated catalyst by centrifugation was washed with acetone to remove oil residues attached to the catalyst surface and pores at reflux condition for 1 h and then dried at 120°C for 3 h [10]. At the end of this treatment, the catalyst was characterized by XRF analysis and the stability was determined by comparing the elemental composition of fresh and used-treated catalyst. In addition, more stable catalysts were three times reused.

The stability and reusability of catalyst can be enhanced by washing with hot water or alcohol [53, 54]. In this context, effect of washing was studied and the catalyst was washed by hot filtration method and 2-propanol to eliminate unstable sulfate groups. In hot filtration method, the catalyst washed with water at 70 °C until obtain a clear solution. Effect of washing with water and alcohol on the stability of catalyst was analyzed. Furthermore, the catalyst with least leaching was reused in the reaction and its reusability performance was analyzed.

## CHAPTER 5

### RESULTS AND DISCUSSION

#### 5.1. Characterization of the Catalysts

The textural, structural and acidic properties of catalyst can have a great impact on their activity in a reaction. Therefore, detailed characterization of them is essentially required in order to interpret their catalytic behavior. In this study, a comprehensive characterization was performed for the catalysts prepared. N<sub>2</sub> adsorption-desorption, FTIR, XRD, NH<sub>3</sub>-TPD, TGA and XRF analysis were carried out and these analyzes provided information about catalysts such as surface area and pore size, chemical bonds in their structure, crystal structure, elemental composition, acidic strength and thermal stability.

##### 5.1.1. SO<sub>4</sub>/ Ti-SBA-15 and SO<sub>4</sub>/SBA-15 Catalysts

Mesoporous structure of SBA-15 and Ti-SBA-15 based catalyst was confirmed with their N<sub>2</sub> adsorption/desorption isotherms as shown Figure 5.1. The catalysts showed type 4 adsorption/desorption isotherms with H1 hysteresis loop that implies their regular mesoporous structure.

The textural properties, namely surface area, pore volume and pore size of SBA-15, SO<sub>4</sub>/SBA-15-(CS), Ti-SBA-15-10, SO<sub>4</sub>/Ti-SBA-15-10(AS), SO<sub>4</sub>/Ti-SBA-15-10(CS), SO<sub>4</sub>/Ti-SBA-15-6(CS) catalysts and their sulphur contents are given in Table 5.1. All the catalysts had high surface area that varying from 315.2 to 766.8 and Ti-SBA-15-10 provided the highest surface area (778.5 m<sup>2</sup>/ g). In addition, mean pore size of all the catalysts were found to be larger than 2 nm which indicates the their mesopore structure. Incorporation of Titanium increased the surface area slightly. On the other hand, sulfation decreased the surface area considerably especially when sulfated with chlorosulfonic acid due to attachment of more sulfate groups on the surface of catalyst.

When the ammonium sulfate and chlorosulfonic acid treatment was compared for Ti-SBA-15 catalysts, sulphur content of SO<sub>4</sub>/Ti-SBA-15-10(AS) and SO<sub>4</sub>/Ti-SBA-15-10(CS) was found as 0.56 and 0.89 wt.%, respectively and it was concluded that chlorosulfonic acid treatment was more effective, which is consistent with literature findings [42]. Moreover, SO<sub>4</sub>/SBA-15-(CS) possessed just 0.14 wt% sulphur whereas increase of sulphur content was observed in the titanium incorporated catalysts since formation of stronger bonds between sulphur, titanium and silicon. Also, increasing of titanium content decreased the surface area of catalyst from 430.3 to 315.2 m<sup>2</sup>/g and increased the sulphur content from 0.89 to 1.49 wt.%. Moreover, increase of titanium content resulted a decrease in pore volume and pore size. It can be due to formation of TiO<sub>2</sub> nanoclusters in the pores of SBA-15 structure.

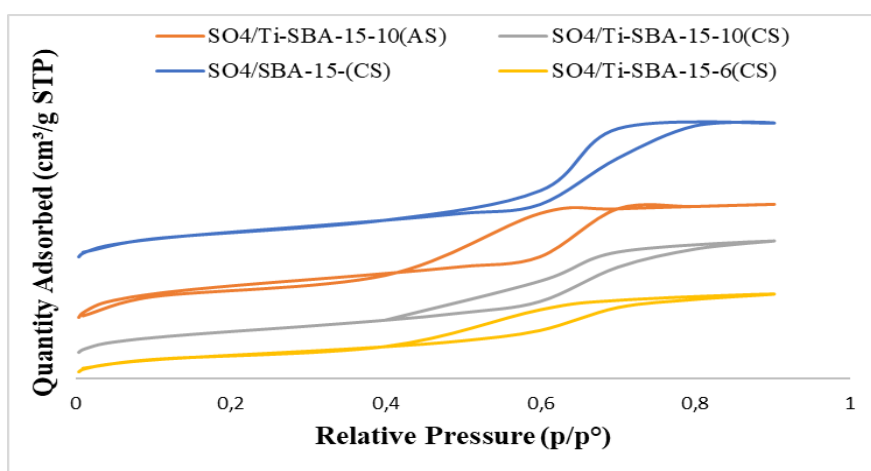


Figure 5.1. N<sub>2</sub> Adsorption/Desorption isotherms of SO<sub>4</sub>/SBA-15-(CS), SO<sub>4</sub>/Ti-SBA-15-10(AS), SO<sub>4</sub>/Ti-SBA-15-10(CS) and SO<sub>4</sub>/Ti-SBA-15-6(CS) catalyst

Table 5.1. Textural properties and sulphur content of SBA-15 and Ti-SBA-15 based catalysts

Catalyst	S <sub>BET</sub> (m <sup>2</sup> /g)	Pore Volume (cm <sup>3</sup> /g)	Pore Size (Å)	Sulphur content (wt.%)
SBA-15	766.8	0.63	47.8	-
SO <sub>4</sub> /SBA-15-(CS)	467.0	0.58	53.6	0.14
Ti-SBA-15-10	778.5	0.45	35.3	-
SO <sub>4</sub> /Ti-SBA-15-10(AS)	647.3	0.49	45.1	0.56
SO <sub>4</sub> /Ti-SBA-15-10(CS)	430.3	0.45	49.0	0.89
SO <sub>4</sub> /Ti-SBA-15-6(CS)	315.2	0.34	47.1	1.49

XRD patterns of Ti-SBA-15-10, SO<sub>4</sub>/Ti-SBA-15-10(AS), SO<sub>4</sub>/Ti-SBA-15-10(CS) and SO<sub>4</sub>/Ti-SBA-15-6(CS) are given in Figure 5.2. Four sharp peaks were observed at 2θ of 25.5, 37.4, 48 and 53 for Ti-SBA-15 which was due to the presence of anatase titanium. However, anatase titanium was stabilized by sulfation of Ti-SBA-15-10 and intensity of these peaks decreased that was in accordance with literature [44]. On the other hand, SO<sub>4</sub>/Ti-SBA-15-6(CS) showed slightly higher intensity than SO<sub>4</sub>/Ti-SBA-15-10(AS) and SO<sub>4</sub>/Ti-SBA-15-10(CS) due to its higher titanium content. XRD patterns of SBA-15 and SO<sub>4</sub>/SBA-15-(CS) are given in Figure 5.3 and a broad peak was observed only at 2θ of 22.0 which is a characteristic amorphous silica peak [56].

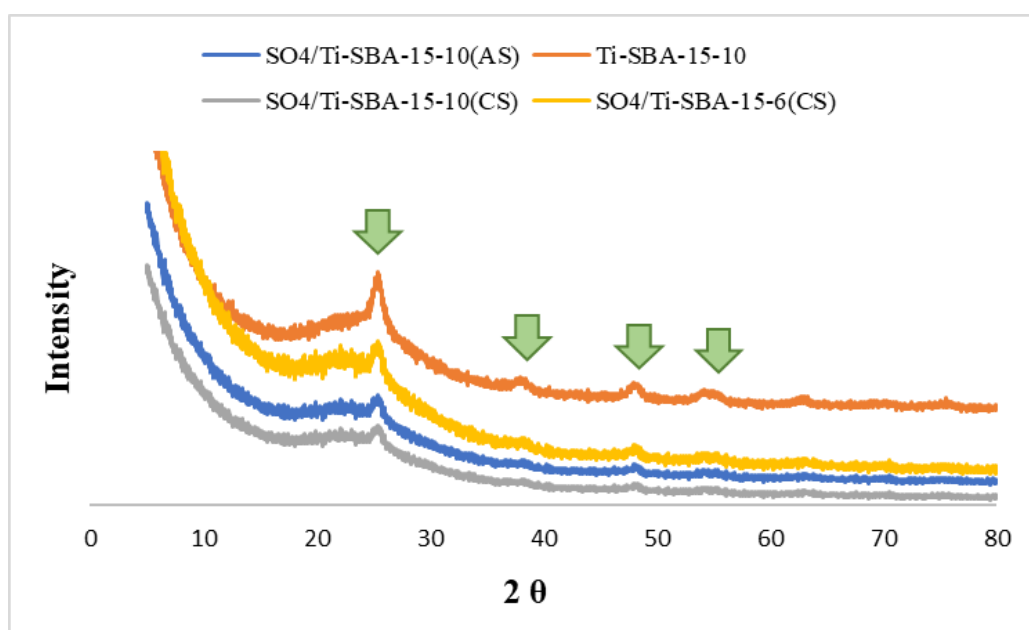


Figure 5.2. XRD patterns of Ti-SBA-15-10, SO<sub>4</sub>/ Ti-SBA-15-10(AS), SO<sub>4</sub>/Ti-SBA-15-10(CS) and SO<sub>4</sub>/Ti-SBA-15-6(CS) catalysts

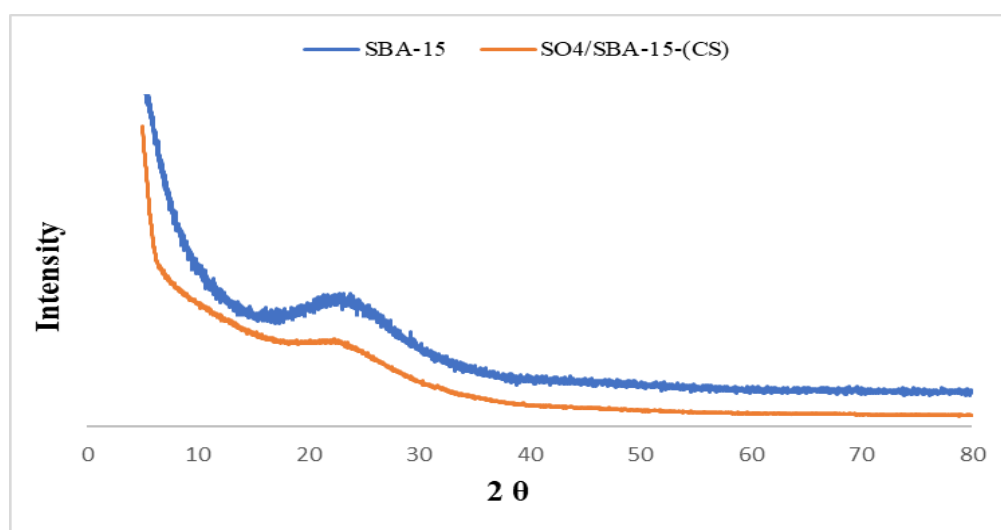


Figure 5.3. XRD patterns of SBA-15 and SO<sub>4</sub>/ SBA-15-(CS) catalysts

Figure 5.4 represents the FTIR spectrum of SO<sub>4</sub>/Ti-SBA-15-10(AS), SO<sub>4</sub>/Ti-SBA-15-10(CS), SO<sub>4</sub>/Ti-SBA-15-6(CS) and SO<sub>4</sub>/SBA-15-(CS) catalysts. They demonstrated a band at 966 cm<sup>-1</sup> owing to Si-O-Ti vibrations. Presence of Si-O bonds in catalysts was confirmed with the bands at 800 and 1069 cm<sup>-1</sup> [57]. The band between 1600 and 1700 cm<sup>-1</sup> is result of vibration of adsorbed water molecule and also a broad band was present at about 3450 cm<sup>-1</sup> which corresponds to surface hydroxyl group and physisorbed water [39]. A similar spectrum was obtained for the SO<sub>4</sub>/SBA-15-(CS) however the band at 960 cm<sup>-1</sup> was attributed to the Si-OH vibration [37]. Although there was an expected peak at 1388 cm<sup>-1</sup> due to vibration of sulfate group, it was not present in the FTIR spectrum of the catalysts [10]. It may be due to overlapping of the sulfated group and Si-O-Si vibrations.

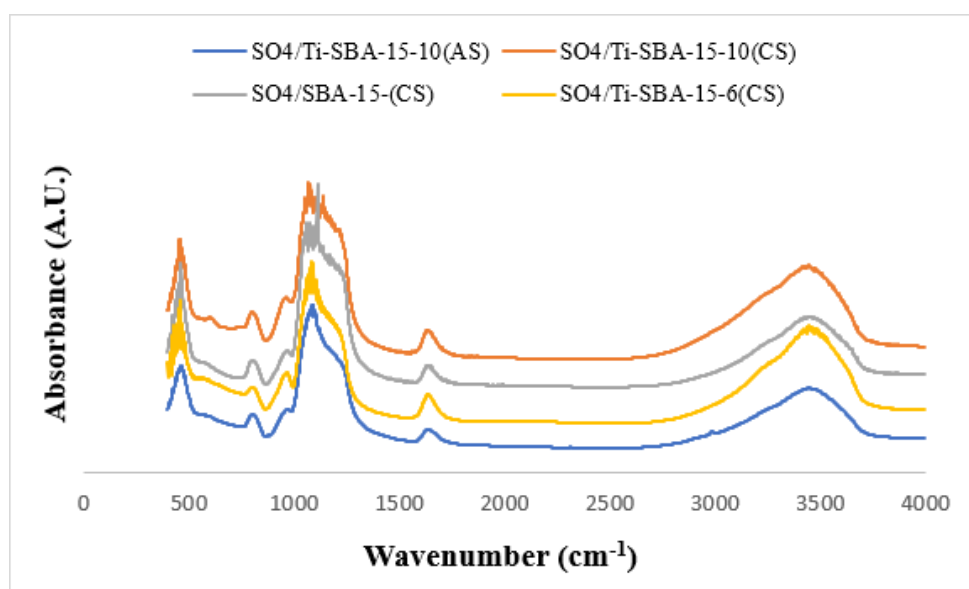


Figure 5.4. FTIR spectra of SO<sub>4</sub>/SBA-15-(CS), SO<sub>4</sub>/Ti-SBA-15-10(AS), SO<sub>4</sub>/Ti-SBA-15-10(CS) and SO<sub>4</sub>/Ti-SBA-15-6(CS) catalysts

The acidic nature of the catalysts was analyzed by NH<sub>3</sub>-TPD analysis. The desorption peaks below 200°C and between 200°C and 300°C indicates weak and moderate acid sites, respectively whereas the peaks above 350°C is as a result of strong acid sites [58]. As shown Figure 5.5, Ti-SBA-15-10 had both weak and strong acid sites but the intensity of peaks was quite low. On the other hand, weak to strong acid sites with a broad high intense single peak between 100-500°C was observed with sulfation of catalysts due to presence of sulfate linkage. In addition, sulfation increased the total acidity of the catalysts significantly. Chlorosulfonic acid provided higher total acidity than ammonium sulfate due higher sulphur contents. This result is in agreement with

the literature [42]. As a result, sulphur loading improved the amount of acid sites and total acidity. Nevertheless, increase of titanium content had a great effect on the acidity of catalyst. It was noted that the strong acid sites and total acidity of the SO<sub>4</sub>/Ti-SBA-15-6(CS) promoted remarkably.

NH<sub>3</sub>-TPD profiles of SBA-15 and SO<sub>4</sub>/SBA-15-(CS) are given in Figure 5.6. SBA-15 had notably very low acidity and chlorosulfonic acid treatment enhanced the total acidity of SBA-15. SO<sub>4</sub>/SBA-15-(CS) showed two desorption peaks that indicates weak and moderate acid sites. Furthermore, it was noticed titanium incorporation promoted total acidity and acid sites by comparison Figure 5.5 and 5.6. This was attributed to increase of sulphur content with titanium incorporation that was confirmed by XRF analysis. In addition, total amount of the acid sites was determined quantitatively by integrating area under the peaks of each catalyst and results are given in the Table 5.2. There was a slight difference between the acidity of SO<sub>4</sub>/Ti-SBA-15-10(AS) and SO<sub>4</sub>/Ti-SBA-15-10(CS). On the hand, acidity of SO<sub>4</sub>/Ti-SBA-15-6(CS) was significantly high.

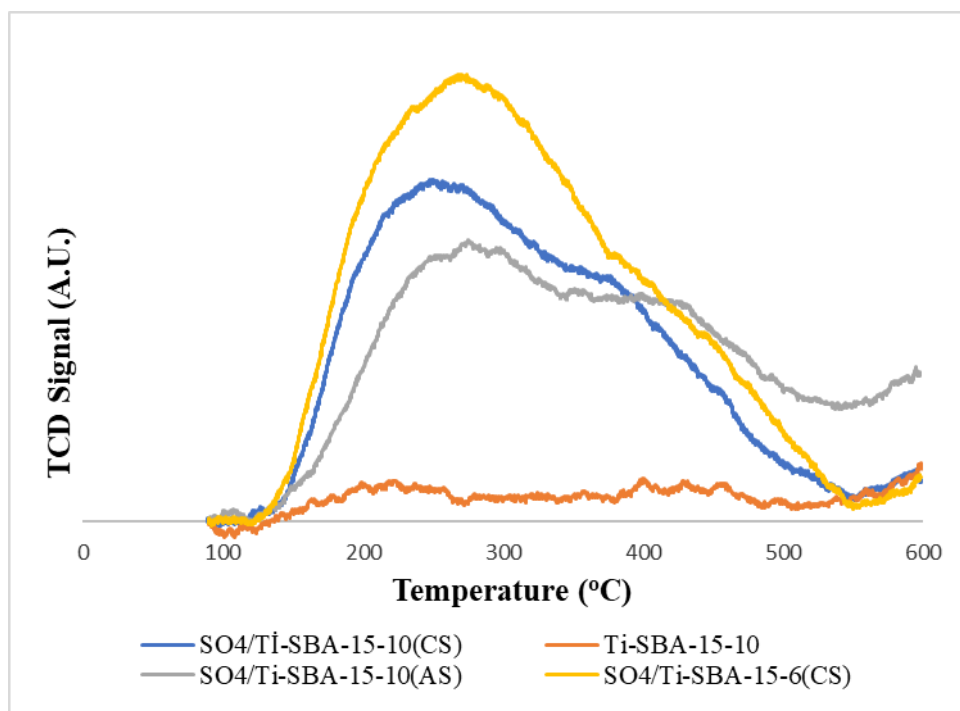


Figure 5.5. NH<sub>3</sub>-TPD analysis of Ti-SBA-15-10, SO<sub>4</sub>/Ti-SBA-15-10(AS), SO<sub>4</sub>/Ti-SBA-15-10(CS) and SO<sub>4</sub>/Ti-SBA-15-6(CS) catalysts

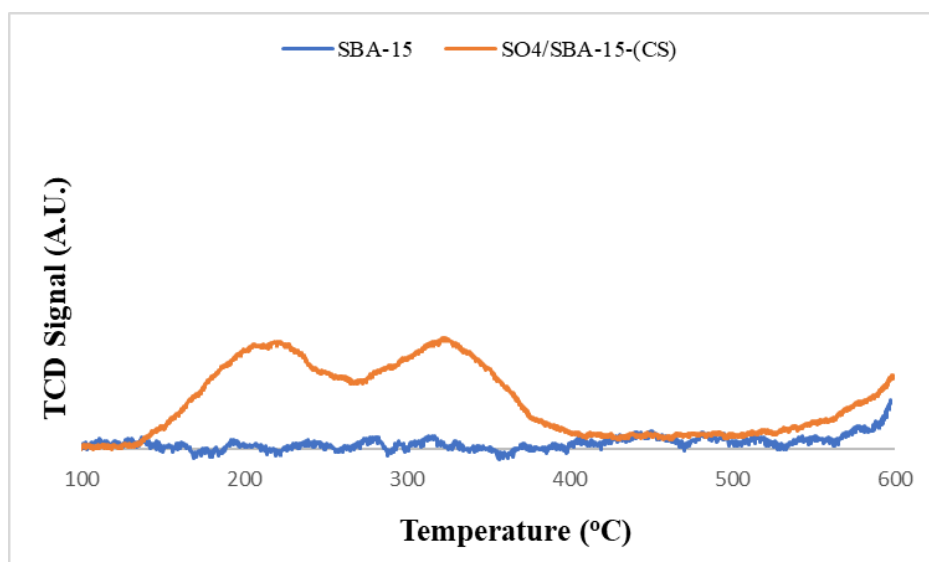


Figure 5.6. NH<sub>3</sub>-TPD analysis of SBA-15 and SO<sub>4</sub>/SBA-15-CS catalysts

Table 5.2. Total acidity of SBA-15, SO<sub>4</sub>/ SBA-15-(CS), Ti-SBA-15-10, SO<sub>4</sub>/ Ti-SBA-15-10(AS), SO<sub>4</sub>/Ti-SBA-15-10(CS) and SO<sub>4</sub>/Ti-SBA-15-6(CS) catalysts

Catalyst	Acidity (mmol NH <sub>3</sub> /gcat)
SBA-15	0.059
SO <sub>4</sub> /SBA-15-(CS)	0.771
Ti-SBA-15-10	0.260
SO <sub>4</sub> /Ti-SBA-15-10(AS)	1.699
SO <sub>4</sub> /Ti-SBA-15-10(CS)	1.765
SO <sub>4</sub> /Ti-SBA-15-6(CS)	2.264

Thermal stability of the catalysts was determined by analyzing their TGA curves which are given in Figure 5.7. Ti-SBA-15 had single weight loss (7 wt.%) between 25 °C and 100°C due to removal of water molecules. SO<sub>4</sub>/Ti-SBA-15-10(AS) demonstrated two significant mass loss. First loss (5 wt.%) was similarly observed between 25 °C and 125 °C which was attributed to desorption of physisorbed water. Second loss (3 wt.%) was at 490 °C which could be due to the decomposition of sulphates [58]. Furthermore, it was noticed that weight loss of Ti-SBA-15 regarding desorption of physisorbed water was greater than sulfated catalysts. This result demonstrated that more hydrophobic nature and so less water adsorption capacity of SO<sub>4</sub>/Ti-SBA-15-10(AS) [59].

On the other hand, behavior of SO<sub>4</sub>/Ti-SBA-15-10(CS), SO<sub>4</sub>/Ti-SBA-15-6(CS) and SO<sub>4</sub>/SBA-15-(CS) was quite different. Weight loss of SO<sub>4</sub>/SBA-15-(CS) was higher than SO<sub>4</sub>/Ti-SBA-15-10(AS). It can be due to improvement of stability by titanium incorporation. However, a remarkable weight loss was found for the SO<sub>4</sub>/Ti-SBA-15-10(CS) and SO<sub>4</sub>/Ti-SBA-15-6(CS). It might be attributed to enhance of sulfur content with chlorosulfonic acid treatment and increase of titanium content. As a result of higher sulfur content, more weight loss may be noted [60].

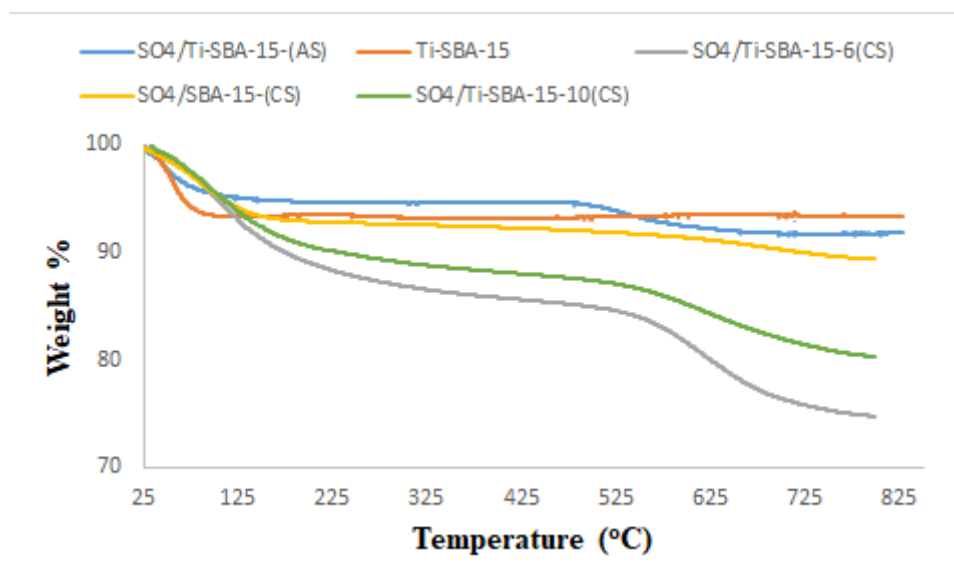


Figure 5.7. Thermal gravimetric analysis of SO<sub>4</sub>/SBA-15-(CS), Ti-SBA-15-10, SO<sub>4</sub>/Ti-SBA-15-10(AS), SO<sub>4</sub>/Ti-SBA-15-10(CS) and SO<sub>4</sub>/Ti-SBA-15-6(CS) catalysts

### 5.1.2. SO<sub>4</sub>/ TiO<sub>2</sub>-SiO<sub>2</sub> and SO<sub>4</sub>/La-TiO<sub>2</sub>-SiO<sub>2</sub> Catalysts

N<sub>2</sub> adsorption/desorption isotherms of SO<sub>4</sub>/TiO<sub>2</sub>-SiO<sub>2</sub>(AS), SO<sub>4</sub>/La-TiO<sub>2</sub>-SiO<sub>2</sub>(AS) and SO<sub>4</sub>/La-TiO<sub>2</sub>-SiO<sub>2</sub>(CS) catalysts are given in Figure 5.8. The catalysts demonstrated type 4 adsorption/desorption isotherms with H4 hysteresis loop and this represents the mesopore structure with slit shaped pores [51]. SO<sub>4</sub>/TiO<sub>2</sub>-SiO<sub>2</sub>(AS) and SO<sub>4</sub>/La-TiO<sub>2</sub>-SiO<sub>2</sub>(AS) possessed narrower H4 hysteresis loops while SO<sub>4</sub>/La-TiO<sub>2</sub>-SiO<sub>2</sub>(CS) showed larger H4 hysteresis loop. It may be due to increase of pore size and pore volume after chlorosulfonic acid treatment.

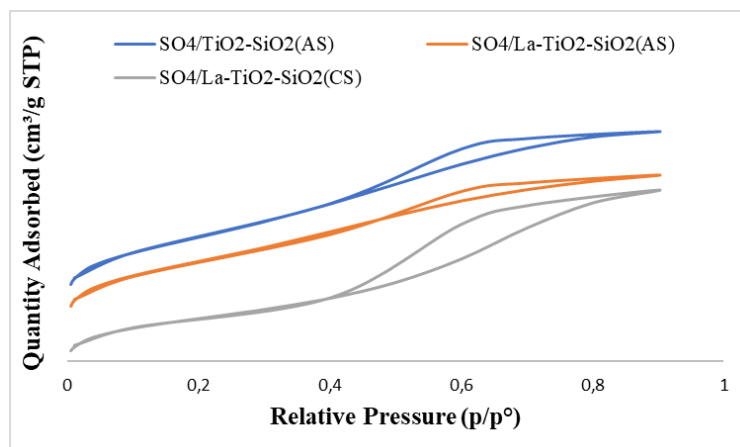


Figure 5.8. N<sub>2</sub> Adsorption/Desorption isotherms of SO<sub>4</sub>/TiO<sub>2</sub>-SiO<sub>2</sub>(AS), SO<sub>4</sub>/La-TiO<sub>2</sub>-SiO<sub>2</sub>(AS) and SO<sub>4</sub>/La-TiO<sub>2</sub>-SiO<sub>2</sub>(CS) catalysts

The catalysts were mesopore and had high surface area as given in Table 5.3. TiO<sub>2</sub>-SiO<sub>2</sub> had the highest surface area (691.4 m<sup>2</sup>/g) and it decreased to 462.2 m<sup>2</sup>/g after sulfation. La incorporation decreased surface area of catalysts. Also, La addition resulted a significant decrease in the pore volume. On the other hand, pore size of catalysts was affected slightly. Sulfation of La-TiO<sub>2</sub>-SiO<sub>2</sub> caused similarly decrease of surface area from 591.2 to 321.7 m<sup>2</sup>/g. Furthermore, high sulphur content was observed in the La incorporated catalysts due to the improvement of the interaction of the sulfate groups and catalysts with La addition. In addition, comparison of SO<sub>4</sub>/La-TiO<sub>2</sub>-SiO<sub>2</sub>(AS) and SO<sub>4</sub>/La-TiO<sub>2</sub>-SiO<sub>2</sub>(CS) catalysts showed that chlorosulfonic acid treatment enhanced the sulphur content more of the catalyst. On the other hand, a significant increase was observed at the pore size of SO<sub>4</sub>/La-TiO<sub>2</sub>-SiO<sub>2</sub>(CS). It might be due to decrease of micropores by strong acid treatment.

Table 5.3. Textural properties and sulphur content of La-TiO<sub>2</sub>-SiO<sub>2</sub>, TiO<sub>2</sub>-SiO<sub>2</sub>, SO<sub>4</sub>/TiO<sub>2</sub>-SiO<sub>2</sub>(AS), SO<sub>4</sub>/La-TiO<sub>2</sub>-SiO<sub>2</sub>(AS) and SO<sub>4</sub>/La-TiO<sub>2</sub>-SiO<sub>2</sub>(CS) catalysts

Catalyst	S <sub>BET</sub> (m <sup>2</sup> /g)	Pore Volume (cm <sup>3</sup> /g)	Pore Size (Å)	Sulphur content (wt.%)
TiO <sub>2</sub> -SiO <sub>2</sub>	691.7	0.62	39.7	-
SO <sub>4</sub> /TiO <sub>2</sub> -SiO <sub>2</sub> (AS)	462.2	0.35	34.4	0.44
La-TiO <sub>2</sub> -SiO <sub>2</sub>	591.2	0.36	33.4	-
SO <sub>4</sub> /La-TiO <sub>2</sub> -SiO <sub>2</sub> (AS)	440.5	0.29	33.5	0.68
SO <sub>4</sub> /La-TiO <sub>2</sub> -SiO <sub>2</sub> (CS)	321.7	0.38	46.1	0.92

Figure 5.9 represents the XRD patterns of  $\text{TiO}_2\text{-SiO}_2$  and  $\text{SO}_4/\text{TiO}_2\text{-SiO}_2(\text{AS})$  catalyst. They demonstrated amorphous silica structure and peaks of anatase titanium crystals was not observed. Figure 5.10 shows that XRD analysis of  $\text{La-TiO}_2\text{-SiO}_2$ ,  $\text{SO}_4/\text{La-TiO}_2\text{-SiO}_2(\text{AS})$  and  $\text{SO}_4/\text{La-TiO}_2\text{-SiO}_2(\text{CS})$  catalysts. There were no peaks related with anatase titanium and La species in their XRD analysis. This confirmed that homogenous distribution of titanium species, high dispersion of La in the catalyst [51].

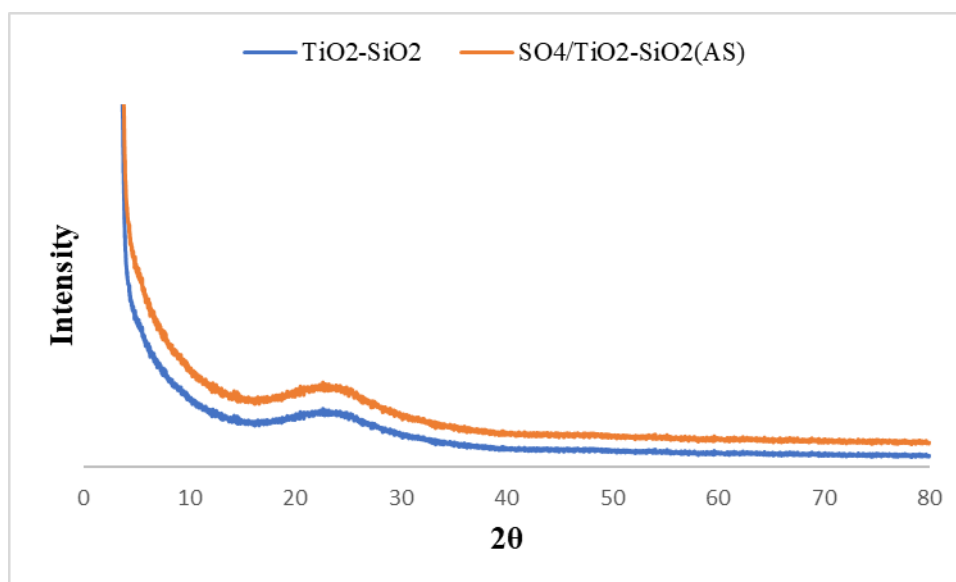


Figure 5.9. XRD patterns of  $\text{TiO}_2\text{-SiO}_2$  and  $\text{SO}_4/\text{TiO}_2\text{-SiO}_2(\text{AS})$  catalysts

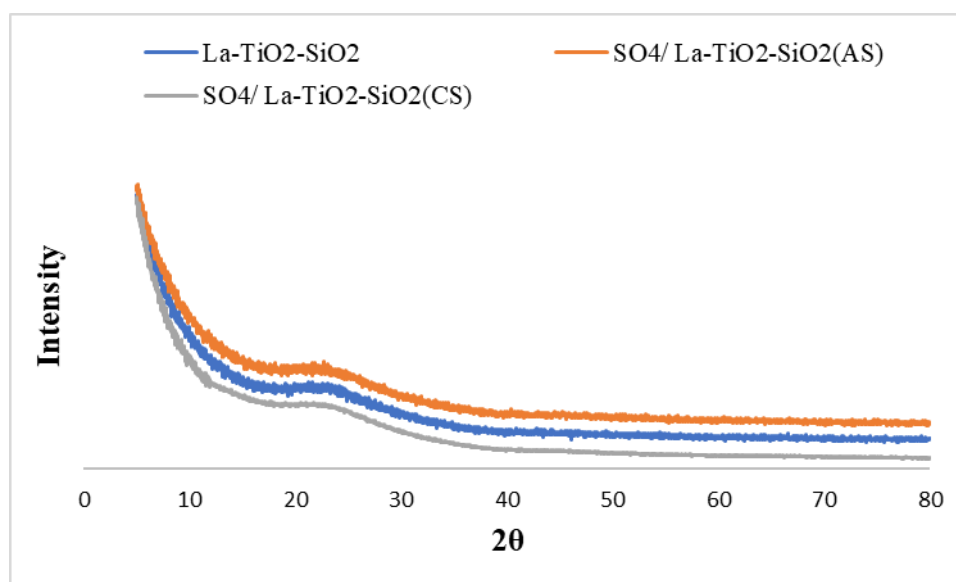


Figure 5.10. XRD patterns of  $\text{La-TiO}_2\text{-SiO}_2$ ,  $\text{SO}_4/\text{La-TiO}_2\text{-SiO}_2(\text{AS})$  and  $\text{SO}_4/\text{La-TiO}_2\text{-SiO}_2(\text{CS})$  catalysts

FTIR spectroscopy of sulphated  $\text{TiO}_2\text{-SiO}_2$  and  $\text{La-TiO}_2\text{-SiO}_2$  catalysts are given in Figure 5.11. A peak was observed at  $455\text{ cm}^{-1}$  due to Si-O-Si bending vibration. Also, peaks were noted at about  $813\text{ cm}^{-1}$  and  $1086\text{ cm}^{-1}$  as a result of symmetrical and asymmetrical stretching of Si-O-Si, respectively [65–67]. Furthermore, presence of  $\text{TiO}_2\text{-SiO}_2$  interaction was confirmed with the Ti-O-Si bond peak at  $947\text{ cm}^{-1}$  [64]. The peaks at about 1650 and 3500 originated from remaining adsorbed water molecules [65]. The intensity of this peak is relatively low for  $\text{SO}_4/\text{La-TiO}_2\text{-SiO}_2(\text{AS})$  and  $\text{SO}_4/\text{La-TiO}_2\text{-SiO}_2(\text{CS})$ . Thus, sulphated  $\text{La-TiO}_2\text{-SiO}_2$  catalyst can have more hydrophobic character and adsorbed less water. Although there was a expected peak between  $980\text{-}1300\text{ cm}^{-1}$  owing to vibration of sulfate groups, it was not present. This might be due to overlapping of the sulfated group and Si-O-Si vibrations [51].

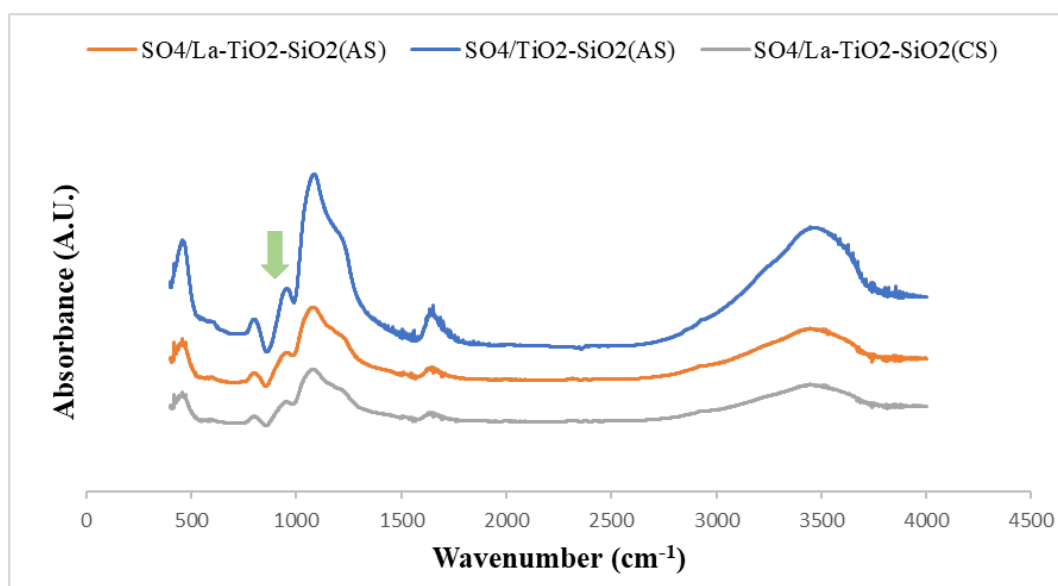


Figure 5.11. FTIR spectra of  $\text{SO}_4/\text{TiO}_2\text{-SiO}_2(\text{AS})$ ,  $\text{SO}_4/\text{La-TiO}_2\text{-SiO}_2(\text{AS})$  and  $\text{SO}_4/\text{La-TiO}_2\text{-SiO}_2(\text{CS})$  catalysts

$\text{NH}_3\text{-TPD}$  analysis of  $\text{TiO}_2\text{-SiO}_2$  and  $\text{SO}_4/\text{TiO}_2\text{-SiO}_2(\text{AS})$  catalysts was displayed in Figure 5.12.  $\text{TiO}_2\text{-SiO}_2$  had weak acid sites whereas their sulfated form had weak, moderate and strong acid sites. In addition, intensity of  $\text{SO}_4/\text{TiO}_2\text{-SiO}_2(\text{AS})$  was greater than  $\text{TiO}_2\text{-SiO}_2$  since total acidity was improved by sulfation. Acidic characteristic of  $\text{La-TiO}_2\text{-SiO}_2$  and  $\text{SO}_4/\text{La-TiO}_2\text{-SiO}_2$  was given in Figure 5.13. Similarly, strong acid sites were obtained by sulfation of  $\text{La-TiO}_2\text{-SiO}_2$ . Comparison of catalysts with and without La revealed that La addition increased the amount of total acid sites of catalysts because higher sulphur was captured on the surface of the catalyst via incorporation of La. It was confirmed with XRF results of catalysts (Table 5.3). Moreover, total amount of the acid

sites were determined quantitatively by integrating area under the peaks of each catalyst and results are given in the Table 5.4. The highest acidity was observed in the  $\text{SO}_4/\text{La-TiO}_2\text{-SiO}_2(\text{CS})$  that was consistent with sulphur content of catalyst obtained from XRF analysis.

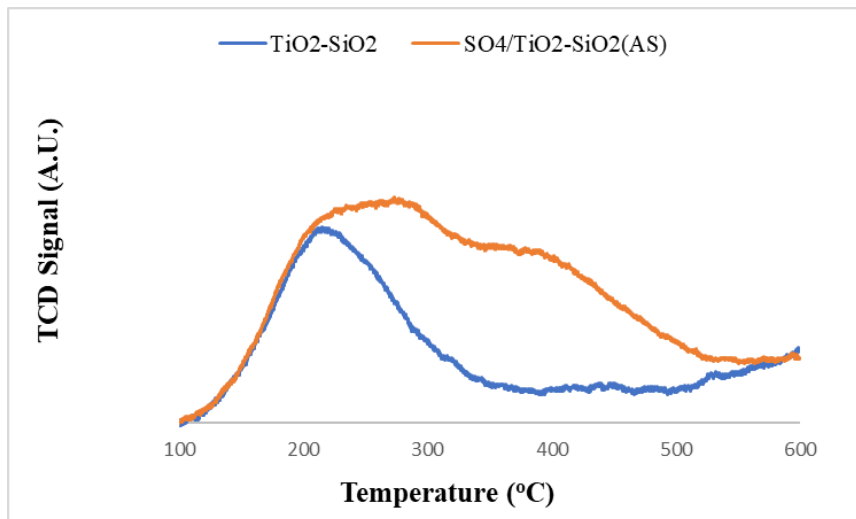


Figure 5.12.  $\text{NH}_3$ -TPD analysis of  $\text{TiO}_2\text{-SiO}_2$  and  $\text{SO}_4/\text{TiO}_2\text{-SiO}_2(\text{AS})$  catalysts

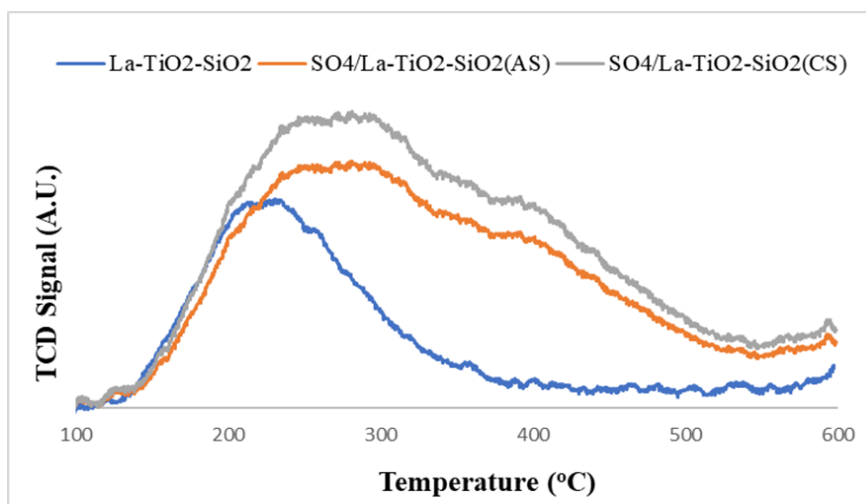


Figure 5.13.  $\text{NH}_3$ -TPD analysis of  $\text{La-TiO}_2\text{-SiO}_2$ ,  $\text{SO}_4/\text{La-TiO}_2\text{-SiO}_2(\text{AS})$  and  $\text{SO}_4/\text{La-TiO}_2\text{-SiO}_2(\text{CS})$  catalysts

Table 5.4. Total acidity of La-TiO<sub>2</sub>-SiO<sub>2</sub>, TiO<sub>2</sub>-SiO<sub>2</sub>, SO<sub>4</sub>/TiO<sub>2</sub>-SiO<sub>2</sub>(AS), SO<sub>4</sub>/La-TiO<sub>2</sub>-SiO<sub>2</sub>(AS) and SO<sub>4</sub>/La-TiO<sub>2</sub>-SiO<sub>2</sub>(CS) catalysts

Catalyst	Acidity (mmol NH <sub>3</sub> /gcat)
TiO <sub>2</sub> -SiO <sub>2</sub>	0.695
SO <sub>4</sub> /TiO <sub>2</sub> -SiO <sub>2</sub> (AS)	1.495
La-TiO <sub>2</sub> -SiO <sub>2</sub>	0.742
SO <sub>4</sub> /La-TiO <sub>2</sub> -SiO <sub>2</sub> (AS)	1.555
SO <sub>4</sub> /La-TiO <sub>2</sub> -SiO <sub>2</sub> (CS)	1.780

The TGA curves of La-TiO<sub>2</sub>-SiO<sub>2</sub>, TiO<sub>2</sub>-SiO<sub>2</sub>, SO<sub>4</sub>/TiO<sub>2</sub>-SiO<sub>2</sub>(AS), SO<sub>4</sub>/La-TiO<sub>2</sub>-SiO<sub>2</sub>(AS) and SO<sub>4</sub>/La-TiO<sub>2</sub>-SiO<sub>2</sub>(CS) catalysts are given in Figure 5.14. The highest thermal stability was obtained with La-TiO<sub>2</sub>-SiO<sub>2</sub>. Thermal stability was enhanced significantly with La addition which is in accordance with literature [53]. All the catalysts initially showed weight loss based on releasing of physisorbed water. Furthermore, another prominent weight loss was observed for the sulfated catalysts due to decomposition of sulphates about 450 °C [66]. As a result, sulfation caused a decrease on the thermal stability of the catalyst. In addition, chlorosulfonic acid treatment (SO<sub>4</sub>/La-TiO<sub>2</sub>-SiO<sub>2</sub>(CS)) caused more weight loss than ammonium sulfate (SO<sub>4</sub>/La-TiO<sub>2</sub>-SiO<sub>2</sub>(AS)) since SO<sub>4</sub>/La-TiO<sub>2</sub>-SiO<sub>2</sub>(CS) had higher sulfur content [60]. However, the sulfated catalysts can be used conveniently since ring opening reactions were performed below 450 °C.

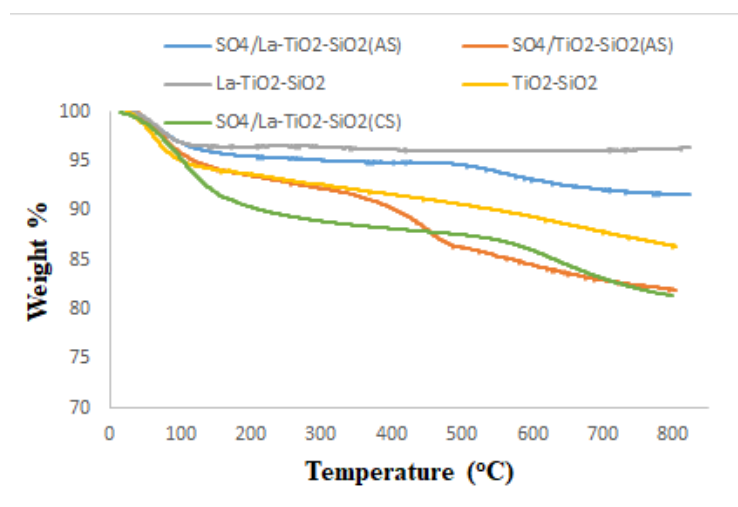


Figure 5.14. Thermal gravimetric analysis of TiO<sub>2</sub>-SiO<sub>2</sub>, La-TiO<sub>2</sub>-SiO<sub>2</sub>, SO<sub>4</sub>/TiO<sub>2</sub>-SiO<sub>2</sub>(AS) and SO<sub>4</sub>/La-TiO<sub>2</sub>-SiO<sub>2</sub>(AS) catalysts

## 5.2 Activity and Stability of the Catalysts

### 5.2.1 Biolubricant Production from Epoxidized Soybean Oil with 2-propanol Reaction

First of all, the ring opening reaction of epoxidized soybean oil was carried out with a commercial acid catalyst Amberlyst-15 in the presence of 2-propanol to specify optimum reaction temperature, alcohol/epoxide mol ratio and catalyst loading. The results are given in Table 5.5. Increasing of temperature from 60°C to 80°C increased the conversion from 10 to 27%. Although temperature had a positive effect on the conversion, the reactions could not carry out above 80°C because of low boiling point of 2-propanol (82.5°C). In addition, effect of alcohol/epoxide mol ratio was investigated. It was determined that high alcohol/epoxide mol ratio was more effective in the reaction. Furthermore, catalyst loading was studied. Higher conversion was obtained with increasing of catalyst loading. As a result, optimum reaction temperature, alcohol/epoxide mol ratio and catalyst loading was found as 80°C, 10/1 and 10 wt.% respectively.

Table 5.5. Ring opening reaction of epoxidized soybean oil with 2-propanol in the presence of Amberlyst-15

Catalyst	Alcohol	Catalyst Amount	Alcohol/epoxide mol ratio	Reaction Condition	Conversion
Amberlyst-15	2-propanol	10 wt%	10/1	60°C, 6h, 1000 rpm	10%
				70°C, 6h, 1000 rpm	14%
				80°C, 6h, 1000 rpm	27%
		7 wt%	80°C, 6h, 1000 rpm	21%	
		7 wt%	80°C, 6h, 1000 rpm	8%	
		10 wt%	80°C, 6h, 1000 rpm	12%	

The activity and stability of SO<sub>4</sub>/Ti-SBA-15-10(AS), SO<sub>4</sub>/La-TiO<sub>2</sub>-SiO<sub>2</sub> and SO<sub>4</sub>/TiO<sub>2</sub>-SiO<sub>2</sub> were tested after determination optimum reaction temperature and alcohol/epoxide mol ratio. Conversion results and sulphur leaching amount are given in Table 5.6.

Table 5.6. Activity and Stability of SO<sub>4</sub>/Ti-SBA-15-10(AS), SO<sub>4</sub>/La-TiO<sub>2</sub>-SiO<sub>2</sub> and SO<sub>4</sub>/TiO<sub>2</sub>-SiO<sub>2</sub> catalysts (Reaction Condition: 80 °C, 6 h, 10/1 alcohol/epoxide mol ratio, 10 wt.% catalyst)

Catalyst	Epoxide Conversion	Catalyst Sulphur Content before reaction (wt.%)	Catalyst Sulphur Content after reaction (wt.%)	Sulphur Leaching
SO <sub>4</sub> /Ti-SBA-15-10(AS)	32%	0.56	0.32	42%
SO <sub>4</sub> /TiO <sub>2</sub> -SiO <sub>2</sub> (AS)	25%	0.44	0.18	62%
SO <sub>4</sub> /La-TiO <sub>2</sub> -SiO <sub>2</sub> (AS)	28%	0.68	0.30	55%

Ti-SBA-15 and La-TiO<sub>2</sub>-SiO<sub>2</sub> were sulfated with different sulfate source which is chlorosulfonic acid to determine the effect of sulfate source on the stability and activity of the catalysts. The results are given in the Table 5.7.

Table 5.7. Activity and Stability of SO<sub>4</sub>/Ti-SBA-15-10(AS), SO<sub>4</sub>/Ti-SBA-15-10(CS), SO<sub>4</sub>/Ti-SBA-15-6(CS), SO<sub>4</sub>/SBA-15-(CS) with reactions of 2-propanol (Reaction Condition: 80 °C, 6 h, 10/1 alcohol/epoxide mol ratio, 10 wt.% catalyst)

Catalyst	Epoxide Conversion	Catalyst Sulphur Content before reaction (wt.%)	Catalyst Sulphur Content after reaction (wt.%)	Sulphur Leaching
SO <sub>4</sub> /Ti-SBA-15-10(AS)	32%	0.56	0.32	42%
SO <sub>4</sub> /Ti-SBA-15-10(CS)	28%	0.89	0.73	17%
SO <sub>4</sub> /Ti-SBA-15-6(CS)	39%	1.49	1.26	15%
SO <sub>4</sub> /SBA-15-(CS)	26%	0.14	0.06	57%
SO <sub>4</sub> /La-TiO <sub>2</sub> -SiO <sub>2</sub> (AS)	28%	0.68	0.30	55%
SO <sub>4</sub> /La-TiO <sub>2</sub> -SiO <sub>2</sub> (CS)	29%	0.92	0.74	20%

The sulphur leaching of Ti-SBA-15-10(AS) decreased from 42% to 17% with chlorosulfonic acid treatment. In addition, it was expected that increase of conversion due to higher sulphur content of SO<sub>4</sub>/Ti-SBA-15-10(CS) but the conversion decreased slightly from 32% to 28%. It can be ascribed to lower surface area of SO<sub>4</sub>/Ti-SBA-15-10(CS) as

shown in the catalyst characterization section (Chapter 5). Since chlorosulfonic acid treatment provided more stable catalyst than ammonium sulphate, studies were proceeded with using chlorosulfonic acid and effect of titanium was investigated. For this purpose,  $\text{SO}_4/\text{SBA-15-(CS)}$  without titanium incorporation,  $\text{SO}_4/\text{Ti-SBA-15-10(CS)}$  with Si/Ti:10 and  $\text{SO}_4/\text{Ti-SBA-15-6(CS)}$  with Si/Ti:6 catalysts were compared. Although  $\text{SO}_4/\text{Ti-SBA-15-6(CS)}$  had even lower surface area, it provided the highest (39%) conversion as a result of its considerable high sulphur content (Table 5.7). As a result, it was concluded that acidity of catalyst should be high for the high catalytic performance. Furthermore, the catalyst stability improved slightly. In addition,  $\text{SBA-15-(CS)}$  catalyst was investigated. It provided 26% conversion however its stability was found as quite low, 57% leaching was observed. In this context, titanium incorporation enhanced considerably stability of catalyst. The lowest leaching and best conversion were obtained with  $\text{SO}_4/\text{Ti-SBA-15-6(CS)}$ . Higher stability of titanium incorporated catalyst is associated with formation of strong chelate bonds between Ti-O-Si that was explained in the literature [50]. In addition, titanium displayed a positive effect on the conversion. It can be due to more acidic nature of catalyst with higher titanium content. Furthermore,  $\text{SO}_4/\text{La-TiO}_2\text{-SiO}_2\text{(AS)}$  and  $\text{SO}_4/\text{La-TiO}_2\text{-SiO}_2\text{(CS)}$  demonstrated similar catalytic performance however stability of  $\text{SO}_4/\text{La-TiO}_2\text{-SiO}_2\text{(CS)}$  was much better. Hereby, leaching of catalysts decreased significantly with chlorosulfonic acid treatment. This result was attributed to the stronger interaction of chlorosulfonic acid with catalyst surface as it reported in the literature [42].

Washing of catalysts with deionized water or solvent can be effective for the elimination for physically absorbed sulfate species [68]. Hence, the leaching can be minimized and more stable catalysts can be obtained. In this regard, the  $\text{SO}_4/\text{Ti-SBA-15-10(CS)}$  was washed with hot water and 2-propanol (70-80°C) until a clear solution was obtained (3 cycle). The photos taken are given in Figure 5.15. Sulphur content of catalyst before and after washing were analyzed. After that, its activity and sulphur content after reaction was tested. As shown Table 5.8, hot water washing caused the loss of most of the sulfate groups. Sulphur content of catalyst decreased from 0.89 to 0.22 after washing. In addition, it had still sulphur leaching in the reaction. Thus, a dramatic decrease was observed in the activity of the catalyst. Besides, washing of the catalyst with 2-propanol resulted less sulphur leaching. However, it exhibited 34% sulphur leaching in the reaction. Consequently, hot water or 2-propanol washing was not found

as suitable for SO<sub>4</sub>/Ti- SBA-15-10(CS) catalyst in terms of improvement of stability. However, it was noticed that the sulphur leaching was more significant with hydration of Bronsted acid sites.

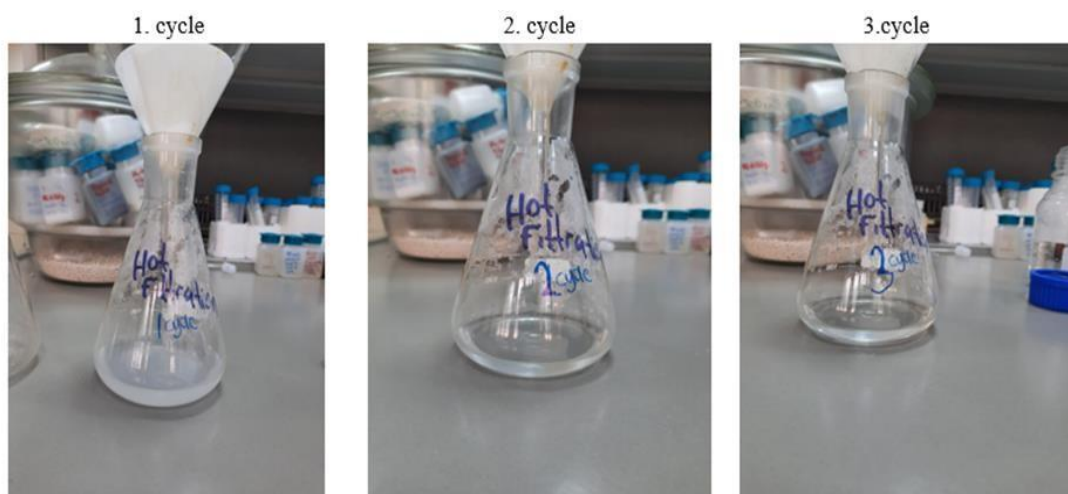


Figure 5.15. Washing of SO<sub>4</sub>/Ti-SBA-15-10(CS)

Table 5.8. Activity and stability of hot filtrated SO<sub>4</sub>/Ti-SBA-15-10(CS) catalyst

Catalyst	Sulphur Content of fresh catalyst (wt.%)	Catalyst Sulphur Content after washing (wt.%)	Epoxide Conversion	Catalyst Sulphur Content after reaction (wt.%)	Sulphur Leaching
SO <sub>4</sub> /Ti-SBA-15-10(CS) *water washed	0.89	0.22	10%	0.15	32%
SO <sub>4</sub> /Ti-SBA-15-10(CS) *2-propanol washed	0.89	0.74	15%	0.49	34%

As a result of all above discussion, most stable and active catalyst was found as SO<sub>4</sub>/Ti-SBA-15-10(CS) and SO<sub>4</sub>/Ti-SBA-15-6(CS). Products obtained with these catalysts were further analyzed with FT-IR and H-NMR analysis. The FT-IR spectrum of epoxidized soybean oil and ring opening reaction products with SO<sub>4</sub>/Ti-SBA-15-10(CS) and SO<sub>4</sub>/Ti-SBA-15-6(CS) are given in the Figure 5.16. The products obtained with SO<sub>4</sub>/Ti-SBA-15-10(CS) and SO<sub>4</sub>/Ti-SBA-15-6(CS) were labelled as 2prop.CSTi10 and 2prop.CSTi6, respectively. The peak between 823-844 cm<sup>-1</sup> was attributed to epoxy groups [69]. This peak was more prominent for the epoxidized soybean oil whereas its intensity decreased in the products showing ring opening of some of the epoxy groups.

Epoxide conversion and attachment of hydroxyl groups via alkoxylation was further confirmed with increasing the intensity of peaks at  $3400\text{ cm}^{-1}$ . This peaks indicates the presence of the hydroxyl O-H stretching [36]. Another essential peak was found at  $1740\text{ cm}^{-1}$  that was ascribed to ester structure of the products. Moreover, there were characteristic peaks for both epoxidized soybean oil and products due to presence of triglyceride in their structure. The peaks at  $725$ ,  $1379$  and  $1463\text{ cm}^{-1}$  implies that  $\text{CH}_2$  rocking vibration,  $\text{CH}_3$  symmetrical bending and  $\text{CH}_2$  bending vibration, respectively [70]. In addition, peaks at  $2927$  and  $2858\text{ cm}^{-1}$  are related with methylene asymmetric and symmetric stretching [71].

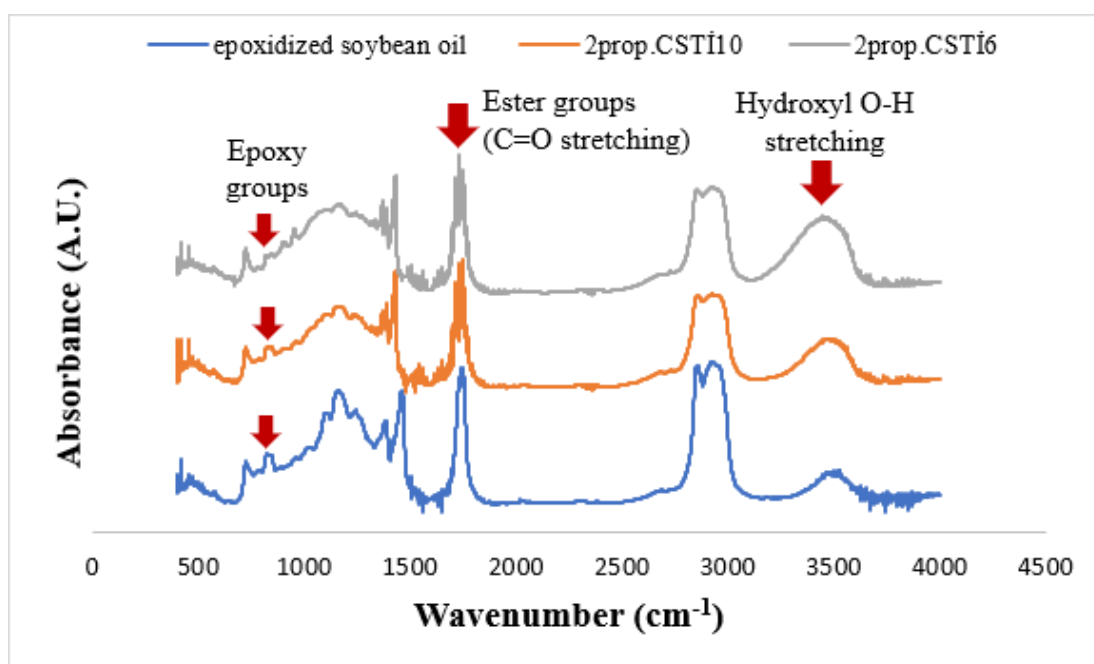


Figure 5.16. FTIR spectrum of epoxidized soybean oil and product of epoxidized soybean oil ring opening reaction (Alcohol: 2-propanol, Catalysts:  $\text{SO}_4/\text{Ti-SBA-15-10}(\text{CS})$  and  $\text{SO}_4/\text{Ti-SBA-15-6}(\text{CS})$  catalysts)

H-NMR spectra of epoxidized soybean oil is presented in Figure 5.17. The peaks of characteristic epoxy groups were observed between 2.8-3.2 ppm region [14]. Also, it was noticed that signals of some common peaks and their peak assignment is given in Table 5.9. The H-NMR spectra of ring opening product of epoxidized soybean oil with 2-propanol by  $\text{SO}_4/\text{Ti-SBA-15-10}(\text{CS})$  catalyst is given in Figure 5.18. As shown below, epoxy groups were still exist however their intensity decreased. Thus,

conversion of some epoxy groups was confirmed (28% conversion). Nonetheless, Figure 5.19 demonstrated that intensity decrease of epoxy groups was more significant since higher conversion was obtained with SO<sub>4</sub>/Ti-SBA-15-6(CS) (39% conversion). Additionally, a new peak appeared at 3.60 ppm owing to attachment OH of 2-propanol to ring opened product [35].

Table 5.9. H-NMR spectrum peak assignment [14]

Functional groups	Peak signals (ppm)
methine proton of $-\text{CH}_2-\text{CH}-\text{CH}_2$ backbone	5.1-5.3
methylene proton of $-\text{CH}_2-\text{CH}-\text{CH}_2-$ glycerol's backbone	4.0-4.4
$\alpha$ - $\text{CH}_2$ to $>\text{C}=\text{O}$	2.2-2.4
$\alpha$ - $\text{CH}_2$ connected epoxy group	1.7-1.9
$\beta$ - $\text{CH}_2$ to $>\text{C}=\text{O}$	1.55-1.7
$\beta$ - $\text{CH}_2$ connected epoxy group	1.4-1.55
terminal $-\text{CH}_3$ groups	0.8-1.0

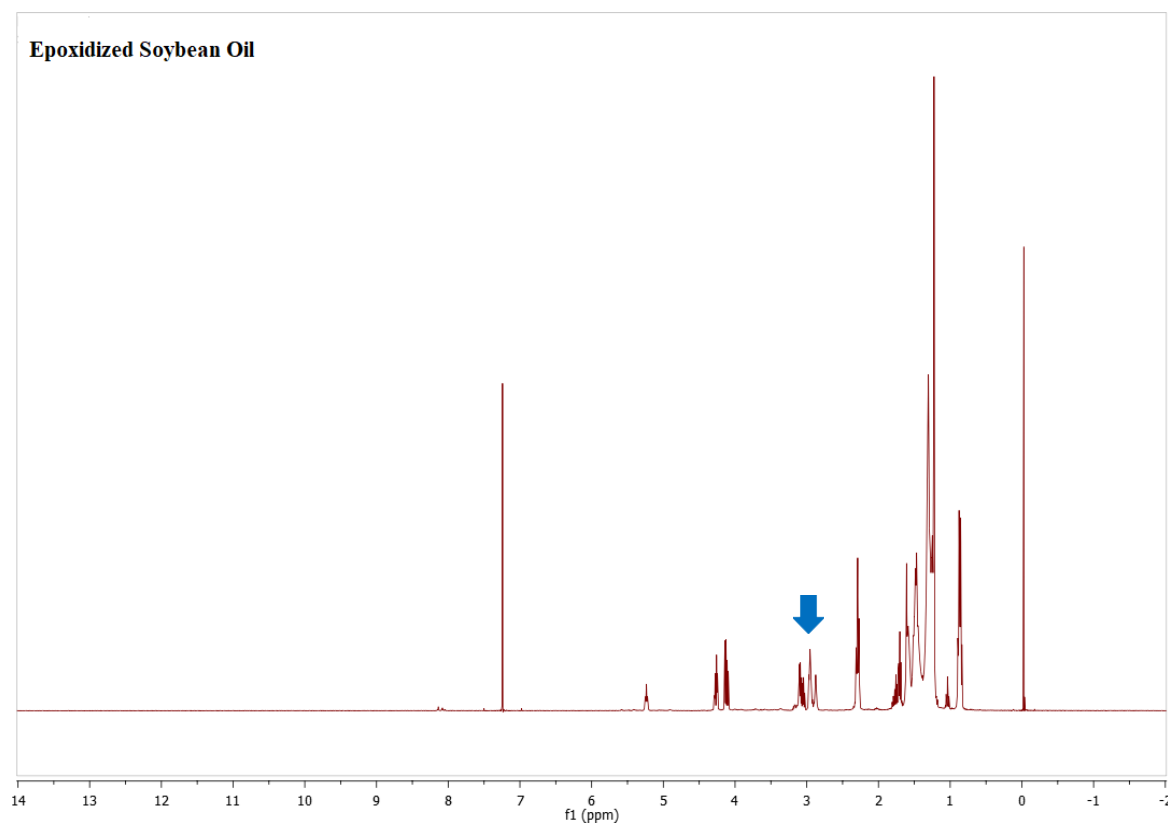


Figure 5.17. H-NMR spectrum of epoxidized soybean oil

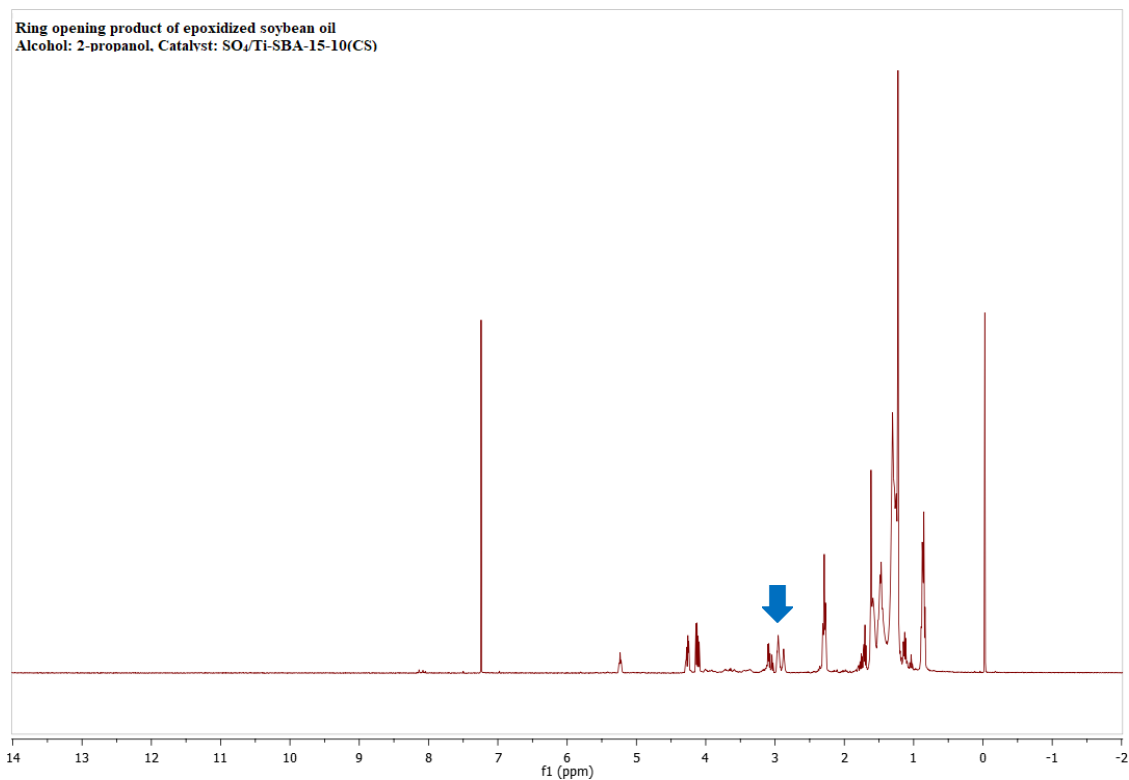


Figure 5.18.  $^1\text{H}$ NMR spectrum of ring opening product with 2-propanol by  $\text{SO}_4/\text{Ti-SBA-15-10}(\text{CS})$  catalyst

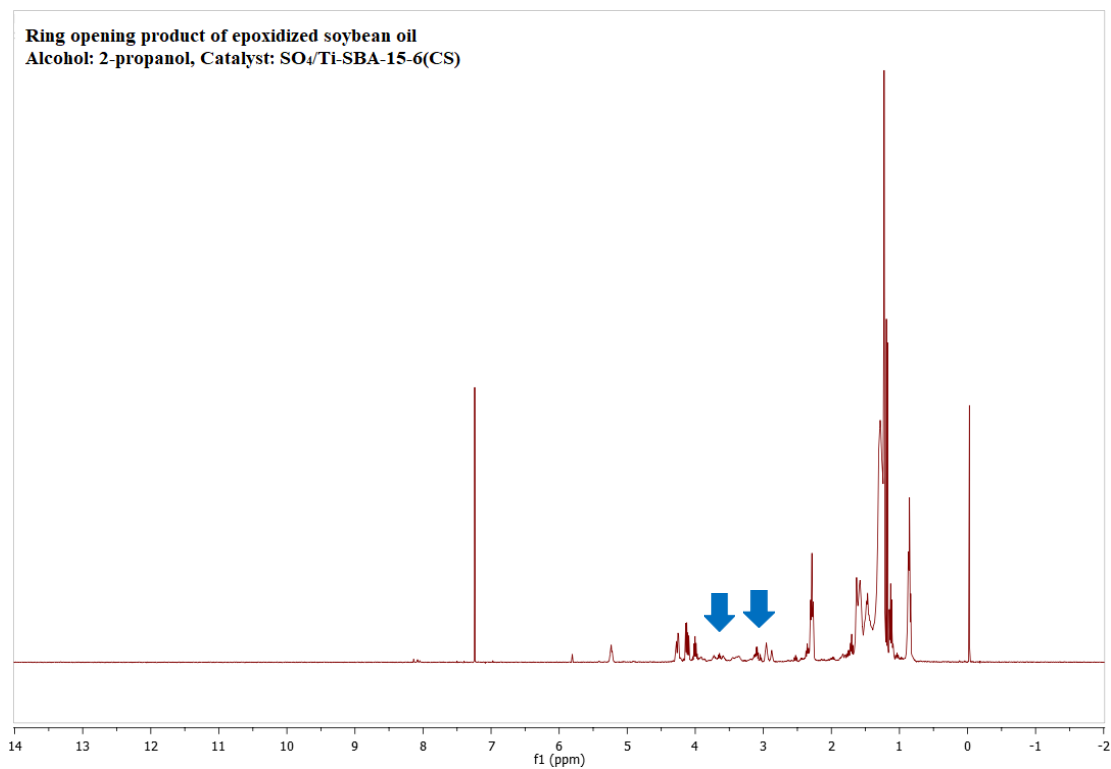


Figure 5.19.  $^1\text{H}$ NMR spectrum of ring opening product with 2-propanol by  $\text{SO}_4/\text{Ti-SBA-15-6}(\text{CS})$  catalyst

Reusability studies  $\text{SO}_4/\text{Ti-SBA-15-10}(\text{CS})$  and  $\text{SO}_4/\text{Ti-SBA-15-6}(\text{CS})$  were also performed. As shown in Figure 5.20, activity of  $\text{SO}_4/\text{Ti-SBA-15-10}(\text{CS})$  decreased from 28% to 9% at the end of three cycle. Similarly, there was activity loss with the  $\text{SO}_4/\text{Ti-SBA-15-6}(\text{CS})$ . These results were attributed to sulphur leaching of catalyst. Sulphur content of  $\text{SO}_4/\text{Ti-SBA-15-10}(\text{CS})$  decreased to from 0.89 to 0.59 wt.% and sulphur content of  $\text{SO}_4/\text{Ti-SBA-15-6}(\text{CS})$  decreased to from 1.49 to 0.88 wt.%.

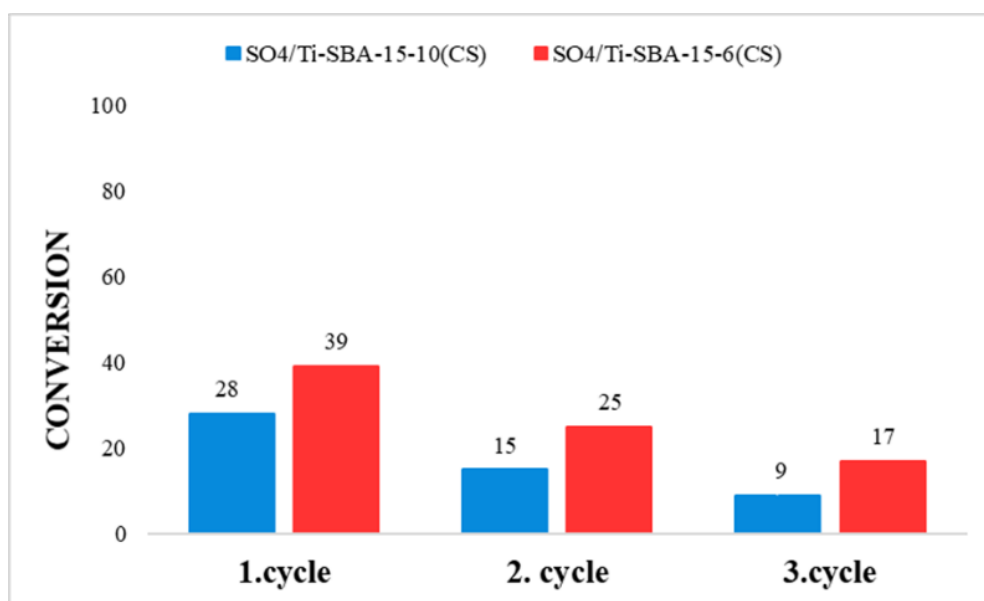


Figure 5.20. Reusability of  $\text{SO}_4/\text{Ti-SBA-15-10}(\text{CS})$  and  $\text{SO}_4/\text{Ti-SBA-15-6}(\text{CS})$  in the reactions of 2-propanol

In conclusion,  $\text{SO}_4/\text{Ti-SBA-15-6}(\text{CS})$  was found as the most stable and active catalyst. Therefore, catalyst loading was studied parametrically with the  $\text{SO}_4/\text{Ti-SBA-15-6}(\text{CS})$ . For this purpose, the catalyst amount was varied from 7 to 20 wt. % according to epoxy soybean oil amount. The results are given in the Figure 5.21. It was observed as a positive effect on the conversion with increasing catalyst loading. It was attained 29% epoxide conversion with 7 wt.% catalyst loading whereas 20 wt.% catalyst loading provided 52 % conversion. Besides catalyst loading, effect of reaction time on conversion was also investigated. Reactions were performed for 3, 6 and 12 h. As shown in Figure 5.22, prolong of reaction time increased the epoxide conversion.

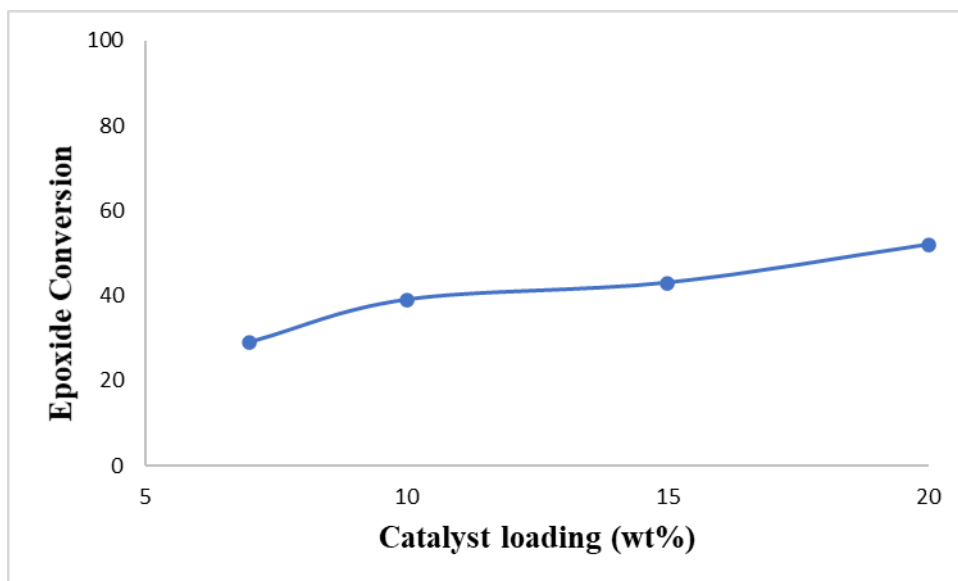


Figure 5.21. Effect of the catalyst loading on the conversion  
(Reaction Condition: 80 °C, 6 h, 10/1 alcohol/epoxide mol ratio, 10 wt.% catalyst)

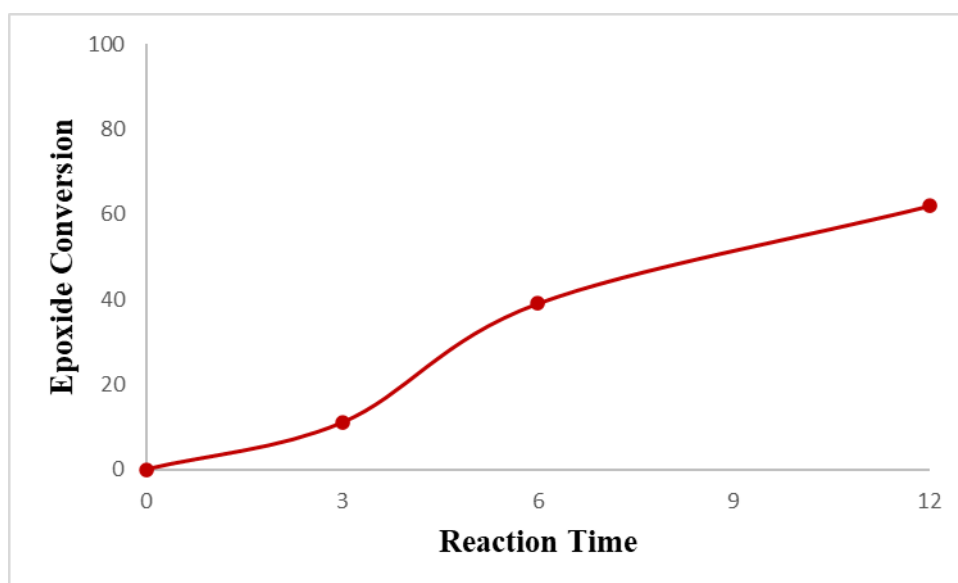


Figure 5.22. Effect of the reaction time on the conversion  
(Reaction Condition: 80 °C, 10/1 alcohol/epoxide mol ratio, 10 wt.% catalyst)

### 5.2.2. Biolubricant Production from Epoxidized Soybean Oil with 2-ethyl hexanol Reaction

Reactions with 2-propanol demonstrated that SO<sub>4</sub>/Ti-SBA-15-10(AS), SO<sub>4</sub>/Ti-SBA-15-10(CS) and SO<sub>4</sub>/Ti-SBA-15-6(CS) were more active and stable catalysts. In this

context, activity of these catalysts was further studied in the ring opening reactions with 2-ethylhexanol. It was reported that in the literature, longer reaction time and higher temperature are required for the long chain branched alcohols [26]. Hence, reaction conditions were studied with Amberlyst-15 prior to activity test of SO<sub>4</sub>/Ti-SBA-15-10(AS), SO<sub>4</sub>/Ti-SBA-15-10(CS) and SO<sub>4</sub>/Ti-SBA-15-6(CS). The results are given in Table 5.10. It was found that 6 h and 80°C were not favorable for the ring opening reaction with 2-ethyl hexanol. On the other hand, prolong reaction period and rise of temperature exhibited a great effect on the conversion. It increased from 18 to 59%. Thus, the results obtained were in line with findings with literature. Also, lower alcohol/epoxide mol ratio (6/1) could be used as reaction followed a different mechanism than 2-propanol. Short alcohols such as 2-propanol follows as Eley-Rideal mechanisms. In this mechanism, there is need for higher amount of alcohol since alcohol is not adsorbed on the catalyst. Long alcohols such as 2-ethylhexanol follows the the Langmuir–Hinshelwood– Hougen–Watson mechanism. In this mechanism, alcohol is adsorbed on the active sites of catalysts [31]. As a result, reactions were further carried out with 6/1 alcohol/epoxide mol ratio at 100°C for 18 h.

Table 5.10. Ring opening reaction epoxidized soybean oil with 2-ethyl hexanol in the presence of Amberlyst-15

Catalyst	Catalyst Amount	Alcohol	Alcohol/epoxide mol ratio	Reaction Condition	Epoxide Conversion
Amberlyst-15	7 wt.%	2-ethyl hexanol	6/1	6h, 80°C 1000 rpm	18%
				6h, 100°C 1000 rpm	30%
				18h, 100°C 1000 rpm	59%

As shown in Table 5.11, promising catalytic performance was obtained in the ring opening reactions with 2-ethyl hexanol. The activity of SO<sub>4</sub>/Ti-SBA-15-10(CS) (80 % conversion) was determined as slightly lower than SO<sub>4</sub>/Ti-SBA-15-10(AS) (85 % conversion). However, chlorosulfonic acid treatment enhanced stability of catalyst. Furthermore, SO<sub>4</sub>/Ti-SBA- 15-6(CS) demonstrated the highest activity since increasing titanium content was advantageous regarding acidic nature of the catalyst. Besides it was noted that SO<sub>4</sub>/Ti- SBA-15-10(CS) and SO<sub>4</sub>/Ti-SBA-15-6(CS) were more stable than SO<sub>4</sub>/Ti-SBA-15- 10(AS). On the other hand, all catalysts were more stable in the reactions with 2-ethyl hexanol than reactions with 2-propanol (see Table 5.6 and 5.7)

even though reactions of 2-ethyl hexanol was performed at higher temperature and longer time. The difference observed in leaching behavior of catalysts can be explained with the study performed by Sadaba et al. (2015) [68]. They stated that reaction medium is a crucial parameter and polarity of medium can affect the stability of the catalysts. More polar solvents can lead to increase of sulphur leaching. In addition, epoxide conversion was above 80% in the reactions of 2-ethylhexanol whereas it was maximum 39 % in the reactions of 2-propanol. Reason of this situation could be due to higher reaction temperature changing from 80 to 100 °C.

Table 5.11. Activity and Stability of SO<sub>4</sub>/Ti-SBA-15-10(AS), SO<sub>4</sub>/Ti-SBA-15-10(CS), SO<sub>4</sub>/Ti-SBA-15-6(CS) reactions of 2-ethylhexanol

Catalyst	Epoxide Conversion (%)	Catalyst Sulphur Content before reaction (wt.%)	Catalyst Sulphur Content after reaction (wt.%)	Sulphur Leaching
SO <sub>4</sub> /Ti-SBA-15-10(AS)	85%	0.56	0.49	12%
SO <sub>4</sub> /Ti-SBA-15-10(CS)	80%	0.89	0.80	10%
SO <sub>4</sub> /Ti-SBA-15-6(CS)	90%	1.49	1.34	10%

It was concluded that SO<sub>4</sub>/Ti-SBA-15-10(CS) and SO<sub>4</sub>/Ti-SBA-15-6(CS) showed less sulphur leaching than SO<sub>4</sub>/Ti-SBA-15-10(AS). Products attained with the SO<sub>4</sub>/Ti-SBA-15-10(CS) and SO<sub>4</sub>/Ti-SBA-15-6(CS) were labelled as 2ethex.CSTi10 and 2ethex.CSTi6, respectively and they were also investigated with FT-IR and H-NMR analysis. FTIR spectra of them and epoxidized soybean oil are given in Figure 5.23. Peaks of epoxy groups (823-844 cm<sup>-1</sup>) was almost disappeared as a result of high catalytic performance of the catalysts [34]. Moreover, an increase was observed in the intensity of hydroxyl stretching peaks for both products but it was more apparent in the 2ethex.CSTi6. Thus, better performance of SO<sub>4</sub>/Ti-SBA-15-6(CS) was confirmed. HNMR spectrum of the products are given in Figure 5.24 and 5.25. Signals of epoxy groups (2.8-3.2 ppm) significantly decreased and a new peak was observed at 3.44 ppm that might be responsible from OH of 2-ethylhexanol [72].

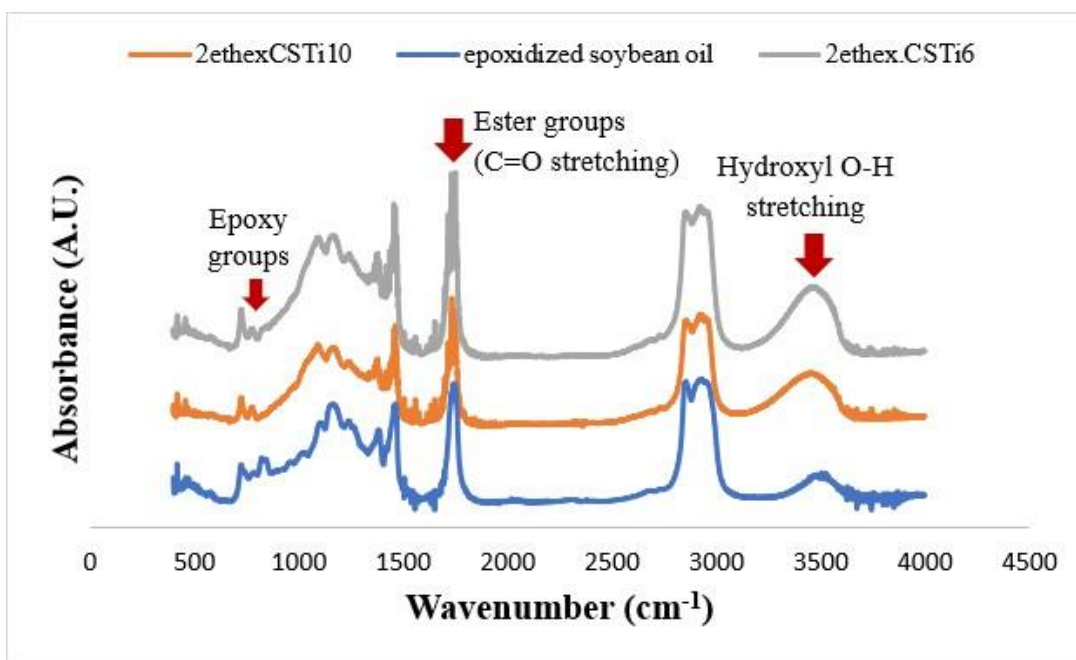


Figure 5.23. FTIR spectrum of epoxidized soybean oil and product of epoxidized soybean oil ring opening reaction (Alcohol: 2-ethyl hexanol, Catalysts:  $\text{SO}_4/\text{Ti-SBA-15-10}(\text{CS})$  and  $\text{SO}_4/\text{Ti-SBA-15-6}(\text{CS})$  catalysts)

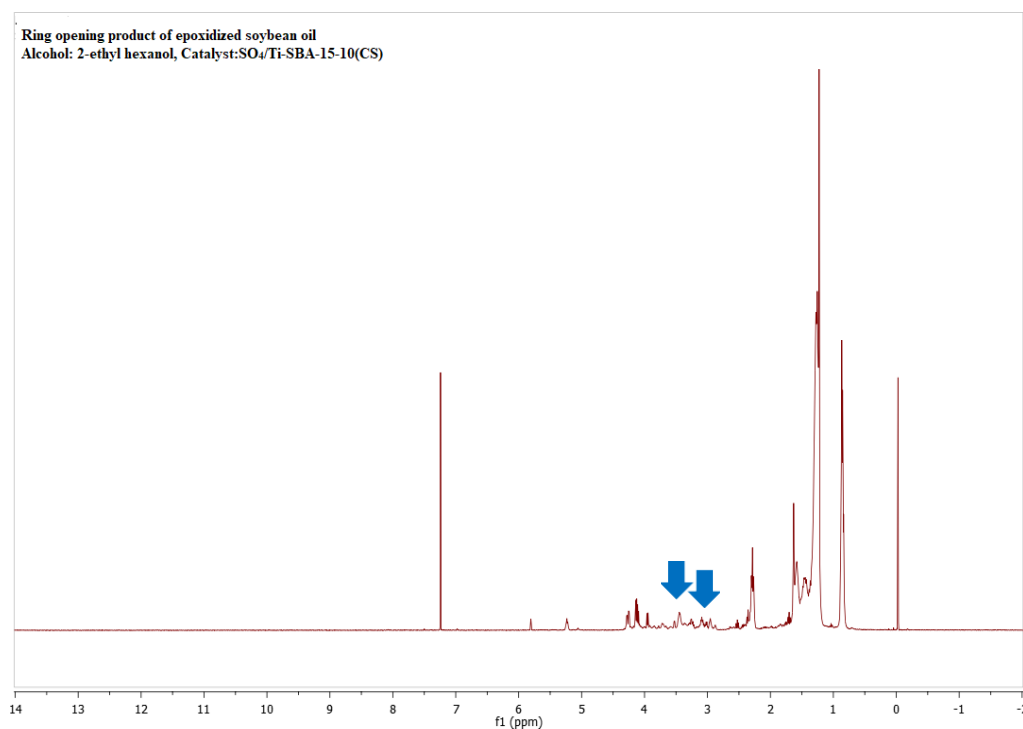


Figure 5.24.  $^1\text{H}$ NMR spectrum of ring opening product with 2-ethyl hexanol by  $\text{SO}_4/\text{Ti-SBA-15-10}(\text{CS})$  catalyst

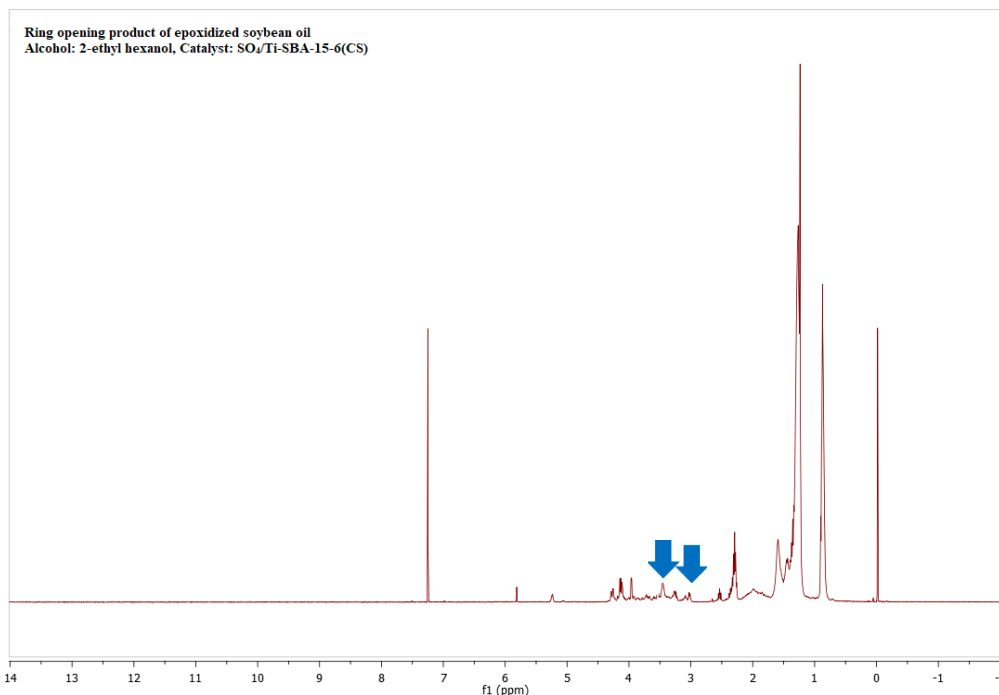


Figure 5.25. HNMR spectrum of ring opening product with 2-ethyl hexanol by  $\text{SO}_4/\text{Ti-SBA-15-6(CS)}$  catalyst

Reusability of  $\text{SO}_4/\text{Ti-SBA-15-6(CS)}$  was examined and it was used in the three successive runs.  $\text{SO}_4/\text{Ti-SBA-15-6(CS)}$  lost its activity in each cycle because of leaching of sulphate groups. Activity results of each run are shown in Figure 5.26. Fresh  $\text{SO}_4/\text{Ti-SBA-15-6(CS)}$  had 1.49 wt.% sulphur content and it decreased the 1.08 wt.% after 3 cycles. Furthermore, parametric study of reaction time showed that epoxide conversion was enhanced by increasing reaction period.

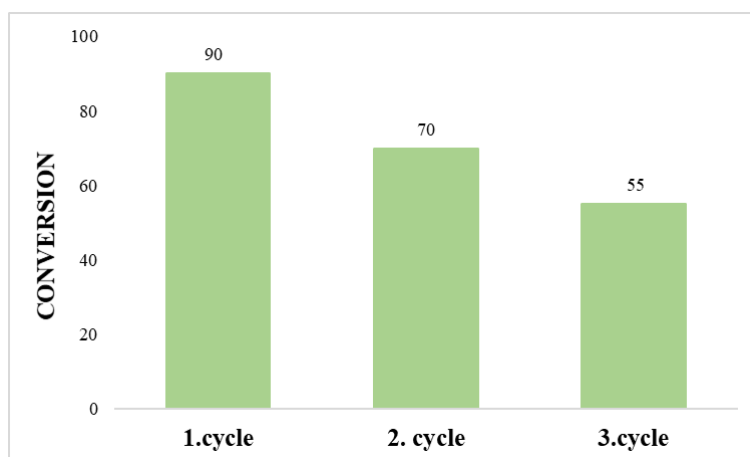


Figure 5.26. Reusability of  $\text{SO}_4/\text{Ti-SBA-15-6(CS)}$  in the reactions of 2-ethyl hexanol

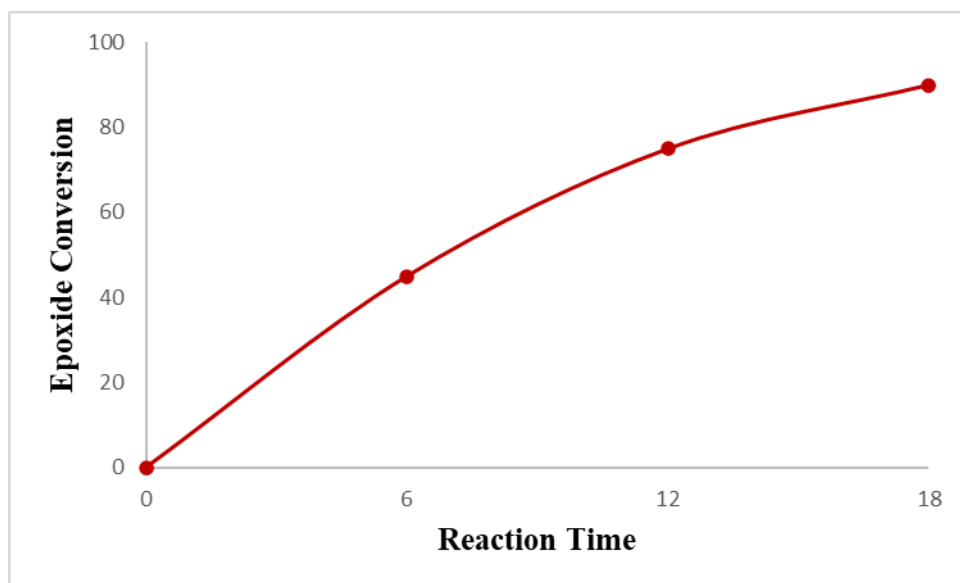


Figure 5.27. Effect of the reaction time on the conversion  
(Reaction Condition: 100 °C, 6/1 alcohol/epoxide mol ratio, 7 wt.% catalyst)

## 5.2. Physicochemical Properties of the Obtained Biolubricants

Physicochemical properties are important parameters for the biolubricants. Biolubricants should have high thermal stability and good low temperature properties. Products obtained with more active and stable catalysts for both alcohols were labelled as shown in Table 5.12. Thermal stability and low temperature behavior of products were analyzed with TGA and DSC analysis, respectively.

Table 5.12. Names of products obtained with more active and stable catalysts

Product name	Alcohol	Catalyst	Conversion	Leaching
2-prop.CSTi-10	2-propanol	SO <sub>4</sub> /Ti-SBA-15-10(CS)	28%	17%
2-prop.CSTi-6		SO <sub>4</sub> /Ti-SBA-15-6(CS)	39%	15%
2-ethex.CSTi-10	2-Ethyl hexanol	SO <sub>4</sub> /Ti-SBA-15-10(CS)	80%	10%
2-ethex.eCSTi-6		SO <sub>4</sub> /Ti-SBA-15-6(CS)	90%	10%

Figure 5.28 shows that thermogravimetric analysis of epoxidized soybean oil, 2-prop.CSTi-10, 2-prop.CSTi-6, 2-ethex.CSTi-10 and 2-ethex.CSTi-6. It was ascertained that epoxidized soybean oil and all products were thermally stable up to 300°C and 95% weight loss was observed between 300-460°C. On the other hand, there was no obvious effect of ring opening reactions on thermal stability. This outcome could be

explained with primary objective of epoxidation and ring opening reactions. Thermal stability is improved by epoxidation as a result of removal of double bonds. However, decrease of unsaturation affects negatively low temperature properties. It is aimed to enhance of low temperature properties via ring opening reactions. In this context, ring opening reactions may have not a prominent effect of on the thermal stability [17].

DSC thermogram of epoxidized of soybean oil, 2-prop.CSTi-10, 2-prop.CSTi-6, 2-ethex.CSTi-10 and 2-ethex.CSTi-6 are given in Figure 5.29. On the contrary thermal stability of products, improvement of low temperature of properties can be observed clearly. Epoxidized soybean oil showed crystallization peak at  $-18^{\circ}\text{C}$ . Similarly, there was a crystallization peak at this temperature for the 2-prop.CSTi-10. As a result of low conversion (28%), better low temperature properties could not be obtained. On the other hand, crystallization peak of 2-prop.CSTi-6 shifted to left and its intensity decreased. Nevertheless, it was noticed that low temperature properties of products from ring opening reactions with 2-ethyl hexanol was further enhanced. Especially, a significant shift and decrease in the intensity for the crystallization peak of 2-ethex.CSTi-6. Consequently, 2-ethyl hexanol was found as more effective for the promotion low temperature properties. Ring opening reactions with 2-ethyl hexanol provided a branching to the structure. It produced a steric hindrance. Thus, crystallization and stacking of molecules could be restrained and better low temperature properties were obtained [18].

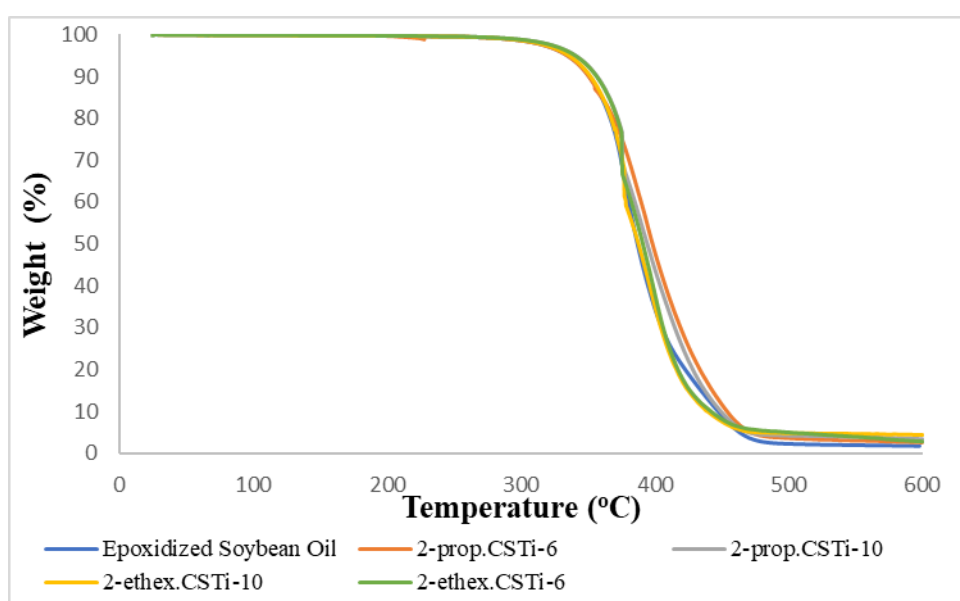


Figure 5.28. Thermal Stability of epoxidized soybean oil and obtained products

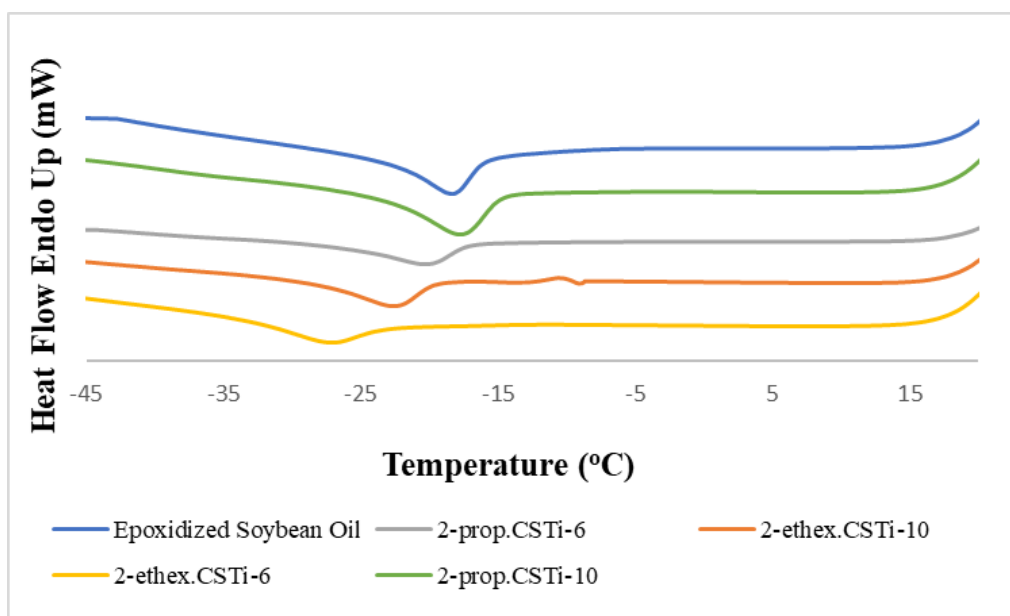


Figure 5.29. Low temperature properties of epoxidized soybean oil and biolubricant samples produced

## CHAPTER 6

### CONCLUSION

Prepared  $\text{SO}_4/\text{SBA-15}$ ,  $\text{SO}_4/\text{Ti-SBA-15}$ ,  $\text{SO}_4/\text{TiO}_2\text{-SiO}_2$  and  $\text{SO}_4/\text{La-TiO}_2\text{-SiO}_2$  catalyst had high surface area (varying between 778 and 315  $\text{m}^2/\text{g}$ ) and mesopore structure. Sulfation of catalysts with ammonium sulfate and chlorosulfonic acid enhanced their total acidity. However, chlorosulfonic acid provided higher total acidity and stronger acid sites. The activities test of catalysts in the ring opening reaction of epoxide soybean oil with 2-propanol demonstrated that prepared catalyst with ammonium sulfate had serious leaching. On the other hand, chlorosulfonic acid treatment significantly caused less leaching. Therefore, chlorosulfonic acid treatment was more favorable than ammonium sulphate regarding acidity and stability of catalysts. Nevertheless, it was found that titanium and lanthanum incorporation had positive effect on the stability of the catalysts.

It was noticed that acidity played an essential role in the activity of catalyst.  $\text{SO}_4/\text{Ti-SBA-15-6}(\text{CS})$  was found as the most stable and active catalyst (62 % epoxide conversion, (12 h)) due to its higher acidity. Promising catalytic result (90 % epoxide conversion, (18 h)) was also obtained with  $\text{SO}_4/\text{Ti-SBA-15-6}(\text{CS})$  in the ring opening reaction with 2-ethyl hexanol. Also, it showed more stable behavior due to difference of reaction medium. Obtained products had high thermal stability and enhanced low temperature properties. Improvement of low temperature properties was more prominent in the reactions performed with 2-ethyl hexanol due to higher epoxide conversion, longer and branched chain structure.

Reusability studies of  $\text{SO}_4/\text{Ti-SBA-15-6}(\text{CS})$  showed a decrease in the epoxide conversion. This decrease was ascribed to sulphur leaching of catalyst. It was suggested that further studies are needed for development of active and stable catalysts.

## REFERENCES

- [1] J. C. J. Bart, E. Gucciardi, and S. Cavallaro, "Markets for biolubricants," in *Biolubricants*, 2013. doi: 10.1533/9780857096326.712.
- [2] K. Alper, K. Tekin, S. Karagöz, and A. J. Ragauskas, "Sustainable energy and fuels from biomass: A review focusing on hydrothermal biomass processing," *Sustainable Energy and Fuels*. 2020. doi: 10.1039/d0se00784f.
- [3] M. Antar, D. Lyu, M. Nazari, A. Shah, X. Zhou, and D. L. Smith, "Biomass for a sustainable bioeconomy: An overview of world biomass production and utilization," *Renewable and Sustainable Energy Reviews*. 2021. doi: 10.1016/j.rser.2020.110691.
- [4] N. K. Attia, S. A. El-Mekkawi, O. A. Elardy, and E. A. Abdelkader, "Chemical and rheological assessment of produced biolubricants from different vegetable oils," *Fuel*, 2020, doi: 10.1016/j.fuel.2020.117578.
- [5] R. Yunus and X. Luo, *Thermochemical Conversion of Plant Oils and Derivatives to Lubricants*, vol. 2. Elsevier Ltd, 2017. doi: 10.1016/bs.aibe.2016.11.001.
- [6] G. Karmakar, P. Ghosh, and B. K. Sharma, "Chemically modifying vegetable oils to prepare green lubricants," *Lubricants*. 2017. doi: 10.3390/lubricants5040044.
- [7] A. Mukhtar *et al.*, "Current status and challenges in the heterogeneous catalysis for biodiesel production," *Renew. Sustain. Energy Rev.*, vol. 157, no. November 2021, p. 112012, 2022, doi: 10.1016/j.rser.2021.112012.
- [8] J. A. Cecilia, D. B. Plata, R. M. A. Saboya, F. M. T. de Luna, C. L. Cavalcante, and E. Rodríguez-Castellón, "An overview of the biolubricant production process: Challenges and future perspectives," *Processes*. 2020. doi: 10.3390/pr8030257.
- [9] K. Gupta, D. R. Roy, V. Subramanian, and P. K. Chattaraj, "Are strong Brønsted acids necessarily strong Lewis acids?," *J. Mol. Struct. THEOCHEM*, 2007, doi: 10.1016/j.theochem.2007.02.013.

- [10] R. V. Sharma and A. K. Dalai, "Synthesis of bio-lubricant from epoxy canola oil using sulfated Ti-SBA-15 catalyst," *Appl. Catal. B Environ.*, 2013, doi: 10.1016/j.apcatb.2013.06.001.
- [11] S. Soltani, U. Rashid, S. I. Al-Resayes, and I. A. Nehdi, "Recent progress in synthesis and surface functionalization of mesoporous acidic heterogeneous catalysts for esterification of free fatty acid feedstocks: A review," *Energy Conversion and Management*. 2017. doi: 10.1016/j.enconman.2016.07.042.
- [12] <https://www.sopa.org>, "No Title," 28.03.2022.
- [13] E. J. Parente *et al.*, "Production of biolubricants from soybean oil: Studies for an integrated process with the current biodiesel industry," *Chem. Eng. Res. Des.*, 2021, doi: 10.1016/j.cherd.2020.11.012.
- [14] P. S. Lathi and B. Mattiasson, "Green approach for the preparation of biodegradable lubricant base stock from epoxidized vegetable oil," *Appl. Catal. B Environ.*, 2007, doi: 10.1016/j.apcatb.2006.06.016.
- [15] S. Almasi, B. Ghobadian, G. Najafi, and M. D. Soufi, "A review on bio-lubricant production from non-edible oil-bearing biomass resources in Iran: Recent progress and perspectives," *Journal of Cleaner Production*. 2021. doi: 10.1016/j.jclepro.2021.125830.
- [16] J. McNutt and Q. S. He, "Development of biolubricants from vegetable oils via chemical modification," *Journal of Industrial and Engineering Chemistry*. 2016. doi: 10.1016/j.jiec.2016.02.008.
- [17] A. Z. Syahir *et al.*, "A review on bio-based lubricants and their applications," *Journal of Cleaner Production*. 2017. doi: 10.1016/j.jclepro.2017.09.106.
- [18] C. H. Chan, S. W. Tang, N. K. Mohd, W. H. Lim, S. K. Yeong, and Z. Idris, "Tribological behavior of biolubricant base stocks and additives," *Renewable and Sustainable Energy Reviews*. 2018. doi: 10.1016/j.rser.2018.05.024.
- [19] J. K. Mannekote, S. V. Kailas, K. Venkatesh, and N. Kathyayini, "Environmentally friendly functional fluids from renewable and sustainable sources-A review," *Renewable and Sustainable Energy Reviews*. 2018. doi: 10.1016/j.rser.2017.05.274.

- [20] N. A. Zainal, N. W. M. Zulkifli, M. Gulzar, and H. H. Masjuki, "A review on the chemistry, production, and technological potential of bio-based lubricants," *Renewable and Sustainable Energy Reviews*. 2018. doi: 10.1016/j.rser.2017.09.004.
- [21] M. D. Soufi, B. Ghobadian, G. Najafi, M. R. Sabzimateki, and T. Yusaf, "TOPSIS multi-criteria decision modeling approach for biolubricant selection for two-stroke petrol engines," *Energies*, 2015, doi: 10.3390/en81212408.
- [22] T. M. Panchal, A. Patel, D. D. Chauhan, M. Thomas, and J. V. Patel, "A methodological review on bio-lubricants from vegetable oil based resources," *Renewable and Sustainable Energy Reviews*. 2017. doi: 10.1016/j.rser.2016.11.105.
- [23] C. Murru, R. Badía-Laiño, and M. E. Díaz-García, "Oxidative Stability of Vegetal Oil-Based Lubricants," *ACS Sustainable Chemistry and Engineering*. 2021. doi: 10.1021/acssuschemeng.0c06988.
- [24] V. B. Borugadda and V. V. Goud, "Epoxidation of castor oil fatty acid methyl esters (COFAME) as a lubricant base stock using heterogeneous ion-exchange resin (IR-120) as a catalyst," 2014. doi: 10.1016/j.egypro.2014.07.249.
- [25] R. Mungroo, N. C. Pradhan, V. V. Goud, and A. K. Dalai, "Epoxidation of canola oil with hydrogen peroxide catalyzed by acidic ion exchange resin," *JAOCs, J. Am. Oil Chem. Soc.*, 2008, doi: 10.1007/s11746-008-1277-z.
- [26] E. M. Monono, D. M. Haagensohn, and D. P. Wiesenborn, "Characterizing the epoxidation process conditions of canola oil for reactor scale-up," *Ind. Crops Prod.*, 2015, doi: 10.1016/j.indcrop.2015.01.061.
- [27] E. Purwanto, "The Synthesis of Polyol from Rice Bran Oil ( RBO ) through Epoxidation and Hydroxylation Reactions," *Master Eng. Sci. Thesis*, no. July, pp. 73–74, 2010.
- [28] R. V. Sharma, A. K. R. Somidi, and A. K. Dalai, "Preparation and properties evaluation of biolubricants derived from canola oil and canola biodiesel," *J. Agric. Food Chem.*, 2015, doi: 10.1021/jf505825k.
- [29] C. S. Madankar, A. K. Dalai, and S. N. Naik, "Green synthesis of biolubricant

- base stock from canola oil,” *Ind. Crops Prod.*, 2013, doi: 10.1016/j.indcrop.2012.11.012.
- [30] R. M. A. Saboya *et al.*, “Synthesis of biolubricants by the esterification of free fatty acids from castor oil with branched alcohols using cationic exchange resins as catalysts,” *Ind. Crops Prod.*, 2017, doi: 10.1016/j.indcrop.2017.04.018.
- [31] R. M. A. Saboya *et al.*, “Assessment of commercial resins in the biolubricants production from free fatty acids of castor oil,” *Catal. Today*, 2017, doi: 10.1016/j.cattod.2016.02.020.
- [32] C. García-Sancho *et al.*, “Influence of pore size and loading for Nb<sub>2</sub>O<sub>5</sub>/SBA-15 catalysts on synthetic ester production from free fatty acids of castor oil,” *Mol. Catal.*, vol. 436, pp. 267–275, 2017, doi: 10.1016/j.mcat.2017.04.036.
- [33] A. R. O. Ferreira, J. Silvestre-Albero, M. E. Maier, N. M. P. S. Ricardo, C. L. Cavalcante, and F. M. T. Luna, “Sulfonated activated carbons as potential catalysts for biolubricant synthesis,” *Mol. Catal.*, 2020, doi: 10.1016/j.mcat.2020.110888.
- [34] Q. Ren, J. Pan, J. Zhou, Y. Na, C. Chen, and W. Li, “Synthesis and tribological studies of branched alcohol derived epoxidized biodiesel,” *Materials (Basel)*, 2015, doi: 10.3390/ma8105326.
- [35] V. B. Borugadda, A. K. R. Somidi, and A. K. Dalai, “Chemical/structural modification of canola oil and canola biodiesel: Kinetic studies and biodegradability of the alkoxides,” *Lubricants*, 2017, doi: 10.3390/lubricants5020011.
- [36] R. Turco, R. Tesser, R. Vitiello, V. Russo, S. Andini, and M. Di Serio, “Synthesis of biolubricant basestocks from epoxidized soybean oil,” *Catalysts*, 2017, doi: 10.3390/catal7100309.
- [37] E. Tututi-Ríos, H. González, D. A. Cabrera-Munguía, A. Gutiérrez-Alejandre, and J. L. Rico, “Acid properties of Sn-SBA-15 and Sn-SBA-15-PrSO<sub>3</sub>H materials and their role on the esterification of oleic acid,” *Catal. Today*, 2021, doi: 10.1016/j.cattod.2021.09.008.
- [38] S. Y. Chen, T. Mochizuki, Y. Abe, M. Toba, and Y. Yoshimura, “Production of

- high-quality biodiesel fuels from various vegetable oils over Ti-incorporated SBA-15 mesoporous silica,” *Catal. Commun.*, 2013, doi: 10.1016/j.catcom.2013.07.021.
- [39] S. Chirra *et al.*, “Synthesis of a novel bifunctional mesoporous Ti-SBA-15-SO<sub>3</sub>H catalyst and studies on their enhanced performance and kinetic modeling of lactic acid esterification reaction with n-butanol,” 2020. doi: 10.1016/j.matpr.2020.12.404.
- [40] E. Killıç and S. Yılmaz, “Fructose dehydration to 5-hydroxymethylfurfural over sulfated TiO<sub>2</sub>-SiO<sub>2</sub>, Ti-SBA-15, ZrO<sub>2</sub>, SiO<sub>2</sub>, and activated carbon catalysts,” *Ind. Eng. Chem. Res.*, 2015, doi: 10.1021/acs.iecr.5b00628.
- [41] R. V. Sharma, C. Baroi, and A. K. Dalai, “Production of biodiesel from unrefined canola oil using mesoporous sulfated Ti-SBA-15 catalyst,” *Catal. Today*, 2014, doi: 10.1016/j.cattod.2014.07.005.
- [42] G. D. Yadav and A. D. Murkute, “Preparation of a novel catalyst UDCaT-5: Enhancement in activity of acid-treated zirconia - Effect of treatment with chlorosulfonic acid vis-à-vis sulfuric acid,” *J. Catal.*, 2004, doi: 10.1016/j.jcat.2004.02.021.
- [43] K. R. Sunajadevi and S. Sugunan, “Para-selective tert-butylation of phenol over nano sulfated titania catalysts prepared via sol-gel route,” *Catal. Letters*, 2005, doi: 10.1007/s10562-005-2134-4.
- [44] R. V. Sharma, K. K. Soni, and A. K. Dalai, “Preparation, characterization and application of sulfated Ti-SBA-15 catalyst for oxidation of benzyl alcohol to benzaldehyde,” *Catal. Commun.*, 2012, doi: 10.1016/j.catcom.2012.09.027.
- [45] D. A. Cabrera Munguia, E. Tututi-Ríos, A. Gutiérrez-Alejandre, J. Luis Rico, and H. González, “Reaction study for the esterification of oleic acid over M-SBA-15-SO<sub>3</sub>H (M=Al, Ti) catalysts.,” 2017. doi: 10.1016/j.egypro.2017.12.098.
- [46] M. Rubaya Rashid, F. Afroze, S. Ahmed, M. S. Miran, and M. Abu Bin Hasan Susan, “Control of the porosity and morphology of ordered mesoporous silica by varying calcination conditions,” 2019. doi: 10.1016/j.matpr.2019.04.119.
- [47] C. Yan *et al.*, “Sulfated zirconia catalysts supported on mesoporous Mg-SBA-15

- with different morphologies for highly efficient conversion of fructose to 5-hydroxymethylfurfural,” *Microporous Mesoporous Mater.*, 2021, doi: 10.1016/j.micromeso.2021.111507.
- [48] H. Tanabe, K., Itoh, M., Morishige, K., & Hattori, “The Effect of Preparation Method on the Acidity of Mixed Oxides. Preparation Of Catalysts I - Scientific Bases For The Preparation Of Heterogeneous Catalysts,” *Proc. First Int. Symp. Held Solvay Res. Cent.*, pp. 65–78, 1975.
- [49] M. B. Gawande, R. K. Pandey, and R. V. Jayaram, “Role of mixed metal oxides in catalysis science - Versatile applications in organic synthesis,” *Catalysis Science and Technology*. 2012. doi: 10.1039/c2cy00490a.
- [50] H. Yang, R. Lu, and L. Wang, “Study of preparation and properties on solid superacid sulfated titania-silica nanomaterials,” *Mater. Lett.*, 2003, doi: 10.1016/S0167-577X(02)00954-0.
- [51] G. N. Shao, R. Sheikh, A. Hilonga, J. E. Lee, Y. H. Park, and H. T. Kim, “Biodiesel production by sulfated mesoporous titania-silica catalysts synthesized by the sol-gel process from less expensive precursors,” *Chem. Eng. J.*, 2013, doi: 10.1016/j.cej.2012.11.059.
- [52] J. Aguado, R. van Grieken, M. J. López-Muñoz, and J. Marugán, “A comprehensive study of the synthesis, characterization and activity of TiO<sub>2</sub> and mixed TiO<sub>2</sub>/SiO<sub>2</sub> photocatalysts,” *Appl. Catal. A Gen.*, 2006, doi: 10.1016/j.apcata.2006.07.003.
- [53] L. Li *et al.*, “Esterification of itaconic acid using Ln~SO<sub>4</sub>2-/TiO<sub>2</sub>-SiO<sub>2</sub> (Ln = La<sup>3+</sup>, Ce<sup>4+</sup>, Sm<sup>3+</sup>) as catalysts,” *J. Mol. Catal. A Chem.*, 2013, doi: 10.1016/j.molcata.2012.11.008.
- [54] Z. Zailan, M. Tahir, M. Jusoh, and Z. Y. Zakaria, “A review of sulfonic group bearing porous carbon catalyst for biodiesel production,” *Renewable Energy*. 2021. doi: 10.1016/j.renene.2021.05.030.
- [55] C. M. Mendaros, A. W. Go, W. J. T. Nietes, B. E. J. O. Gollem, and L. K. Cabatingan, “Direct sulfonation of cacao shell to synthesize a solid acid catalyst for the esterification of oleic acid with methanol,” *Renew. Energy*, 2020, doi:

10.1016/j.renene.2020.01.066.

- [56] P. Zhang, P. Liu, M. Fan, P. Jiang, and A. Haryono, "High-performance magnetite nanoparticles catalyst for biodiesel production: Immobilization of 12-tungstophosphoric acid on SBA-15 works effectively," *Renew. Energy*, 2021, doi: 10.1016/j.renene.2021.05.033.
- [57] P. Devi, U. Das, and A. K. Dalai, "Production of glycerol carbonate using a novel Ti-SBA-15 catalyst," *Chem. Eng. J.*, 2018, doi: 10.1016/j.cej.2018.04.030.
- [58] S. Gopinath, P. S. M. Kumar, K. A. Y. Arafath, K. V. Thiruvengadaravi, S. Sivanesan, and P. Baskaralingam, "Efficient mesoporous SO<sub>4</sub><sup>2-</sup>/Zr-KIT-6 solid acid catalyst for green diesel production from esterification of oleic acid," *Fuel*, 2017, doi: 10.1016/j.fuel.2017.04.090.
- [59] V. N. Mutlu and S. Yılmaz, "Synthesis of butyl glucoside over sulphated Zr-SBA-15 and tungstophosphoric acid incorporated SBA-15 catalysts," *Catal. Today*, 2021, doi: 10.1016/j.cattod.2020.04.060.
- [60] Y. Zhang, W. T. Wong, and K. F. Yung, "Biodiesel production via esterification of oleic acid catalyzed by chlorosulfonic acid modified zirconia," *Appl. Energy*, 2014, doi: 10.1016/j.apenergy.2013.11.044.
- [61] N. Azizi, M. Edrisi, and F. Abbasi, "Mesoporous silica SBA-15 functionalized with acidic deep eutectic solvent: A highly active heterogeneous N-formylation catalyst under solvent-free conditions," *Appl. Organomet. Chem.*, 2018, doi: 10.1002/aoc.3901.
- [62] R. De Clercq *et al.*, "Titania-Silica Catalysts for Lactide Production from Renewable Alkyl Lactates: Structure-Activity Relations," *ACS Catal.*, 2018, doi: 10.1021/acscatal.8b02216.
- [63] X. Zhang, F. Zhang, and K. Y. Chan, "Synthesis of titania-silica mixed oxide mesoporous materials, characterization and photocatalytic properties," *Appl. Catal. A Gen.*, 2005, doi: 10.1016/j.apcata.2005.01.037.
- [64] Y. Du, L. Zhou, Z. Liu, and J. Lei, "Hierarchical porous HPW/titania-silica material with superior adsorption-catalytic oxidation activity for multi-ring thiophenic sulfur compounds," *New J. Chem.*, 2020, doi: 10.1039/c9nj05793e.

- [65] N. Azizi and M. Edrisi, "Deep eutectic solvent immobilized on SBA-15 as a novel separable catalyst for one-pot three-component Mannich reaction," *Microporous Mesoporous Mater.*, 2017, doi: 10.1016/j.micromeso.2016.11.009.
- [66] A. A. Dabbawala, S. M. Alhassan, D. K. Mishra, J. Jegal, and J. S. Hwang, "Solvent free cyclodehydration of sorbitol to isosorbide over mesoporous sulfated titania with enhanced catalytic performance," *Mol. Catal.*, 2018, doi: 10.1016/j.mcat.2018.05.009.
- [67] Y. Li, X. D. Zhang, L. Sun, J. Zhang, and H. P. Xu, "Fatty acid methyl ester synthesis catalyzed by solid superacid catalyst SO<sub>4</sub><sup>2-</sup>/ZrO<sub>2</sub>-TiO<sub>2</sub>/La<sup>3+</sup>," *Appl. Energy*, 2010, doi: 10.1016/j.apenergy.2009.06.030.
- [68] I. Sadaba, M. Lopez Granados, A. Riisager, and E. Taarning, "ChemInform Abstract: Deactivation of Solid Catalysts in Liquid Media: The Case of Leaching of Active Sites in Biomass Conversion Reactions," *ChemInform*, 2015, doi: 10.1002/chin.201540246.
- [69] A. Adhvaryu and S. Z. Erhan, "Epoxidized soybean oil as a potential source of high-temperature lubricants," *Ind. Crops Prod.*, 2002, doi: 10.1016/S0926-6690(01)00120-0.
- [70] D. Favero *et al.*, "Renewable polyol obtained by microwave-assisted alcoholysis of epoxidized soybean oil: Preparation, thermal properties and relaxation process," *J. Mol. Liq.*, 2019, doi: 10.1016/j.molliq.2019.04.078.
- [71] M. Kurańska, H. Benes, K. Polaczek, O. Trhlikova, Z. Walterova, and A. Prociak, "Effect of homogeneous catalysts on ring opening reactions of epoxidized cooking oils," *J. Clean. Prod.*, 2019, doi: 10.1016/j.jclepro.2019.05.096.
- [72] R. D. Kulkarni, P. S. Deshpande, S. U. Mahajan, and P. P. Mahulikar, "Epoxidation of mustard oil and ring opening with 2-ethylhexanol for biolubricants with enhanced thermo-oxidative and cold flow characteristics," *Ind. Crops Prod.*, 2013, doi: 10.1016/j.indcrop.2013.06.006.